UPTAKE OF CHLORIDE-36 AND SODIUM-22 BY THE CHOROID PLEXUS—CEREBROSPINAL FLUID—BRAIN SYSTEM OF THE IMMATURE AND MATURE RAT: EVIDENCE FOR ACTIVE CHLORIDE TRANSPORT BY THE CHOROIDAL EPENDYMA

by

Quentin Roberts Smith

A dissertation submitted to the faculty of
The University of Utah in partial fulfillment of the requirements
for the degree of

Doctor of Philosophy

Department of Pharmacology

The University of Utah

August 1980

THE UNIVERSITY OF UTAH GRADUATE SCHOOL

SUPERVISORY COMMITTEE APPROVAL

of a dissertation submitted by

Quentin Roberts Smith

I have read this dissertation and have found it to be of [illegible] quality for a doctoral degree.

[illegible]
Date

Conrad E. Johanson, [illegible]
Cochairman, Supervisory Committee

I have read this dissertation and have found it to be of satisfactory quality for a doctoral degree.

Jul 15 1980
Date

Dix n M. Woodbury, Ph.
Cochairman, Supervisory Committee

I have read this dissertation and have found it to be of satisfactory quality for a

[illegible]
Date

Donal J. Reed, Ph.D.
Member, Supervisory Committee

I have read this dissertation and hav[illegible] quality for a doctoral degree.

[illegible]
Date

[illegible] Kemp, P[illegible]
Me[illegible]ber, Supervisory Committee

I have read this dissertation and have found it to be of satisfactory quality for a doctoral degree.

15, 1980
Date

J. [illegible]alter Woodbury, [illegible]
Me[illegible]r, Supervisory Committee

THE UNIVERSITY OF UTAH GRADUATE SCHOOL

FINAL READING APPROVAL

To the Graduate Council of The University of Utah:

I have read the dissertation of Quentin Roberts Smith in its final form and have found that (1) its format, citations, and bibliographic style are consistent and acceptable; (2) its illustrative materials including figures, tables, and charts are in place; and (3) the final manuscript is satisfactory to the Supervisory Committee and is ready for submission to the Graduate School.

Conrad E. Johanson, Ph.D.
Member, Supervisory Committee

Approved for the Major Department

Chairman/Dean

Approved for the Graduate Council

James L.
Dean of The Graduate

ABSTRACT

Transport and permeability properties of the blood-cerebrospinal fluid and blood-brain barriers were determined by kinetic analysis of radioisotope uptake from the plasma into the central nervous system of adult and infant rats. For adult rats (5 wk of age), ^{36}Cl and ^{22}Na uptake into the lateral ventricle (LVCP) and fourth ventricle (4VCP) choroid plexuses were resolved into two components, a fast component ($t_{1/2}$ 0.02-0.05 h) which represents isotope distribution within the extracellular and residual erythrocyte compartments and a slow component ($t_{1/2}$ 0.85-1.93 h) representing isotope movement into the epithelial cell compartment. Calculated LVCP and 4VCP cell [Cl], 67 mmol/kg cell H_2O, were 3.9x greater than that predicted for passive distribution by the membrane potential. It is postulated that Cl is actively transported into the choroid ependymal cell across the basolateral membrane; the energy for active Cl transport may be the Na electrochemical potential gradient which is twice that of the Cl electrochemical potential difference. ^{36}Cl and ^{22}Na uptake into the cerebrospinal fluid (CSF) were resolved into two components, a fast component ($t_{1/2}$ 0.18 h, fractional volume 0.24) and a slow component ($t_{1/2}$ 1.2 h, fractional volume 0.76). Evidence suggests that the fast component represents isotope movement across the blood-CSF barrier, i.e., the choroid plexuses. The slow component may reflect isotope

exchange primarily from brain extracellular fluid into the CSF. Cerebral cortex and cerebellum uptake of ^{36}Cl and ^{22}Na were resolved into two components. The fast component ($t_{1/2}$ 0.02-0.05 h, fractional volume 0.04-0.08) is comprised of the vascular compartment and a small perivascular space. The slow component ($t_{1/2}$ 1.1-1.7 h, fractional volume 0.92-0.96) represents isotope movement across the blood-brain barrier into the brain extracellular and cellular compartments. The extracellular fluid volume of the cerebral cortex and cerebellum was estimated as ~13% from the initial slope of the brain space versus CSF space curve. Like the choroid plexuses, the glial cell compartment of the brain would appear to actively accumulate Cl from 2-6x that predicted for passive distribution. The relative permeability of the blood-CSF and blood-brain barriers to ^{36}Cl, ^{22}Na, and ^{3}H-mannitol was determined by calculating permeability surface-area products (PA). Analysis of the PA values for all three isotopes indicates that the effective permeability of the choroidal epithelium (blood-CSF barrier) is significantly greater than that of the cerebral cortex or cerebellum capillary endothelium (blood-brain barrier).

Analysis of radioisotope uptake by the 1- and 2-wk rat central nervous system revealed significant maturational differences from that of the 5-wk rat. The calculated LVCP and 4VCP cell [Cl] and [Na] were markedly greater in the 1-wk than in the 5-wk rat. Likewise, a significant CSF fast component was not observed for radioisotope uptake at 1 wk of age. It is postulated that while the immature choroid plexus can actively accumulate Cl across the

basolateral membrane of the cell, the mechanisms which regulate Cl exit from the choroidal cell into the CSF have not fully developed. Thus, at 1 wk, epithelial cell [Cl] and [Na] were substantially greater than at 2 or 5 wk because ion transport into the choroidal cell across the basolateral membrane was not coupled with ion movement from the cell into the CSF. The onset of choroid plexus fluid secretion ($\sim$ 2 wk), as indicated by the volume of the CSF fast component, corresponds in time to the decrease in choroid plexus cell [Cl] and [Na] (1-2 wk). Lastly, the cerebral cortex and cerebellum PA for all three radioisotopes decreased significantly between 1 and 5 wk of age (barrier tightening) while the CSF (fast component) PA to ^{36}Cl and ^{22}Na increased with age (transepithelial choroid plexus NaCl transport).

TABLE OF CONTENTS

LIST OF FIGURES

LIST OF TABLES

ACKNOWLEDGMENTS

Gratitude is expressed to all members of the Department of Pharmacology for their contributions to my graduate training.

I am particularly grateful to Dr. Conrad E. Johanson for his unselfish guidance, support, and friendship throughout the course of my education at the University of Utah. Also, special thanks are expressed to Dr. Dixon M. Woodbury for his personal concern for my development and for his direction and inspiration.

I wish to express my gratitude to Drs. Donal J. Reed, John W. Kemp, and J. Walter Woodbury for their thoughtful criticisms and suggestions while serving as members of my thesis committee.

I would also like to thank Wayne A. Bamossy for his technical assistance and professional typing of this manuscript.

Finally, a special note of thanks is extended to my wife, Helen Thorsheim, for her love and understanding while I labored toward the doctoral degree.

This work was supported by NIH grants NS 13988, GM 07579, and AM 20935.

PART ONE

UPTAKE OF CHLORIDE-36 AND SODIUM-22 BY THE CHOROID PLEXUS-CEREBROSPINAL FLUID SYSTEM: EVIDENCE FOR ACTIVE CHLORIDE TRANSPORT BY THE CHOROIDAL EPENDYMA

INTRODUCTION

The nature of choroid plexus Cl transport, whether passive diffusion, facilitated diffusion, or active transport, has remained an issue in CSF physiology since HOGBEN et al. (1960) reported evidence for active Cl transport into the dogfish CSF. WOODBURY (1967) and MAREN & BRODER (1970) proposed Cl secretion into CSF to explain decreases in the CSF ^{36}Cl space upon perchlorate and acetazolamide treatment, respectively. Furthermore, BOURKE et al. (1970) and ABBOTT et al. (1971) measured a constant rate of Cl uptake into the CSF over a plasma [Cl] range of 60-120 mmol/l, indicating some mechanism for accumulating Cl into the CSF. In 1972, two reports were published which provided good evidence for passive Cl diffusion across the choroidal ependyma. First, MINER & REED (1972) did not detect any appreciable Cl electrochemical potential gradient from serum ultrafiltrate to nascent choroid plexus CSF. Second, in the in vitro frog choroid plexus, WRIGHT (1972) found that the unidirectional fluxes across the ependyma were equal and agreed with the Ussing flux ratio equation for passive ionic distribution. Thus, Cl movement into the CSF was conceived as primarily the result of active Na transport with Cl following passively down the electrical gradient created by Na movement.

In recent years, there has been a marked increase in interest in active transepithelial Cl transport, partly due to the recognition that active Cl

transport is a far more widespread phenomenon than previously appreciated. Many epithelial tissues similar in histology and physiology to the choroid plexus, i.e., renal proximal tubule, ileum, and gall bladder, have been shown to accumulate Cl intracellularly and produce an active transepithelial movement of Cl (FRIZZELL et al., 1979). Significantly, the ciliary body, a CNS epithelial tissue similar to the choroid plexus, transports Cl actively from plasma to aqueous humor (COLE, 1977). Furthermore, Cl transport has become especially important to the neuroscientist due to the demonstration of Cl accumulation by astrocytes (BOURKE & NELSON, 1972a; GILL et al., 1974; KIMELBERG et al., 1979). Thus, an examination of the mechanism of Cl transport (passive or active) by the mammalian choroid plexus is in order. To that end, we measured the distribution of Cl within the epithelial cell of the mammalian choroid plexus by the compartmentation technique to determine if Cl was accumulated within the cell against an electrochemical potential gradient. In addition, we analyzed the kinetics of ^{36}Cl and ^{22}Na uptake into the choroid plexus-cerebrospinal fluid system to relate ^{36}Cl and ^{22}Na movement across the choroid plexus to their uptake into the CSF. Lastly, we examined both the LVCP and 4VCP to determine regional differences and similarities between the choroid plexuses.

MATERIALS AND METHODS

One hundred forty-four Sprague-Dawley rats (90-110 g) were utilized in the present investigation: 99 and 45 in the *in vivo* and *in vitro* studies, respectively. All animals were allowed free access to water and Purina rat chow.

In vivo experimental protocol

Four hours prior to sacrifice each animal was lightly anesthetized with ether and bilaterally nephrectomized by ligation of the renal pedicles. All radioisotopes were injected intraperitoneally, except for the ^{51}Cr-tagged erythrocytes which were delivered intravenously. Three separate studies were performed *in vivo*. In the first study, *in vivo* uptake curves were determined for ^{36}Cl, ^{22}Na, and ^{3}H-mannitol. A total of 54 animals was divided into two groups of 27 rats; each animal received 0.1 μCi/g of either ^{36}Cl or ^{22}Na at 1/12, 1/6, 1/4, 1/2, 1, 2, 4, 6, or 8 h prior to sacrifice. Similarly, ^{3}H-mannitol was injected intraperitoneally to 12 rats at 1/12, 1/6, 1/4, or 1 h before death. In the second study, chemical determinations of Na and Cl content were performed on samples from 12 rats, in order to compare chemical and radioisotope steady-state spaces. Lastly, in the third study, tissue water content, extracellular space, and residual erythrocyte volume were measured to allow calculation of the concentration of Na and Cl in the parenchymal cells of the sampled tissues. In 12 animals, the tissue volumes

of distribution of two saccharides commonly used to quantify extracellular space, mannitol and inulin, were determined as the 1-h tissue space after injection of 0.5 μCi/g of ^{3}H-mannitol or ^{3}H-inulin. Water content, ^{3}H-mannitol space (1 h) and ^{51}Cr-tagged erythrocyte volume (10 min) were measured in an additional 9 animals. ^{51}Cr-tagged erythrocytes were prepared by incubating rat erythrocytes for 1 h in 0.9% NaCl containing 1 mCi/ml ^{51}Cr. Subsequently, the red blood cells were washed three times with non-radioactive saline to remove the unbound isotope and were injected via the inferior vena cava 10 min prior to sacrifice.

Sampling of tissues and fluids

Just prior to sacrifice, each animal was anesthetized with ether. A 4 ml sample of blood was obtained from the abdominal aorta with a heparinized syringe. Approximately 100 μl of the blood sample was placed in a tared vial and weighed on a Sartorius balance; the remainder was centrifuged for 10 min and the plasma collected for analysis. Within 2 min after exsanguination, an 80-100 μl sample of CSF was taken from the cisterna magna and weighed. Only samples free of visible erythrocyte contamination were saved for analysis. Following decapitation and removal of the brain, the lateral ventricle and fourth ventricle choroid plexuses were quickly exposed and collected with the aid of a stereoscopic dissecting microscope and ophthalmologic forceps. After removal of the meninges, a slice of gray matter from the parietal cerebral cortex and one lobe of the cerebellum were placed in tared vials and weighed. For comparison with the CNS, a sample of submaxillary salivary gland and skeletal muscle was collected and weighed for analysis.

In vitro experimental protocol

Two experimental studies were performed in vitro. In the first group, 27 rats were utilized to measure lateral ventricle and fourth ventricle choroid plexus uptake of ^{36}Cl (1000 dpm/μl) and ^{3}H-inulin (2000 dpm/μl) at 1/2, 1, 2, 4, 6, 8, 10, 20, and 30 min. In the second group, the chemical sodium and chloride content, ^{3}H-inulin space, and water content were measured in the choroid plexuses of 18 rats after 30 min of in vitro incubation. To perform the incubations, the LVCP and 4VCP were excised as described in the preceding section. The tissues were then placed in 5 ml of artificial CSF containing (in mM) 117.6 NaCl, 18.0 $NaHCO_3$, 3.0 KCl, 2.0 urea, 1.4 $CaCl_2$, 0.8 $MgCl_2$, 0.7 Na_2HPO_4, and 12.1 dextrose. The solution was maintained at 37° C in a Metabolyte Water Bath Shaker (New Brunswick Sci. Co.) and aerated with a humidified mixture of 95.6% O_2 and 4.4% CO_2 (pCO_2 of solution ~ 28 mm Hg). After 30 min, the plexuses were taken from the bath, wiped on a glass slide to remove adhering artificial CSF and placed on a small (~1 mg) piece of aluminum foil for weighing.

Analytical techniques

Samples containing ^{36}Cl or ^{3}H activity were analyzed with a Nuclear Chicago Isocap 300 liquid scintillation counter. Tissues and fluids were digested overnight at 60° C in a volume of 1 M piperidine which was 10x that of the sample wet weight. One-half ml of the digested sample was then added to 10 ml of Biofluor Scintillation Cocktail (New England Nuclear) and thoroughly mixed before counting. ^{22}Na and ^{51}Cr activity were directly assayed

for gamma radioactivity by counting the vials on a Beckman Biogamma counter without any further sample preparation.

The wet weight of most tissues and fluids was measured directly with a Sartorius balance. Due to the small size of the choroid plexus (1-2 mg), evaporative water loss was significant within a few seconds after removing the tissue from the brain. Thus, the wet weight of the choroid plexuses was determined indirectly. Upon excision of either the LVCP or 4VCP, the tissue was placed on a pre-weighed aluminum foil and immediately placed on a Cahn electrobalance. The tissue weight was recorded at 1/4 min intervals up to 2 min after the plexus was removed from the brain. It has been demonstrated previously that the log tissue weight vs. time plot is linear for at least 3 min ($r > 0.999$; JOHANSON et al., 1976). A least squares linear regression was utilized to provide an extrapolated y-intercept, the antilog of which was taken as the fresh plexus wet weight. Tissue dry weights were recorded after desiccation to constant weight in a 105° C oven.

Tissue and fluid electrolye (Na, K, Cl) contents were determined as follows. Tissues other than the choroid plexus were extracted overnight in 4 ml of a solution containing HNO_3 (0.02 M) and Li_2SO_4 (7.5 mM). For Na and K analysis, 50 μl of each extracted solution was diluted with 2 ml of the HNO_3-Li solution. Samples were prepared for Cl content determination by combining 1 ml of the extracted solution with 3.5 ml of a 1:6 mixture of gelatin reagent (6.2 g gelatin/l H_2O, 0.10 g/l thymol blue, and 0.10 g/l thymol) and nitric acid reagent (6.4 ml conc. HNO_3/l and 100 ml/l glacial acetic acid), respectively. Each choroid plexus tissue was extracted with 1 ml of

the HNO_3-Li solution. Then, the sample was analyzed for Na-K content without further modification or prepared for assay of Cl content by addition of 3.5 ml of the gel-acid solution. Due to the small size of the rat choroid plexuses, both LVCP and the 4VCP from each animal were pooled for Cl analysis. Twenty μl of plasma or CSF was diluted 1/200 with the HNO_3-Li solution. Final modifications for analysis were the same as those for the choroid plexus-extracted solutions. All samples, along with appropriate standards, were analyzed for Na and K with an Instrumentation Laboratory Flame Photometer and for Cl with a Cotlove Chloridometer (amperometric titration of Ag).

Calculations

The tissue or CSF content of ^{36}Cl, ^{22}Na, ^{3}H-mannitol, or ^{3}H-inulin was expressed as a volume of distribution or space (%) = 100 x (dpm/g tissue or CSF)/(dpm/g plasma H_2O x D.F.) where D.F. is the appropriate Donnan factor, i.e., 1.05 for a monovalent cation, 0.95 for a monovalent anion, and 1.00 for an uncharged molecule. The product of g plasma H_2O and D.F. is referred to as g extracellular fluid. A chemical Cl or Na space was determined as 100 x (mmol Cl or Na/kg tissue or CSF)/(mmol Cl or Na/kg extracellular fluid). Similarly, ^{51}Cr-tagged erythrocyte volume was expressed as a space (%) = 100 x (dpm/g tissue)/(dpm/g erythrocytes). Lastly, water content (%) was determined as 100 x (tissue wet weight-tissue dry weight)/(tissue wet weight).

Parenchymal cell ion concentrations were calculated using the formula:

$$[X]cell = \frac{(X)tissue - (X)e - (X)r}{Vtissue - Ve - Vr}$$

where (X) = Na, K, or Cl content (mmol/kg wet weight), V = fractional volume of water, e = extracellular fluid, and r = residual erythrocytes. Extracellular water volume was estimated with two markers, ^{3}H-mannitol and ^{3}H-inulin. Residual erythrocyte water volume was determined as the product of the tissue erythrocyte space and the erythrocyte water content (70%). (X)e and (X)r were calculated as [X]eVe and [X]rVr, respectively. Cell ^{36}Cl or ^{22}Na spaces were obtained by modifying the above equation, substituting radioisotope space (tissue, extracellular fluid, and residual erythrocytes) for Cl or Na content. Finally, Cl, Na, or K equilibrium potentials were calculated using the Nernst equation: $Ex\ (mV) = (61/z)\log_{10}([X]e \text{ or } csf/[X]\,cell)$, where z = the valence of the ion X.

Radioisotope uptake curves were resolved into components by a modification of the graphical analysis method of SOLOMON (1949). Briefly, uptake spaces were subtracted from the steady-state space and the difference was plotted vs. time on semilogarithmic paper. Linear portions of the subtracted line (In space vs. time) were analyzed by a least squares linear regression program which provided the slope $\pm$ S.E.M., intercept $\pm$ S.E.M. and (correlation coefficient)^2. The slope, equivalent to the rate constant (k) of the component, was converted to a half-time ($t_{1/2}$) by the formula $t_{1/2} = (\ln 2)/k$. The exp (y-intercept) corresponded to the volume of distribution of the component. When appropriate, another component could be resolved by subtracting the values predicted by the line from those early values which were not fitted to the line and plotting the difference vs. time on semilogarithmic paper. Again, linear portions of the line (In space vs. time) were analyzed

by linear regression. Except for the CSF, the second component was determined by only 2-3 experimental points, at t = 0, 1/12, and/or 1/6 h; in those instances the reported volume and half-time are indicated only as a relative description of the component and thus standard errors or 95% confidence limits are not reported.

Student's t test was used to determine statistical significance. For component volume and half-time data, 95% confidence limits are reported because upon conversion from rate constant to half-time and from y-intercept (ln) to exp (y-intercept) the standard errors were no longer symmetrical.

Materials

^{3}H-mannitol (0.123 mCi/g), ^{3}H-inulin (389 mCi/g), ^{51}Cr-sodium chromate (0.252 mCi/g), and ^{22}Na-NaCl (carrier free) were obtained from New England Nuclear; ^{36}Cl-NaCl (12.7 mCi/g) was purchased from ICN Chemical and Radioisotope Division. Radiochemical and chemical purity were reported as > 99% by the companies.

RESULTS

In vivo experiments

In order to maintain a constant level of plasma radioactivity, rats were bilaterally nephrectomized 4 h prior to sacrifice. The time course of plasma ^{36}Cl, ^{22}Na, or ^{3}H-mannitol activity was analyzed by linear regression for the in vivo uptake studies. From 1/12 to 8 h, the slope of the regression line was not significantly different from 0 for either ^{36}Cl ($P = 0.28$) or ^{22}Na ($P = 0.47$). The slope of the ^{3}H-mannitol regression line was not statistically significant ($P = 0.54$) from 1/12 to 1 h. For all three radioisotopes, the standard deviation of the plasma activity was approximately 7% of the mean. Nephrectomy (4 h) did not alter plasma, choroid plexus cell or CSF ion concentrations (Na, K, and Cl) as compared to unoperated-control animals (unpublished results), in contrast to longer periods (> 6 h) of azotemia (FERGUSON & WOODBURY, 1969). Thus, the tissue and CSF uptake curves were based on a constant level of isotope in the plasma.

^{36}Cl and ^{22}Na uptake are shown for the LVCP and for the 4VCP in Fig. 1. A steady-state distribution of ^{36}Cl was achieved in both the LVCP and 4VCP after 4-6 h. In contrast, the LVCP and 4VCP differed in the time to reach a ^{22}Na steady-state space, LVCP $\sim$ 6-8 h and 4VCP $\sim$ 4-6 h. As with the rate of uptake, the ^{36}Cl steady-state spaces of the LVCP and 4VCP were approximately equal, 55.2 and 55.8%, respectively. These spaces agree well

Fig. 1. The uptake of ^{36}Cl and ^{22}Na into the LVCP and 4VCP as a function of time after administration. The left-hand portion of the figure represents penetration of the isotopes into the LVCP and the right-hand portion their movement into the 4VCP. Either ^{36}Cl or ^{22}Na (0.1 μCi/g) was injected at various times prior to sacrifice into 4-h nephrectomized rats. Tissue radioactivity was expressed as a space (%) = 100 x (dpm/g tissue)/(dpm/g extracellular fluid). Values are means $\pm$ S.E.M. for 3 animals.

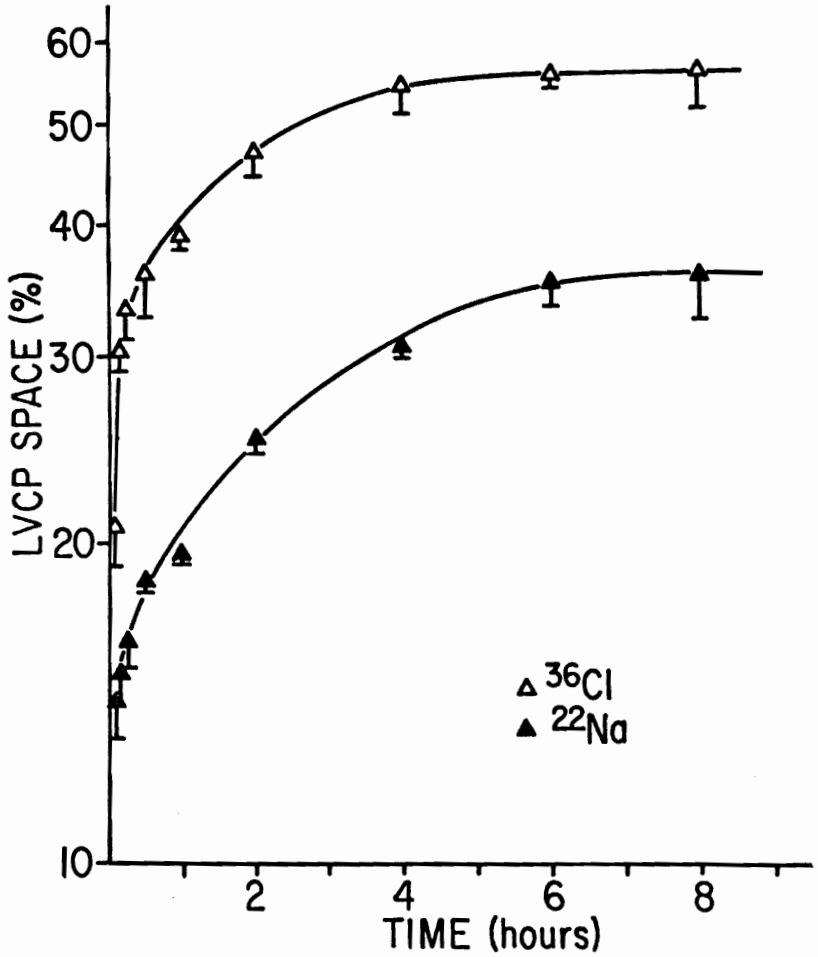
60
50
40
30
20
10
LVCP SPACE (%)
2
4
6
8
TIME (hours)
△ 36Cl
▲ 22Na

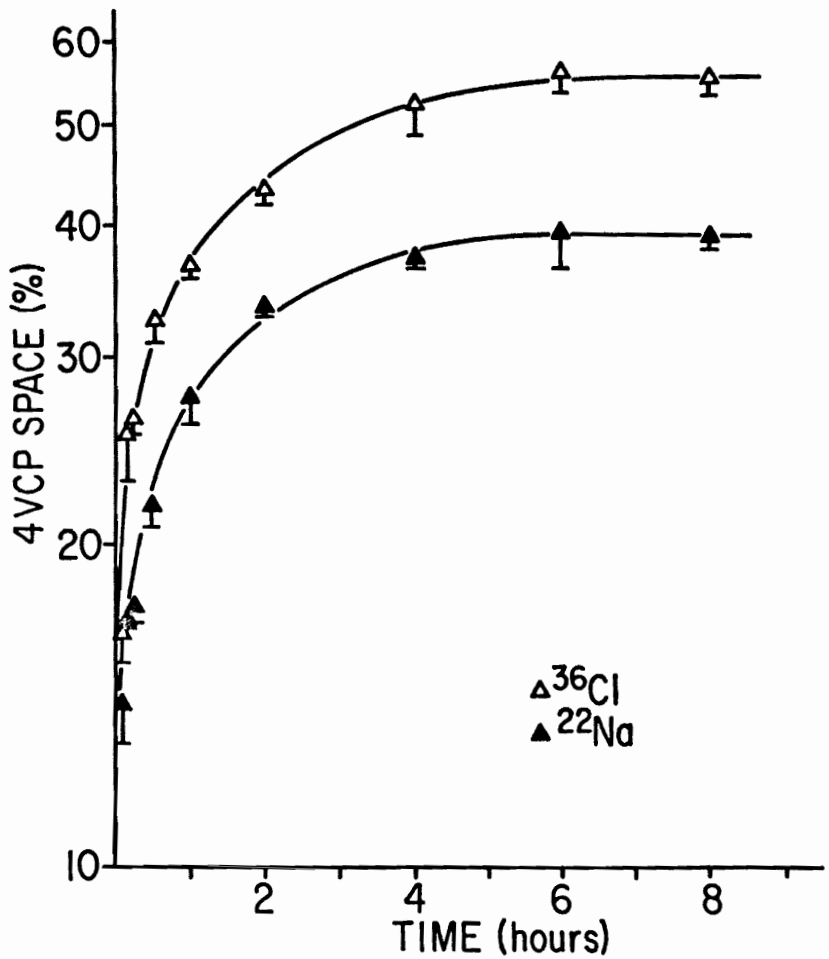
60
50
40
30
20
10
4VCP SPACE (%)
2
4
6
8
TIME (hours)
△ 36Cl
▲ 22Na

with the chemically determined, pooled LVCP and 4VCP Cl space of 56.2%, equivalent to a choroid plexus Cl content of 64 ± 1 (S.E.M.) mmol/kg wet tissue and an extracellular fluid [Cl] of 114 ± 1 mmol/kg H_2O. The 4VCP ^{22}Na steady-state space, 39.2%, was greater than the LVCP ^{22}Na space, 35.8%; this difference was also seen in the chemically measured Na space for the 4VCP (38.5%) and for the LVCP (36.0%). With an extracellular fluid [Na] of 143 ± 1 mmol/kg H_2O, the corresponding choroid plexus Na contents were 4VCP 56 ± 2 mmol/kg wet tissue and LVCP 51 ± 2 mmol/kg. Thus, no evidence for inexchangeable or "bound" Na or Cl was observed in either the in vivo LVCP or 4VCP. While radio-potassium uptake by the choroid plexus was not examined, the K content, as measured by flame photometry, was 95 ± 2 mmol/kg wet tissue for the LVCP and 93 ± 1 mmol/kg for the 4VCP.

CSF uptake of ^{22}Na and ^{36}Cl required approximately 6 h to reach a steady-state distribution (Fig. 2), similar to the choroid plexuses. At early uptake times (< 1/2 h), the CSF ^{22}Na and ^{36}Cl spaces were not significantly different. Later, the ^{36}Cl values approached a steady-state space of 116.7% and the ^{22}Na values approached 111.8%. Both the chemically determined CSF Na and Cl spaces were of less magnitude than the spaces obtained with the radioisotopes. A CSF Na space of 108.5% (155 ± 1 mmol/kg H_2O) was obtained by flame photometry; a CSF Cl space of 105.3% (120+1 mmol/kg) was determined by amperometric titration ($P<0.05$). This discrepancy occurred only with the CSF; all other samples, i.e., skeletal muscle, salivary gland, cerebral cortex, and cerebellum, had equivalent chemical and radioisotope spaces. The CSF [K] was 0.77 times that of the plasma [K] of 4.1 ± 0.1

Fig. 2. The uptake of ^{36}Cl and ^{22}Na into the CSF as a function of time after administration. Values are expressed as a space (%) = 100 x (dpm/g CSF)/(dpm/g extracellular fluid). Each point represents a mean $\pm$ S.E.M. for 3 animals. Error bars are not shown when they fell within the limits of the squares.

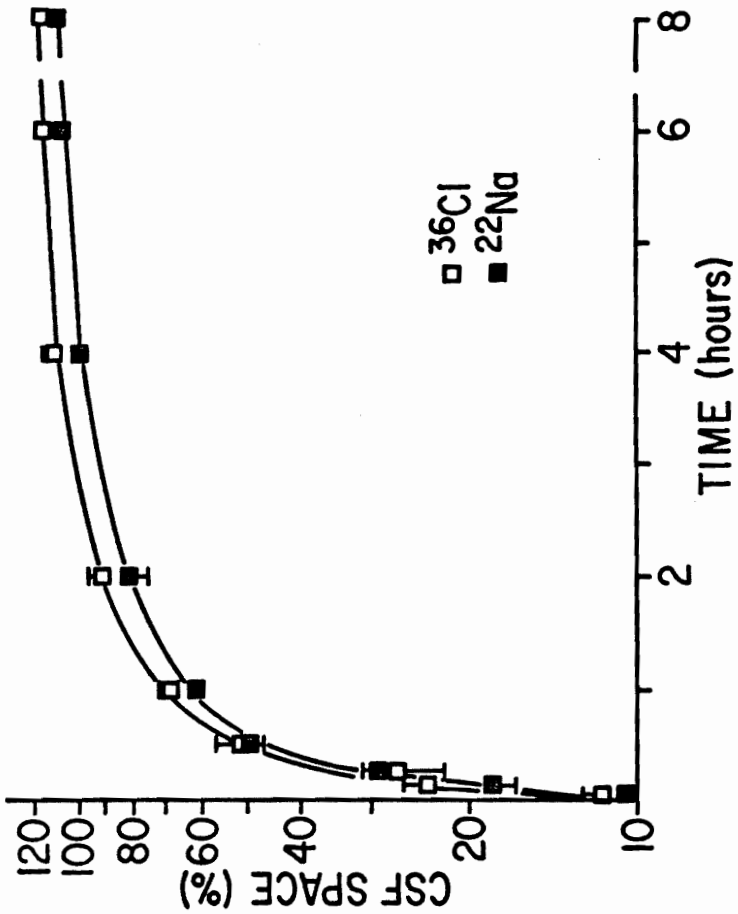
CSF SPACE (%)
120
100
80
60
40
20
10
2
4
6
8
TIME (hours)
□ 36Cl
■ 22Na

mmol/kg H_2O.

In contrast to the CNS, both radioisotopes attained steady-state levels in the submaxillary salivary gland and the skeletal muscle within 15 min. ^{22}Na (14.7%) and ^{36}Cl (13.8%) spaces were not significantly different from the chemically measured volumes of 14.6% and 14.2%, respectively ($P > 0.05$). Similarly, salivary gland ^{22}Na (23.4%) and ^{36}Cl (38.4%) spaces were not different statistically from the corresponding chemically determined values.

^{36}Cl and ^{22}Na uptake into the CNS were resolved into components by a modification of the method of graphical analysis (see Methods). An example of the procedure is shown in Fig. 3 for ^{36}Cl uptake by the LVCP. Parameters obtained from analysis of the LVCP, 4VCP, and CSF uptake curves for ^{22}Na and ^{36}Cl are summarized in Table 1. Choroid plexus ^{36}Cl and ^{22}Na uptake curves were resolved into two components. The fast component for both the LVCP and 4VCP had a rapid $t_{1/2}$ (0.02-0.05 h) and filled a volume 0.45 and 0.36 that of the ^{36}Cl and ^{22}Na steady-state spaces, respectively. Marked differences were noted in the choroid plexus slow components; whereas ^{36}Cl was taken up into the slow components of the LVCP and 4VCP at an approximately equal rate ($t_{1/2}$ = 1.0-1.3 h), the ^{22}Na uptake into the 4VCP slow component was twice as fast as that into the LVCP. The difference between the LVCP and 4VCP ^{22}Na steady-state spaces was accounted for in the slow component volumes, 21.9% for the LVCP and 26.3% for the 4VCP ($P < 0.05$). Graphical analysis of the CSF uptake curves revealed that ^{22}Na and ^{36}Cl were kinetically equivalent. Uptake curves for both radioisotopes

Fig. 3. Graphical analysis of the components of LVCP ^{36}Cl uptake (shown in Fig. 1) as a function of time after administration. The slow component of isotope uptake into the LVCP was resolved by subtracting the tissue spaces from the steady-state space and plotting the difference as a function of time. The slope and y-intercept were obtained by fitting the linear portion of the graph to a straight line by the least squares method. The fast component was estimated by subtracting the spaces predicted by the extrapolated slow component line from the early time period spaces which were not fitted to the slow component line (generally, the 0, 5, and 10 min spaces for the choroid plexuses), and plotting the difference versus time. Again, a slope and y-intercept were obtained by linear regression. For the slow component, each point represents a mean $\pm$ S.E.M. for 3 animals. Only mean values were utilized to obtain the fast component and thus no error limits are indicated.

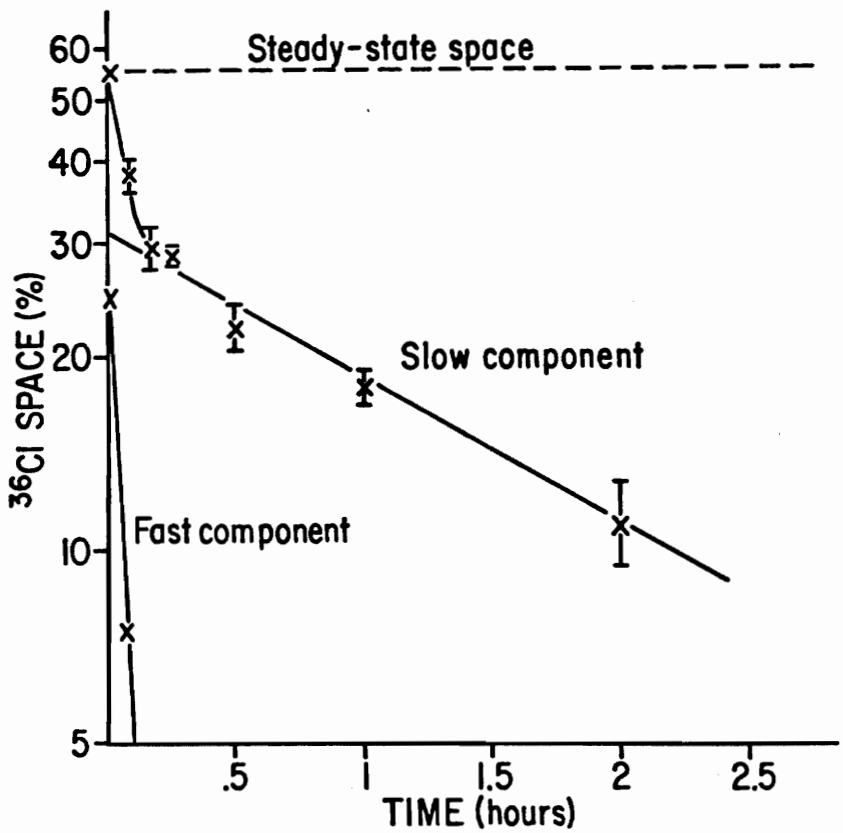
Steady-state space
Slow component
Fast component
^{36}Cl SPACE (%)
60
50
40
30
20
10
5
.5
1
1.5
2
2.5
TIME (hours)

TABLE 1. ANALYSIS OF COMPONENTS OF ^{36}Cl AND ^{22}Na UPTAKE CURVES

Compartment	Isotope	Fast component			Slow component			Steady-state isotope space (%)
		$t_{1/2}$ (h)	Vd (%)	fractional volume	$t_{1/2}$ (h)	Vd (%)	fractional volume	
LVCP	^{36}Cl	0.03	25.5	0.46	1.00 (0.72-1.63)	29.7 (22.0-40.2)	0.54	55.2 (51.6-58.8)
	^{22}Na	0.02	13.9	0.39	1.93 (1.68-2.26)	21.9 (20.8-23.0)	0.61	35.8 (30.7-40.9)
4VCP	^{36}Cl	0.05	24.7	0.44	1.32 (1.04-1.81)	31.1 (26.5-36.4)	0.56	55.8 (50.9-60.7)
	^{22}Na	0.02	12.9	0.33	0.85 (0.70-1.02)	26.3 (23.2-29.9)	0.67	39.2 (35.1-43.3)
CSF	^{36}Cl	0.19 (0.11-0.40)	25.7 (17.2-37.4)	0.22	1.06 (0.93-1.23)	91.0 (73.1-112.6)	0.78	116.7 (114.4-119.0)
	^{22}Na	0.18 (0.15-0.21)	28.9 (22.6-35.6)	0.26	1.31 (1.17-1.49)	82.9 (65.6-104.8)	0.74	111.8 (109.5-114.1)

Radioisotope uptake curves were resolved into components by the method of graphical analysis (see Fig. 3) and fitted to straight lines by linear regression. The $t_{1/2}$, half-time, was obtained by dividing ln 2 by the slope (k) of the regression line. Vd, volume of distribution, was calculated as the exp (y-intercept of the regression line). The fractional volume is the Vd expressed as a fraction of the asymptote (steady-state plateau) of the uptake curve. Values in parentheses are the 95% confidence limits for the parameter.

resolved into a fast component (fractional volume 0.24) and a slow component (fractional volume 0.76). The ^{36}Cl and ^{22}Na half-times for each component were not significantly different ($P > 0.05$).

^{3}H-mannitol uptake by the LVCP and 4VCP was analyzed by graphical analysis (Fig. 4). The uptake curves of both tissues reached steady-state levels within 15 min after i.p. injection of the isotope. In contrast to ^{36}Cl and ^{22}Na uptake by the choroid plexuses, the ^{3}H-mannitol uptake curves resolved into a single fast component ($t_{1/2}$ 0.05 h) for both the LVCP and 4VCP.

The 1-h space of ^{3}H-mannitol and ^{3}H-inulin was analyzed for several tissues and fluids (Table 2). Whereas the two saccharides distributed equally in the skeletal muscle ($P > 0.05$), ^{3}H-mannitol equilibrated in a 17-27% larger space than ^{3}H-inulin in salivary gland, LVCP, and 4VCP. No evidence for significant penetration of ^{3}H-mannitol into erythrocytes was obtained. Thus, the difference in the tissue volumes filled by the two saccharides probably reflects the differences in molecular size; mannitol molecular weight = 182, and inulin molecular weight ~5500 g/mol. The importance of size is best indicated by the significantly greater rate of uptake of ^{3}H-mannitol than ^{3}H-inulin by the cerebral cortex, cerebellum, and CSF. Finally, tissue water content and residual erythrocyte volume were determined in order to calculate cell electrolyte space and concentration. Both LVCP tissue water content ($80.6 \pm 0.2\%$) and residual erythrocyte volume ($7.5 \pm 1.5\%$) were greater than 4VCP water content (79.8 ± 0.1) and erythrocyte volume (6.5 ± 1.2). Calculated epithelial cell water content was 56-60% of tissue weight for the LVCP and 58-61% for the 4VCP, exact values dependent on

Fig. 4. The uptake of ^{3}H-mannitol by the LVCP as a function of time after administration. ^{3}H-mannitol (0.5 μCi/g) was injected at various times prior to sacrifice into 4-h nephrectomized rats. LVCP radioactivity ($\Delta - \Delta$) was expressed as a space (%) = 100 x (dpm/g tissue)/(dpm/g plasma H_2O). The uptake of ^{3}H-mannitol was resolved into 1 component by subtracting the 0, 5, 10, and 15 min spaces from the steady-state space and plotting the difference (X-X). Each point represents a mean $\pm$ S.E.M. for 3 animals.

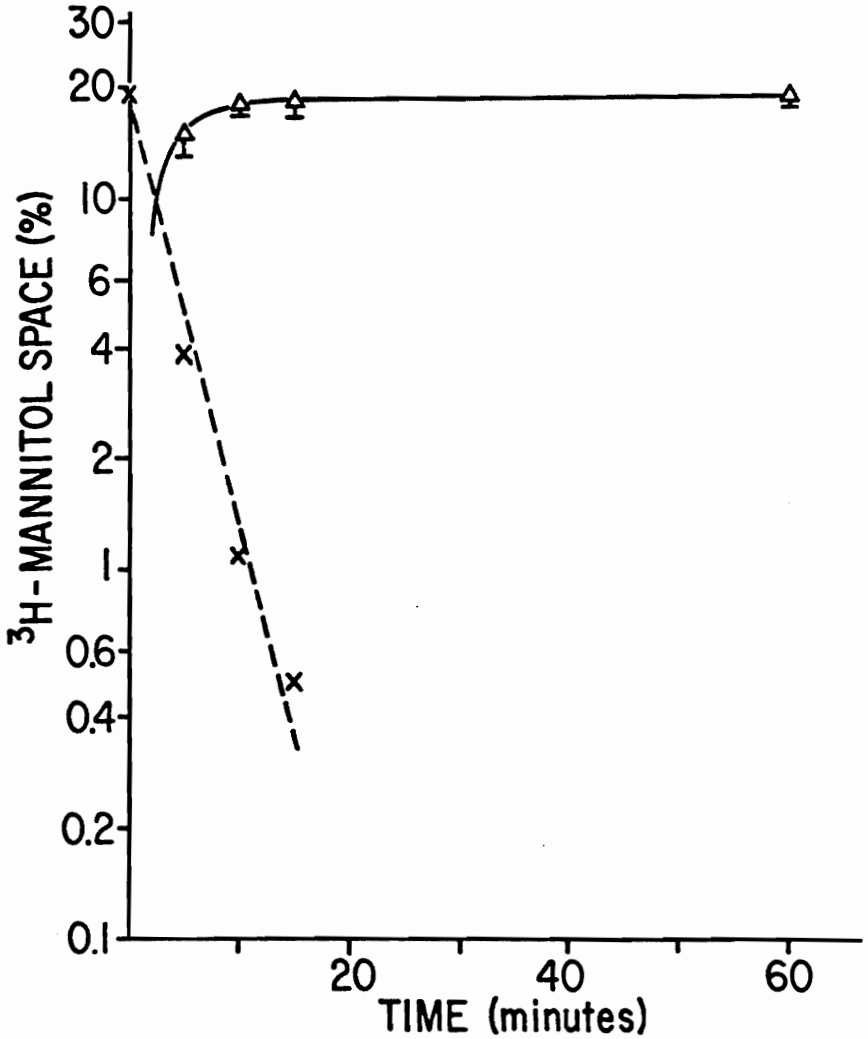
30
20
10
6
4
2
1
0.6
0.4
0.2
0.1
^{3}H-MANNITOL SPACE (%)
20
40
60
TIME (minutes)

TABLE 2. COMPARISON OF THE TISSUE VOLUME OF DISTRIBUTION OF TWO TRACERS USED TO QUANTIFY EXTRACELLULAR FLUID

TISSUE	^{3}H-mannitol space molecular weight = 182 g/mol	^{3}H-inulin space molecular weight ≈ 5500 g/mol
Lateral ventricle choroid plexus	19.1 ± 0.6*	15.8 ± 0.5
Fourth ventricle choroid plexus	17.1 ± 0.3*	14.6 ± 0.4
Cerebral cortex	2.43 ± 0.06*	1.64 ± 0.17
Cerebellum	2.86 ± 0.05*	1.98 ± 0.30
Skeletal muscle	11.2 ± 0.4	10.3 ± 0.4
Salivary gland	24.5 ± 1.1*	19.2 ± 0.4

^{3}H-mannitol or ^{3}H-inulin (0.5 μCi/g) was injected intraperitoneally into 4-h nephrectomized rats at 1 h prior to sacrifice. Tissue and CSF radioactivity was expressed as a space (%) = 100 x (dpm/g tissue)/(dpm/g plasma H_2O). Values are presented as means ± S.E.M. for N = 6 rats. *$P < 0.05$ (^{3}H-mannitol space vs. ^{3}H-inulin space) by Student's t test.

whether the ^{3}H-mannitol or ^{3}H-inulin space was utilized to estimate extracellular fluid volume.

Calculated choroid plexus cell [Na] and [Cl] are summarized in Table 3. Three methods of calculation were utilized. Two of the calculations corrected for non-epithelial cell ion and water by subtracting erythrocyte and extracellular fluid (mannitol or inulin) contributions. In the third calculation, the ^{22}Na or ^{36}Cl fast component was utilized as non-epithelial cell volume, including both extracellular and erythrocyte fractions. Generally, the three methods of calculation produce comparable ion concentrations; LVCP [Na] of 46 and [Cl] of 67 mmol/kg cell H_2O, and 4VCP [Na] of 56 and [Cl] of 67 mmol/kg cell H_2O. Though only chemical measurements of in vivo choroid plexus tissue K content were performed, the calculated LVCP and 4VCP cell [K] were 150 $\pm$ 3 and 149 $\pm$ 4 mmol/kg cell H_2O, respectively. With the Nernst equation, a calculated LVCP cell E_{Na} of +30 mV (reference: interstitial fluid) and a cell E_{Cl} of -14 mV were obtained. Similarly, for the 4VCP cell an E_{Na} of +25 and an E_{Cl} of -14 mV were calculated. Because the CSF [Na] and [Cl] were similar to the choroid plexus interstitial fluid concentrations, the E_{Na} and E_{Cl} (reference: CSF) were only a few mV different from the interstitial fluid reference values (see Fig. 5).

The uptake of ^{36}Cl and ^{22}Na into the LVCP and 4VCP cell H_2O, and the CSF, from 1/4 to 6 h after injection of the isotope is shown in Table 4. For ^{36}Cl, the LVCP, 4VCP, and CSF relative concentrations were not significantly different at any of the 6 time periods; each compartment was filled at approximately the same rate. In contrast, ^{22}Na was taken up by the 4VCP

TABLE 3. CALCULATED CHOROID PLEXUS CELL [Na] AND [Cl] USING DIFFERENT ESTIMATES OF EXTRACELLULAR AND ERYTHROCYTE VOLUME

Calculation: values used to estimate non-epithelial ion and water content	Lateral ventricle choroid plexus [Na]cell	[Cl]cell	Fourth ventricle choroid plexus [Na]cell	[Cl]cell
	(mmol/kg cell H_2O)		(mmol/kg cell H_2O)	
^{3}H-mannitol space and ^{51}Cr-erythrocyte volume	41.9 ± 2.8	67.2 ± 2.8	53.8 ± 1.3	68.4 ± 2.6
^{3}H-inulin space and ^{51}Cr-erythrocyte volume	47.8 ± 2.8	70.0 ± 2.7	57.9 ± 1.2	70.5 ± 2.4
^{22}Na or ^{36}Cl fast component volume	46.9 ± 2.3	62.4 ± 2.8	56.1 ± 0.9	63.2 ± 2.9

Choroid plexus cell [Na] or [Cl] were calculated by subtracting extracellular and erythrocyte contributions from the tissue ion content and water content according to the formula: [X] = (Xtissue - Xe - Xr)/(Vtissue - Ve - Vr) where X = Na or Cl content, V = water content, e = extracellular fluid, and r = erythrocyte. In the third calculation, ^{22}Na and ^{36}Cl fast components were used as estimates of nonepithelial electrolyte and water spaces. Values are means ± S.E.M. for N = 6 rats.

TABLE 4. RELATIVE CONCENTRATIONS OF ^{36}Cl AND ^{22}Na IN VARIOUS COMPARTMENTS AS A FUNCTION OF TIME

Compartment	Time after injection of the radioisotope (hours)					
	1/4	1/2	1	2	4	6
^{36}Cl						
Extracellular fluid	100	100	100	100	100	100
LVCP cell H_2O	30	47	55	77	95	98
4VCP cell H_2O	24	42	52	70	93	97
Cerebrospinal fluid	23	44	57	79	96	99
^{22}Na						
Extracellular fluid	100	100	100	100	100	100
LVCP cell H_2O*	2	13	22	47	75	92
4VCP cell $H_2O^{\dagger}$	12	30	58	78	94	103
Cerebrospinal fluid	26	44	55	73	92	97

^{36}Cl or ^{22}Na was injected into rats at various times prior to sacrifice. Tissues and samples were analyzed for radioactivity and the values expressed as a space (%) = 100 x (dpm/g tissue or CSF)/(dpm/g extracellular fluid). Relative concentrations (%) were obtained by expressing the value as a percent of the steady-state plateau. Choroid plexus tissue data were converted to choroid plexus cell H_2O using the compartmentation data, i.e., water content, ^{3}H-inulin space, and ^{51}Cr-tagged erythrocyte volume (see Results). Each value is expressed as a mean for N = 3 animals. Standard errors are generally < 5% of the respective means. *$P < 0.05$ (LVCP cell H_2O vs. CSF) by Student's t test. $^{\dagger}P < 0.05$ (4VCP cell H_2O vs. CSF) by Student's t test.

at a significantly greater rate than the CSF, while the LVCP was filled at a significantly slower rate than the CSF (Table 4). At each time period, the respective spaces for ^{36}Cl and ^{22}Na in CSF were statistically equivalent ($P > 0.05$).

As for the choroid plexus, tissue electrolyte and compartment values were used to calculate salivary gland and skeletal muscle cell [Cl] and [Na]. While both salivary gland and skeletal muscle cell [Na] were equal, 10 mmol/kg cell H_2O, salivary gland cell [Cl] (36 mmol/kg H_2O) was significantly greater than skeletal muscle cell [Cl] (6 mmol/kg H_2O) ($P < 0.05$). A calculated salivary gland cell E_{Cl} of -30 mV (reference: interstitial fluid) and a cell E_{Na} of +70 mV were obtained using the Nernst equation. Similarly, a cell E_{Cl} of -78 mV and a cell E_{Na} of +72 mV were determined for the skeletal muscle.

In vitro experiments

^{36}Cl and ^{3}H-inulin uptake by the in vitro LVCP and 4VCP were extremely rapid compared to the in vivo isotope uptake. Steady-state spaces of ^{36}Cl ($55.3 \pm 1.2\%$) and ^{3}H-inulin ($40.2 \pm 2.0\%$) were reached after only 1 min of exposure of the tissue to the radioisotope. The in vitro spaces obtained for the LVCP and 4VCP were not significantly different ($P > 0.05$).

Chemically determined choroid plexus (LVCP plus 4VCP) Cl content (70 ± 1 mmol/kg wet tissue) and artificial CSF [Cl] (126 ± 1 mmol/kg H_2O) result in a tissue Cl space (55.6%) equivalent to the radioisotope space (55.3%). LVCP Na content increased by 15 mmol/kg in vitro, whereas K

content decreased by 30 mmol/kg, as determined by flame photometry. However, calculation of epithelial cell electrolyte concentrations revealed that in vivo and in vitro cell [K] (150 mmol/kg cell H_2O) were not significantly different. Cell [Na] decreased from 45 to 36 mmol/kg H_2O after 30 min of in vitro incubation, though the difference was not statistically significant ($P > 0.05$). A 17 mmol/kg cell H_2O decline in cell [Cl] was observed (50 ± 4 mmol/kg H_2O) in vitro ($P < 0.05$). Thus, as noted in vivo, the in vitro choroid plexus cell was able to maintain a high E_{Cl} of -24 mV when both the K and Na gradients (cell to artificial CSF) were not significantly altered.

DISCUSSION

Calculation of intracellular choroid plexus epithelial cell [Cl] and [Na] from tissue electrolyte and water content measurements requires knowledge of the Cl and Na content and water volume of several compartments within the choroid tissue. Fortunately, the choroid plexus is a simple epithelium, consisting only of a highly vascularized connective tissue core surrounded by a single layer of cuboidal epithelial cells. Unlike more complex epithelial tissues, i.e., salivary gland, kidney, and intestine, the ependymal cells of the choroid plexus are primarily one cell type. Thus, the plexus is a convenient tissue for compartmentation of tissue electrolytes. With measurements of exchangeable ion content, extracellular space, and residual erythrocyte volume, tissue ion content can be converted to calculated choroidal epithelial cell [Cl] and [Na].

The equivalence of the chemical and radioisotope tissue spaces in the choroid plexus indicates that within the time period of the in vivo experiments (8 h), all of the tissue Cl and Na was exchangeable. Specifically, no evidence was found for an inexchangeable or "bound" fraction of Cl or Na in the LVCP or 4VCP. Furthermore, the rapid (1 min) uptake of ^{36}Cl by the in vitro choroid plexus into a space equal in volume to the chemically determined Cl space indicates that all of the choroid plexus Cl was freely exchangeable even over a short (1-3 min) time period. ABRAMOW et al. (1967) reported

that only 10% of the rabbit kidney tubule Cl did not exchange with ^{36}Cl within 90 min. Similar results were obtained by FRIZZELL et al. (1973) for ^{36}Cl uptake by the rabbit ileum. Slowly exchanging Na fractions have been reported for epithelial tissues (CIVAN, 1978); the inexchangeable fraction rarely exceeds 30% of the total Na content. In the present study, the small differences between the chemical and radioisotope CSF spaces for Na or Cl are not explicable on the basis of ion binding (^{36}Cl space > Cl space and ^{22}Na space > Na space) and are presumably attributable to evaporation by the radioisotope CSF samples. While ^{22}Na and ^{36}Cl CSF specimens had to be weighed after collection, the CSF for chemical analysis was frozen immediately upon sampling.

Extracellular, stromal, and erythrocyte contributions to choroid plexus tissue ion and water content were quantified by the volume of distribution (Vd) of ^{3}H-saccharides and ^{51}Cr-tagged erythrocytes, and by component analysis of the ^{36}Cl and ^{22}Na uptake curves. The fast components of the choroid plexus ^{36}Cl and ^{22}Na uptake curves were similar in half-time to that of the extracellular marker, ^{3}H-mannitol ($t_{1/2}$ 0.02-0.05 h). Yet, the Vd of the isotopes (^{3}H-saccharides, fast component ^{36}Cl and ^{22}Na) in the LVCP and 4VCP varied from 13-25%. In both the LVCP and 4VCP, the volumes ranged from ^{22}Na fast component (13-14%), ^{3}H-inulin space (14-16%), ^{3}H-mannitol space (17-19%), to ^{36}Cl fast component (24-25%). However, with a correction for the ^{36}Cl content of the residual erythrocytes in the choroid plexus, the ^{36}Cl fast component volume (18-19%) was not significantly different from the ^{3}H-mannitol space. Similarly, the ^{22}Na fast component Vd

(the ^{22}Na content of the residual erythrocytes was < 0.1% of the tissue ^{22}Na space) was not different statistically from the ^{3}H-inulin space. The 4% difference in Vd between the ^{3}H-mannitol and ^{3}H-inulin spaces may reflect differential penetration of the tracers into choroid plexus stromal elements. In the intestine, ^{3}H-mannitol distributes within the mucosal space whereas ^{3}H-inulin fills only a fraction of that compartment (GRIM et al., 1973). In the present study, both markers filled equivalent volumes in the skeletal muscle; however, the salivary gland ^{3}H-mannitol space (24.5%) was ~5% greater than the ^{3}H-inulin space (19.2%). If ^{3}H-mannitol distributed within the salivary gland connective tissue and ducts, regions perhaps not penetrated by ^{3}H-inulin, a 5% difference between the marker volumes would be expected (SCHNEYER et al., 1972). The estimates of QUAY (1966) of the rat ependymal cell, stromal cell, and erythrocyte volumes are consistent with a 5-10% stromal cell space. And, the high Cl content of connective tissue would lead to a larger choroid plexus Cl space than sodium space (~Δ4%). Thus, the volumes in LVCP and 4VCP of erythrocytes (7%), extracellular fluid (15%), and stroma (~4%) were obtained from the distribution of the ^{36}Cl fast component, ^{3}H-mannitol, ^{3}H-inulin, ^{22}Na fast component, and ^{51}Cr-tagged erythrocytes. Subtraction of the water volume of these compartments from the choroid plexus tissue water content (80%) would determine an epithelial cell volume of 56-60% of the wet tissue weight.

The slow component ($t_{1/2}$ 0.9-1.9 h) of the choroid plexus ^{36}Cl and ^{22}Na uptake curves undoubtedly represents radioisotope uptake by the epithelial cells. JOHANSON & WOODBURY (1978) observed similar kinetics for

the uptake of ^{14}C-urea by the rat LVCP. They attributed the slow build-up of ^{14}C-urea within the choroidal epithelium to a sieving effect in the basolateral membrane concurrent with a rapid equilibration with the CSF across the apical membrane. As shown in Table 4, the plexus ^{36}Cl and ^{22}Na cell spaces were similar to the corresponding CSF values. Evidently the choroid plexus basolateral membrane has a low permeability to Na and Cl, as for ^{14}C-urea. In contrast, both the similarity of the choroidal cell and CSF isotope spaces in vivo, and the rapid distribution of ^{36}Cl in the choroid plexus in vitro, would indicate that the apical membrane permeability of the LVCP and 4VCP to Na and Cl is considerably greater than the permeability of the basolateral membrane. A similar difference in permeabilities of the two membranes to I and K has been observed in the in vitro frog choroid plexus (WRIGHT, 1978a, b). Thus, a basolateral membrane with a low permeability to ions and small hydrophilic molecules (urea) in series with a permeable apical membrane may characterize the choroidal epithelium.

The conclusion of the preceding paragraph was reached in part by juxtaposing radioisotope activity in the choroid plexus cell to that in the CSF as sampled from the cisterna magna. Though lateral ventricle and fourth ventricle CSF isotope radioactivities were not determined directly, rat cisternal CSF may represent a reasonable approximation of the activity in the ventricular fluid. First, the agreement between the in vivo LVCP and 4VCP ^{36}Cl space as a function of uptake time (Table 4) is consistent with the rapid equilibration of ^{36}Cl between the in vitro choroid plexus and the incubation medium. A similar observation for ^{14}C-urea strengthens the conclusion (JOHANSON

& WOODBURY, 1978). Second, the difference in the rate of ^{22}Na uptake by the rat LVCP and 4VCP is not consistent with a rapid isotope equilibration within the ventricular fluid followed by a slow penetration into the cisternal CSF; the CSF $t_{1/2}$ (slow component) for ^{22}Na uptake was intermediate between the $t_{1/2}$ for uptake into the LVCP and 4VCP. This is in contrast to SWEET et al. (1950) who found ^{22}Na uptake into human ventricular CSF four times as rapid as penetration into cisternal CSF. The difference in ^{22}Na uptake by the LVCP and 4VCP in the present study probably reflects apical membrane permeability or transport differences instead of regional variation in the ventricular CSF ^{22}Na uptake rate.

Epithelial cell [Cl] and [Na] were calculated utilizing three separate estimates of nonepithelial ion and water content. As shown in Table 3, the three methods of calculation give comparable [Cl] and [Na] for the LVCP and 4VCP. Fig. 5 summarizes the ependymal cell electrolyte concentrations and potentials for the rat LVCP along with data for the interstitial and cerebrospinal fluids. Similar values were obtained for the rat 4VCP, except that the cell [Na] was 56 mmol/kg cell H_2O ($E_{Na\ interstitial}$ +25 mV and $E_{Na\ CSF}$ +27 mV). In both the LVCP and 4VCP, the E_{Cl}, Cl equilibrium potential (-14 to -15 mV), was from 35 to 50 mV more positive than the E_m, resting membrane potential, as reported for the rabbit (-50 to -65 mV) and frog (-50 mV) choroid plexuses (WELCH & SADLER, 1965; WRIGHT, 1978b). Similarly, the E_{Na} (+30 to +32 mV) for the LVCP and 4VCP was from 80 to 95 mV more positive than the resting membrane potential (JOHANSON et al., 1974). Chloride was accumulated 3.9 times that

Fig. 5. A schematic representation of the choroidal epithelium separating the interstitial and cerebrospinal fluids. In the upper half of the figure, [Na], [K], and [Cl] as determined by the compartmentation technique are shown for the interstitial fluid, LVCP cell H_2O, and CSF. In the lower half of the figure, calculated passive membrane potentials for Na, K, and Cl are indicated for both the basolateral membrane and apical membrane of the choroid epithelial cell. Literature values for the membrane potential (E_m) and transepithelial potential are included at the bottom of the figure (Welch & Sadler, 1965; Wright, 1978). For the 4VCP, K and Cl concentrations and passive membrane potentials are equivalent to those of the LVCP. However, 4VCP cell [Na] was 56 mmol/kg H_2O with a +25 mV E_{Na} across the basolateral membrane and a +27 mV E_{Na} across the apical membrane.

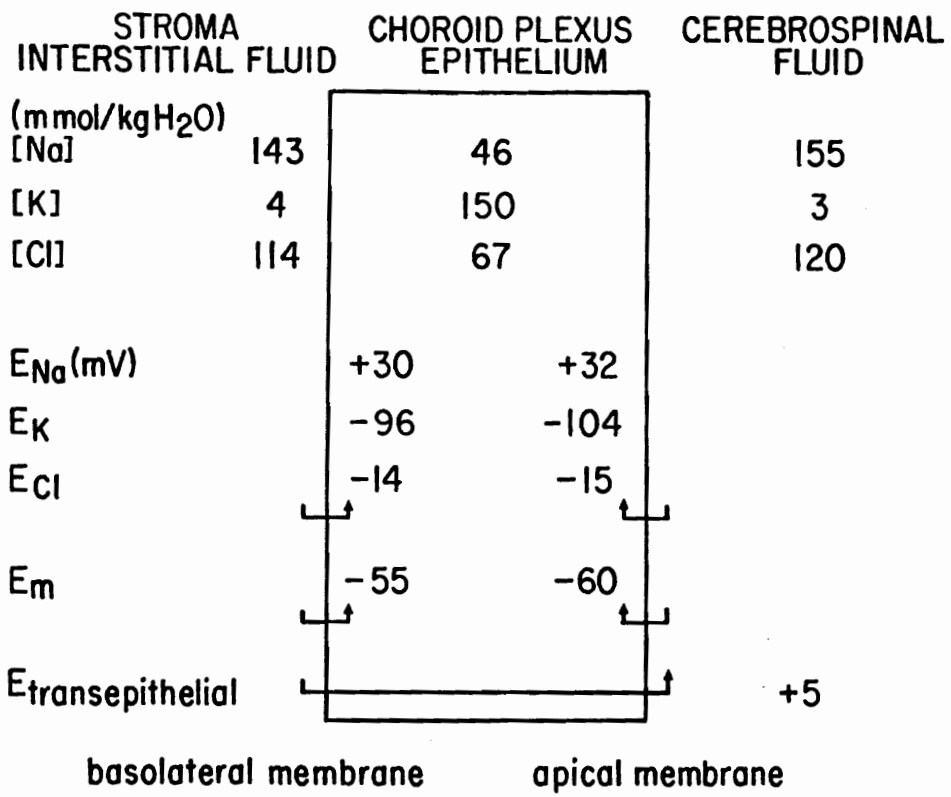
STROMA
INTERSTITIAL FLUID
CHOROID PLEXUS
EPITHELIUM
CEREBROSPINAL
FLUID
(mmol/kgH2O)
[Na]
143
46
155
[K]
4
150
3
[Cl]
114
67
120
ENa(mV)
+30
+32
EK
-96
-104
ECl
-14
-15
Em
-55
-60
Etransepithelial
+5
basolateral membrane
apical membrane

predicted for passive distribution according to the basolateral membrane potential. Comparable values for Cl accumulation have been obtained in the renal proximal tubule (2-3x), gallbladder (2.3x), and intestine (3.4x) using ^{36}Cl compartmentation, ion sensitive electrodes, and electron probe (ABRAMOW et al., 1967; FRIZZELL et al., 1973; SPRING & KIMURA, 1978; DUFFEY et al., 1978; GUPTA et al., 1978; and DUFFEY et al., 1979). The energy source for active Cl transport by the choroid plexus may be the Na electrochemical potential difference, which is 2 times that of the Cl potential difference. As proposed by FRIZZELL et al. (1979), Cl would be taken up into the choroid plexus epithelial cell across the basolateral membrane by a Na-coupled Cl cotransport mechanism. At the apical membrane, Cl would move out of the cell into the CSF along a favorable electrochemical potential gradient. Net chloride transport would be from the plasma into the CSF, as the results of HOGBEN et al. (1960) and BOURKE et al. (1970) would indicate. Further experiments are being conducted to establish both the presence of transepithelial Cl transport by the choroid plexus and the mechanism of that transport. In conclusion, evidence is presented which indicates that the choroid plexus, like other Cl transporting epithelia, accumulates Cl against a 36-50 mV electrochemical gradient.

^{36}Cl and ^{22}Na uptake into the CSF were resolved into two components, a fast component ($t_{1/2}$ 0.18 h, fractional volume 0.24) and a slow component ($t_{1/2}$ 1.2 h, fractional volume 0.76) for each isotope. Similar half-times and volumes were reported for ^{22}Na uptake into the CSF by SOLOMON (1949) and LEVIN & PATLAK (1972). ^{14}C-urea uptake into the CSF was

resolved by JOHANSON & WOODBURY (1978) into two components with $t_{1/2}$ and volumes comparable to those of ^{22}Na. As suggested by LEVIN & PATLAK (1972), the fast component probably represents isotope exchange across the blood-CSF barrier, i.e., the choroid plexuses. Further evidence which supports the localization of the CSF fast component to the choroid plexus is the fact that acetazolamide treatment (20 mg/kg) which inhibits choroid plexus fluid production by > 95% (MELBY & REED, 1978) eliminates the fast component of ^{36}Cl uptake by the rat CSF (unpublished results). Similarly, MILHORAT (1971) reported a 33% decrease in CSF production in choroid plexectomized monkeys, a comparable volume to that of the CSF fast component in the present study. The slow component may represent isotope exchange primarily from brain extracellular fluid into the CSF. ^{36}Cl and ^{22}Na uptake rate constants for the CSF obtained during ventriculo-cisternal perfusion experiments (~0.9 h) (VOGH & MAREN, 1975) are comparable to the slow compartment rate constants (~0.8 h) obtained in the present study. Acetazolamide treatment decreases CSF flow 50% as measured by ventriculo-cisternal perfusion, suggesting that a considerable fraction of the CSF (~50%) originates from extrachoroidal sources (BOURKE & NELSON, 1972b). Thus, based on kinetic data, fractional volumes and rate constants can be measured for ^{36}Cl and ^{22}Na entry into the CSF from choroidal and extrachoroidal sites.

Salivary gland and skeletal muscle cell $[Cl]$ and $[Na]$ compare favorably with literature values (SCHNEYER et al., 1972; JOHANSON et al., 1974; WILLIAMS et al., 1971). In contrast to the choroid plexus, E_{Cl} and E_m were in close agreement in the salivary gland and skeletal muscle, which

would predict a passive distribution of Cl in these tissues. However, the possibility of active Cl transport by the salivary gland cannot be excluded due to the heterogeneous cell population of that tissue, i.e., 70% acinar cells and 30% duct cells (SCHNEYER et al., 1972). The uniform epithelial cell population of the choroid plexus simplifies the interpretation of compartment data and makes the utilization of the compartmentation technique a valid procedure for determining cell electrolytes.

REFERENCES

ABBOTT J., DAVSON H., GLEN I. & GRANT N. (1971) Chloride transport and potential across the blood-CSF barrier. Brain Res. 29, 185-193.

ABRAMOW M., BURG B. & ORLOFF J. (1967) Chloride flux in rabbit kidney tubules in vitro. Am. J. Physiol. 213, 1249-1253.

BOURKE R.S., GABELNICK H.L. & YOUNG O. (1970) Mediated transport of chloride from blood into cerebrospinal fluid. Exp. Brain Res. 10, 17-38.

BOURKE R.S. & NELSON K.M. (1972a) Further studies on the K-dependent swelling of primate cerebral cortex in vivo: The enzymatic basis of the K-dependent transport of chloride. J. Neurochem. 19, 663-685.

BOURKE R.S. & NELSON K.M. (1972b) Studies on the site of mediated transport of chloride from blood into cerebrospinal fluid: Effects of acetazolamide. J. Neurochem. 19, 1225-1232.

CIVAN M.M. (1978) Intracellular activities of sodium and potassium. Am. J. Physiol. 234, F261-F269.

COLE D.F. (1977) Secretion of the aqueous humor. Exp. Eye Res. Suppl., 161-176.

DUFFEY M.E., THOMPSON S.M., FRIZZELL R.A. & SCHULTZ S.G. (1979) Intracellular chloride activites and active chloride absorption in the intestinal epithelium of the winter flounder. J. Membrane Biol. 50, 331-341.

DUFFEY M.E., TURNHEIM K., FRIZZELL R.A. & SCHULTZ S.G. (1978) Intracellular chloride activities in rabbit gallbladder: Direct evidence for the role of the sodium-gradient in energizing "uphill" chloride transport. J. Membrane Biol. 42, 229-245.

FERGUSON R.K. & WOODBURY D.M. (1969) Penetration of ^{14}C-inulin and ^{14}C-sucrose into brain, cerebrospinal fluid, and skeletal muscle of developing rats. Exp. Brain Res. 7, 181-194.

FRIZZELL R.A., FIELD M. & SCHULTZ S.G. (1979) Sodium-coupled chloride transport by epithelial tissues. Am. J. Physiol. 236, F1-F8.

FRIZZELL R.A., NELLANS H.N., ROSE R.C., MARKSCHEID-KASPI L. & SCHULTZ S.G. (1973) Intracellular Cl concnetrations and influxes across the brush border of rabbit ileum. Am. J. Physiol. 224, 328-337.

GILL T.H., YOUNG O.M. & TOWER D.B. (1974) The uptake of ^{36}Cl into astrocytes in tissue culture by a potassium-dependent saturable process. J. Neurochem. 23, 1011-1018.

GRIM E., SIMONDS, A., OELJEN C. & CHENG J. (1973) Inulin and mannitol distribution volumes in canine small intestinal tissues in vivo. Am. J. Physiol. 224, 186-190.

GUPTA B.L., HALL T.A. & NAFTALIN R.J. (1978) Microprobe measurement of Na, K and Cl concentration profiles in epithelial cells and intercellular spaces of rabbit ileum. Nature 272, 70-73.

HOGBEN C.A.M., WISTRAND P. & MAREN T.H. (1960) Role of active transport of chloride in formation of dogfish cerebrospinal fluid. Am. J. Physiol. 199, 124-126.

JOHANSON C.E., REED D.J. & WOODBURY D.M. (1974) Active transport of sodium and potassium by the choroid plexus of the rat. J. Physiol., Lond. 241, 359-372.

JOHANSON C.E., REED D.J. & WOODBURY D.M. (1976) Developmental studies of the compartmentalization of water and electrolytes in the choroid plexus of the neonatal rat brain. Brain Res. 116, 35-48.

JOHANSON C.E. & WOODBURY D.M. (1978) Uptake of [^{14}C]urea by the in vivo choroid plexus-cerebrospinal fluid-brain system: identification of sites of molecular sieving. J. Physiol., Lond. 275, 167-176.

KIMELBURG H.K., BIDDLECOME S. & BOURKE R.S. (1979) SITS-inhibitable Cl transport and Na-dependent H production in primary astroglial cultures. Brain Res. 173, 111-124.

LEVIN V. & PATLAK C.S. (1972) A compartmental analysis of ^{24}Na kinetics in rat cerebrum, sciatic nerve and cerebrospinal fluid. J. Physiol., Lond. 224, 559-561.

MAREN T.H. & BRODER L.E. (1970) The role of carbonic anhydrase in anion secretion into the cerebrospinal fluid. J. Pharmacol. exp. Ther. 172, 197-202.

MELBY J. & REED D.J. (1978) Effect of acetazolamide and furosemide on CSF production by cat choroid plexus in situ. Soc. Neurosci. Abstr. 7, 246.

MILHORAT T.H., HAMMOCK M.K., FENSTERMACHER J.D., RALL D.P. & LEVIN V.A. (1971) Cerebrospinal fluid production by the choroid plexus and brain. Science, N.Y. 173, 330-332.

MINER L.C. & REED D.J. (1972) Composition of fluid obtained from choroid plexus tissue isolated in a chamber in situ. J. Physiol., Lond. 227, 127-139.

QUAY N.B. (1966) Regional differences in metabolism and composition of choroid plexuses. Brain Res. 2, 378-389.

SCHNEYER L.H., YOUNG J.A. & SCHNEYER C.A. (1972) Salivary secretion of electrolytes. Physiol. Rev. 52, 720-777.

SOLOMON A.K. (1949) Equations for tracer experiments. J. Clin. Invest. 28, 1297-1307.

SPRING K.R. & KIMURA G. (1978) Chloride reabsorption by renal proximal tubules of necturus. J. Membrane Biol. 38, 233-254.

SWEET W.H., SELVERSTONE B. & SOLOWAY S. (1950) Studies on formation, flow and absorption of cerebrospinal fluid. II. Studies with heavy water in normal man, in American College of Surgeons Surgical Forum, pp. 376-381. W.B. Saunders Co., Philadelphia.

VOGH B.P. & MAREN T.H. (1975) Sodium, chloride, and bicarbonate movement from plasma to cerebrospinal fluid in cats. Am. J. Physiol. 228, 673-683.

WELCH K. & SADLER K. (1965) Electrical potentials of choroid plexus of the rabbit. J. Neurosurg. 22, 344-351.

WILLIAMS J.A., WITHROW C.D. & WOODBURY D.M. (1971) Effects of ouabain and diphenylhydantoin on transmembrane potentials, intracellular electrolytes, and cell pH of rat muscle and liver in vivo. J. Physiol., Lond. 213, 101-115.

WOODBURY D.M. (1967) Distribution of nonelectrolytes and electrolytes in the brain as affected by alterations in cerebrospinal fluid secretion, in Progress in Brain Research (LAJTHA A. & FORD D.H., eds.), Vol. 29, pp. 297-313. Elsevier Publ. Co., Amsterdam.

WRIGHT E.M. (1972) Mechanisms of ion transport across the choroid plexus. J. Physiol., Lond. 226, 545-571.

WRIGHT E.M. (1978a) Anion transport by choroid plexus epithelium, in Membrane Transport Processes (HOFFMAN J.F., ed.), pp. 293-307. Raven Press, New York.

WRIGHT E.M. (1978b) Transport processes in the formation of the cerebrospinal fluid. Rev. Physiol. Biochem. Pharmacol. 83, 1-34.

PART TWO

UPTAKE OF CHLORIDE–36 AND SODIUM–22 BY THE BRAIN-CEREBROSPINAL FLUID SYSTEM: COMPARISON OF THE PERMEABILITY OF THE BLOOD-BRAIN AND BLOOD-CSF BARRIERS

INTRODUCTION

The slow rate of ^{36}Cl and ^{22}Na uptake from the blood into the brain has been interpreted to indicate the presence of a barrier between the blood and the brain extracellular space (MANERY & BALE, 1941; MANERY & HAEGE, 1941). The anatomical substrate of the blood-brain and blood-CSF barriers has been attributed to the zonulae occludentes between the endothelial cells of cerebral capillaries (blood-brain barrier) and the epithelial cells of the choroid plexus (blood-CSF barrier) (BRIGHTMAN & REESE, 1969). Thus, ^{36}Cl or ^{22}Na movement into the CNS would be a function of barrier permeability (transcellular and paracellular) to the isotope and the rate of transport of the isotope across the barrier (FENSTERMACHER, 1975). Transport of Na has been demonstrated at the choroidal epithelium (WRIGHT, 1972) and at the cerebral capillary endothelium (EISENBERG & SUDDITH, 1979). While a number of studies have examined ^{36}Cl and/or ^{22}Na uptake into brain tissue (DAVSON, 1955; REED et al., 1964; VERNADAKIS & WOODBURY, 1965), there is a paucity of data on regional uptake of isotopes into the CNS. LUCIANO (1968) obtained autoradiographic evidence for heterogeneity in ^{22}Na uptake into the brain tissue. Furthermore, BOULDIN & KRIGMAN (1975) found the choroid epithelial zonulae occludentes more permeable to La than were the cerebral capillary junctions, suggesting that the choroid plexus is a "leaky" epithelium as compared to the "tight" cerebral

capillaries. Thus, considerable evidence exists for differential movement of ^{22}Na or ^{36}Cl across not only the blood-brain and blood-CSF barriers but also across various areas of the blood-brain barrier itself.

To determine analytically the regional differences in barrier permeability, we analyzed ^{36}Cl, ^{22}Na, and ^{3}H-mannitol uptake into the cerebral cortex gray matter, cerebellum, cisternal CSF, and choroid plexuses (lateral and fourth ventricle). The experimental design enabled a comparison of the relative permeability of each region of the barrier to the three isotopes. Furthermore, with estimates of surface area from other studies, the permeability of the blood-brain and blood-CSF barriers was compared. Lastly, the compartmental distribution of Cl and Na in the CNS (extracellular, neuronal, and glial) was examined, including an in vivo determination of the brain extracellular space.

MATERIALS AND METHODS

The experimental protocol, methods, and materials are described fully in the preceding paper of this dissertation (see PART ONE). Briefly, three series of experiments were conducted on Sprague-Dawley rats (90-110 g) nephrectomized under ether anesthesia 4 h prior to the time samples were taken. In the first series, ^{36}Cl and ^{22}Na uptake into regions of the CNS were measured from 1/12 to 8 h after injection in 54 rats (27 for ^{36}Cl and 27 for ^{22}Na). Similarly, ^{3}H-mannitol uptake was analyzed from 1/12 to 1 h after injection in 12 rats. In the second series, the chemically determined Cl and Na contents were measured utilizing amperometric titration of Ag and flame photometry (12 rats). Lastly, in the third series, the tissue water content, ^{3}H-mannitol space (1 h), ^{3}H-inulin space (1 h), and ^{51}Cr-tagged erythrocyte volume (10 min) were determined for analysis of tissue compartments.

Radioisotope volumes of distribution or spaces (^{36}Cl, ^{22}Na, and ^{3}H) were calculated using the formula: Space (%) = 100 x (dpm/g tissue or CSF)/(dpm/g plasma H_2O x D.F.) where D.F. represents the appropriate Donnan factor. For the residual erythrocyte volume (^{51}Cr), the denominator of the calculation was adjusted from (dpm/g plasma H_2O x D.F.) to (dpm/g erythrocytes). Uptake curves were resolved into components (generally 2) by a modification of the method of graphical analysis (SOLOMON, 1949). From such

analysis, component rate constants (k) and volumes of distribution (Vd) were obtained; permeability surface-area products (PA) were calculated either as PA = (k x Vd)/100 (BRADBURY & CROWDER, 1976), or as PA = initial slope of the curve of isotope space versus time (Fig. 9) (BRADBURY, 1979). Finally, glia cell ion concentrations were determined using the formula:

$$[X] = \frac{(X)\text{tissue} - (X)n - (X)e - (X)\text{res}}{V\text{tissue} - Vn - Ve - V\text{res}}$$ where (X) = Na or Cl content (mmol/kg),

V = fractional volume of water, n = neuronal, e = extracellular, and res = rapidly equilibrating space.

RESULTS

As noted in the preceding paper (see PART ONE), regression analysis of plasma radioactivity as a function of time yielded a slope which was not significantly different from 0 for either ^{36}Cl ($P = 0.28$), ^{22}Na ($P = 0.47$), or ^{3}H-mannitol ($P = 0.54$). Furthermore, the standard deviation of the plasma activity was 7% of the mean activity for all three isotopes. Thus, the following results were analyzed and interpreted on the basis of a stable plasma level of isotope.

In Fig. 6, curves for tracer uptake into the cerebral cortex, cerebellum, and CSF are shown for ^{36}Cl (left-hand side) and ^{22}Na (right-hand side). For both isotopes, a steady-state distribution in the cerebral cortex was not reached until ~8 h after injection. ^{36}Cl and ^{22}Na penetrated into the cerebellum at a faster rate, attaining a steady-state level after ~5 h. Steady-state spaces equivalent in magnitude were obtained with radioisotope and chemical techniques. For example, the chemically determined cerebral cortex Cl content (31.5 ± 0.9 mmol/kg) and Na content (47.1 ± 0.3 mmol/kg) and the chemically determined cerebellum Cl content (30.6 ± 0.7 mmol/kg) and Na content (45.9 ± 0.4 mmol/kg) were measured. Conversion to a "space" with the extracellular fluid [Cl] = 114 ± 1 mmol/kg H_2O and [Na] = 143 ± 1 produced values not significantly different from the isotope steady-state spaces of Table 5. As for the brain tissue, ^{36}Cl and ^{22}Na attained a

Fig. 6. The uptake of ^{36}Cl and ^{22}Na into the cerebral cortex, cerebellum, and CSF as a function of time after administration. The left-hand portion of the figure represents ^{36}Cl penetration into the CNS and the right-hand portion represents ^{22}Na movement into the CNS. Either ^{36}Cl or ^{22}Na (0.1 μCi/g) was injected at various times prior to sacrifice into 4-h nephrectomized rats. Tissue radioactivity was expressed as a space (%) = 100 x (dpm/g tissue or CSF)/(dpm/g extracellular fluid). Each point represents a mean $\pm$ S.E.M. for 3 animals.

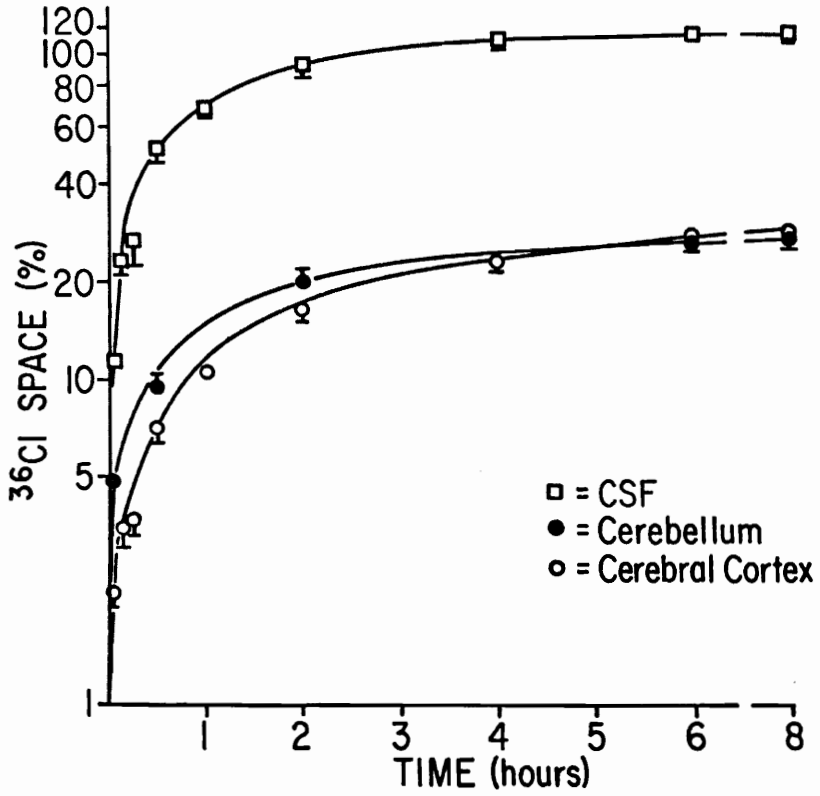
120
100
80
60
40
20
10
5
1
^{36}Cl SPACE (%)
1
2
3
4
5
6
8
TIME (hours)
□ = CSF
● = Cerebellum
○ = Cerebral Cortex

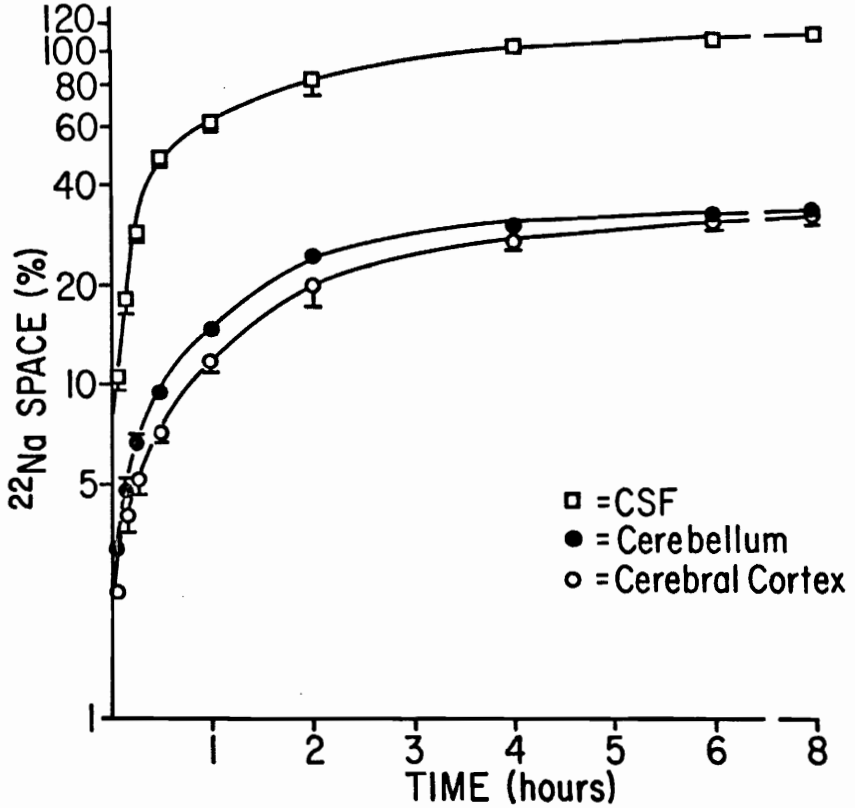
120
100
80
60
40
20
10
5
1
^{22}Na SPACE (%)
1
2
3
4
5
6
8
TIME (hours)
□ =CSF
● = Cerebellum
○ = Cerebral Cortex

TABLE 5. ANALYSIS OF COMPONENTS OF ^{36}Cl AND ^{22}Na UPTAKE CURVES

Compartment	Isotope	Fast component			Slow component			Steady-state isotope space (%)
		$t_{1/2}$ (h)	Vd (%)	fractional volume	$t_{1/2}$ (h)	Vd (%)	fractional volume	
Cerebral cortex	^{36}Cl	0.03	1.0	0.04	1.69 (1.44-2.04)	27.0 (25.2-28.9)	0.96	28.0 (27.2-28.8)
	^{22}Na	0.02	1.4	0.04	1.55 (1.33-1.84)	31.0 (29.0-33.3)	0.96	32.4 (31.1-33.7)
Cerebellum	^{36}Cl	0.05	2.1	0.08	1.05 (0.78-1.59)	24.3 (19.3-31.9)	0.92	26.4 (25.9-26.9)
	^{22}Na	0.02	1.3	0.04	1.11 (1.04-1.18)	31.4 (30.4-32.4)	0.96	32.7 (31.9-33.5)
Cerebrospinal fluid	^{36}Cl	0.19 (0.11-0.40)	25.7 (17.2-37.4)	0.22	1.06 (0.93-1.23)	91.0 (73.7-112.6)	0.78	116.7 (114.4-119.0)
	^{22}Na	0.18 (0.15-0.21)	28.9 (25.6-32.6)	0.26	1.31 (1.17-1.49)	82.9 (65.6-104.6)	0.74	111.8 (109.5-114.1)

Radioisotope uptake curves were resolved into components by the method of graphical analysis and fitted to straight lines by linear regression. The $t_{1/2}$, half-time, was obtained by dividing ln 2 by the slope (k) of the regression line. Vd, volume of distribution, was calculated as the exp (y-intercept of the regression line). The fractional volume is the Vd expressed as a fraction of the asymptote (steady-state plateau) of the uptake curve. Values in parentheses are the 95% confidence limits for the parameter.

steady-state distribution in the CSF after ~6 h; the respective CSF isotope spaces (Table 5) were comparable to the chemical Cl (105.3%) and Na (108.5%) spaces. Although radio-K uptake was not analyzed, the chemically determined K contents of the cerebral cortex, cerebellum, CSF, and extracellular fluid were 100.3 ± 1.2, 99.7 ± 1.0, 3.1 ± 0.1, and 4.1 ± 0.1 mmol/kg, respectively.

The components of the isotope uptake curves are summarized in Table 5 for the cerebral cortex, cerebellum and CSF. Uptake into the cerebral cortex and cerebellum resolved into 2 components; a fast component ($t_{1/2}$ 0.02-0.05 h) and a slow component ($t_{1/2}$ 1.1-1.7 h). The slow component volume represented 92-96% of the total ^{36}Cl or ^{22}Na space. The ^{36}Cl and ^{22}Na slow component $t_{1/2}$ were not significantly different from each other in either the cerebral cortex or cerebellum. However, the average (^{36}Cl, ^{22}Na) cerebellum slow component $t_{1/2}$ (1.1 h) was significantly less than that for the cerebral cortex (1.6 h). The CSF radioisotope uptake curves were resolved into 2 components; for ^{36}Cl, the CSF slow component $t_{1/2}$ was comparable to the cerebellum slow component $t_{1/2}$; whereas, the ^{22}Na CSF $t_{1/2}$ (1.31 h) was intermediary between the cerebral cortex (1.55) and the cerebellum (1.11) $t_{1/2}$.

Because of the slow movement of both ^{36}Cl and ^{22}Na from plasma into the CNS, the CSF isotope activity represents a better measure of the activity in the fluid bathing the brain cells than does the plasma. If ^{36}Cl and ^{22}Na distributed mainly into the brain extracellular space at early uptake times, then the initial slope of the brain activity/CSF activity would estimate the

extracellular volume of the brain. A graph of the ^{36}Cl cerebral cortex space (corrected for the fast component volume) as a function of the CSF space is shown in Fig. 7. The initial slope (extracellular space) for the cerebral cortex was 12.6 ± 1.3% for ^{36}Cl and 14.2 ± 1.1% for ^{22}Na. Similarly, the initial slope for the cerebellum was 11.8 ± 1.5% for ^{36}Cl and 14.4 ± 1.7% for ^{22}Na.

In order to calculate cell ion concentrations within the CNS, the tissue water content, ^{3}H-inulin space (1 h), and ^{51}Cr-tagged erythrocyte volume were measured. The cerebellum water content (79.2 ± 0.1%) tended to be greater than that of the cerebral cortex (78.8 ± 0.2%). A similar trend was observed in the ^{3}H-inulin space (1 h) in cerebellum (2.0 ± 0.7) and cerebral cortex (1.6 ± 0.4%), and in the ^{51}Cr-erythrocyte volume, cerebellum (0.9 ± 0.1) and cerebral cortex (0.5 ± 0.1%). The ^{3}H-inulin spaces for the cerebral cortex and cerebellum were comparable to the ^{36}Cl or ^{22}Na fast component volumes (Table 5).

Cerebral cortex and cerebellum cell ion concnetrations were determined by subtracting fast component and extracellular contributions from the tissue electrolyte and water contents. Cell [Na], [K], and [Cl] were calculated as 34 ± 2, 156 ± 4, and 22 ± 2 mmol/kg cell H_2O for the cerebral cortex and 33 ± 3, 156 ± 3, and 18 ± 2 for the cerebellum, respectively. Further compartmentation into neuronal and glial cell concentrations required estimates of relative neuronal/glial cell volume and the concentration of the ion in one of the two cell compartments. HERTZ (1977) and POPE (1978) have estimated the volume ratio of neurons to glia in the cerebral cortex at ~2/1.

Fig. 7. The uptake of ^{36}Cl by the cerebral cortex as a function of the uptake of ^{36}Cl by the CSF. The initial slope of the curve is an estimate of the cerebral cortex extracellular fluid volume. ^{36}Cl (0.1 μCi/g) was injected into 4-h nephrectomized rats at various times prior to sacrifice. Cerebral cortex and CSF activity were expressed as a space (%) = 100 x (dpm/g cerebral cortex or CSF)/(dpm/g extracellular fluid). For each time point, the cerebral cortex and corresponding CSF ^{36}Cl space were plotted. The initial slope was determined by linear regression. Each point represents a mean for 3 animals.

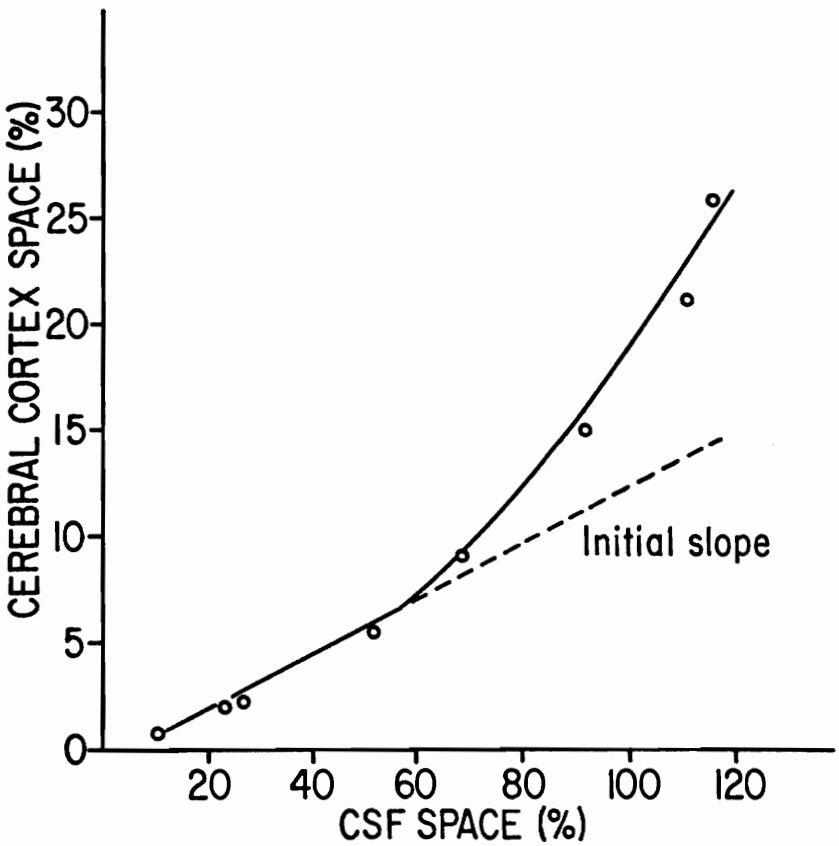
CEREBRAL CORTEX SPACE (%)
0
5
10
15
20
25
30
20
40
60
80
100
120
CSF SPACE (%)
Initial slope

And, the Cl distribution across the mammalian neuronal membrane is generally considered to be passive, i.e., $E_{Cl} = E_m \approx -70$ mV (KATZMAN & PAPPIUS, 1973). Fig. 8 is a schematic of Cl distribution within the cerebral cortex, cerebellum, and CSF based on a neuronal/glial cell volume of 2/1 and a passive distribution of Cl within the neuronal cells ($[Cl] = 10$ mmol/kg cell H_2O). For the cerebral cortex, decreasing the neuronal/glial volume ratio from 3/1, 2/1, 1/1, to 1/2 would determine a glial cell $[Cl]$ of 58, 46, 34, and 28 mmol/kg cell H_2O, respectively. Over the same neuronal/glial volume range, the cerebellum glial cell $[Cl]$ varies from 45, 36, 27 to 23 mmol/kg cell H_2O. Thus, Cl would appear to be accumulated within glial cells to a level 2-6 times that in neuronal cells.

Permeability surface-area products (PA) were determined directly as the initial slope of the isotope space versus time plot (as shown in the upper-half of Fig. 9 for ^{36}Cl uptake into the cerebral cortex), or indirectly as the product of the rate constant and the volume of distribution of a component (as shown in the lower-half of Fig. 9 for the resolved ^{36}Cl uptake curve for the cerebral cortex). Both techniques yielded comparable PA values for ^{36}Cl and ^{22}Na uptake into the various regions of the CNS. However, the precision of the second technique was greater ($\sim$2x) due to larger numbers of points that could be included in the analysis (4 time points were utilized in the upper-half analysis of Fig. 9 compared to 8 points in the lower-half). Furthermore, the indirect technique produced PA values for both components of ^{36}Cl or ^{22}Na uptake into the CSF. Thus, the PA values for ^{36}Cl and ^{22}Na, as calculated from the component analysis, are summarized in Table 6

Fig. 8. Schematic representation of chloride distribution within the cerebral cortex, cerebellum, and CSF. Values for the Cl content of tissues and fluid were obtained from the steady-state distribution of ^{36}Cl. The extracellular fluid (ECF) volume of the cerebral cortex and cerebellum were obtained from the initial slope of the brain tissue space/CSF space curve (Fig. 2). The [Cl] of the ECF was taken to be similar to that of the CSF. A neuronal cell volume twice that of the glial cell volume was assumed (Hertz, 1977; Pope, 1978). Lastly, a passive distribution (E_m = -70 mV) of Cl was utilized to calculate neuronal cell [Cl]. Glial cell [Cl] was determined by subtraction of extracellular and neuronal cell contributions to tissue Cl and water content. Volume was expressed as a percent of tissue wet weight; [Cl] concentration was reported as mmol/kg H_2O. Each value represents a mean for 6 or more animals.

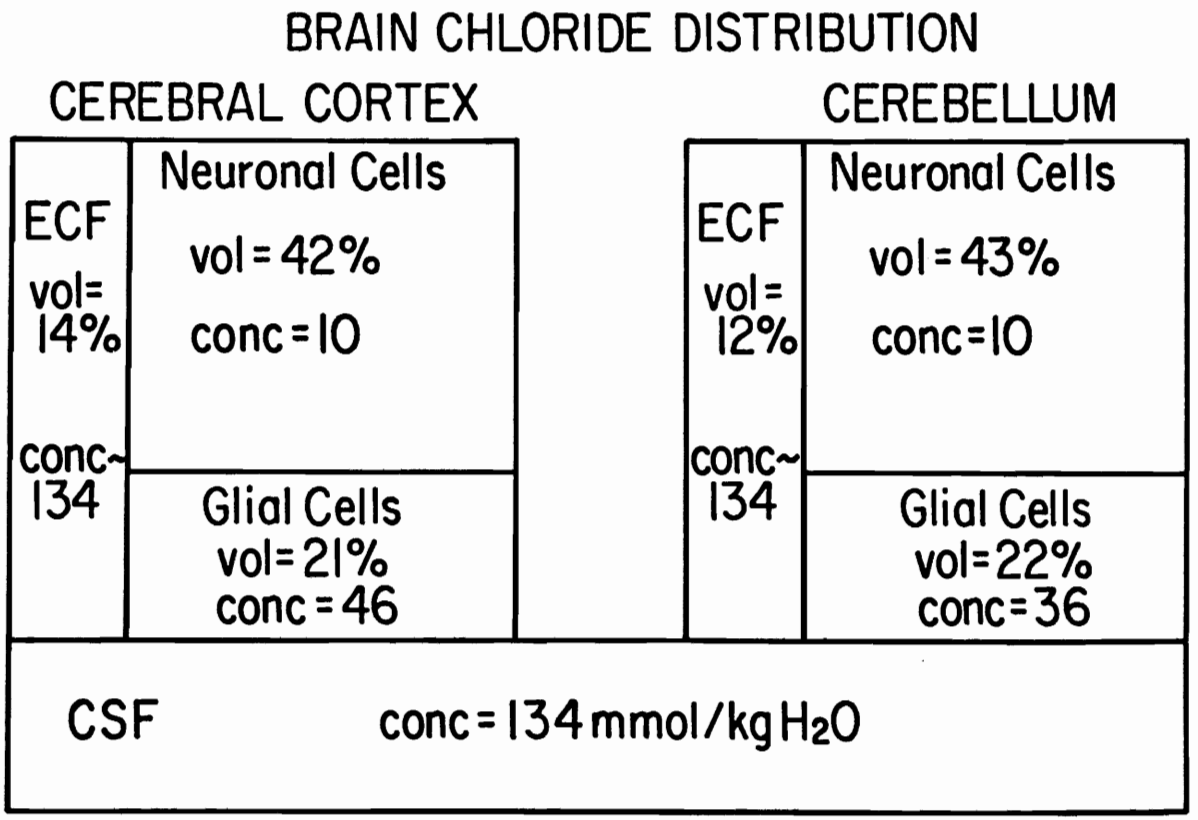
BRAIN CHLORIDE DISTRIBUTION
CEREBRAL CORTEX
CEREBELLUM
ECF
vol=
14%
conc~
134
Neuronal Cells
vol=42%
conc=10
Glial Cells
vol=21%
conc=46
ECF
vol=
12%
conc~
134
Neuronal Cells
vol=43%
conc=10
Glial Cells
vol=22%
conc=36
CSF
conc=134 mmol/kg H2O

Fig. 9. Two graphical methods for determining the permeability surface-area product (PA) for ^{36}Cl uptake into the cerebral cortex. In the upper-half of the figure, the cerebral cortex ^{36}Cl space was plotted as a function of time after ^{36}Cl administration. The initial slope (PA) of the curve was determined by linear regression. In the lower-half of the figure, the slow component was resolved by graphical analysis and a rate constant (k) was determined by linear regression. Then, the rate constant was converted to PA by the formula: $PA = k \times Vd/100$, where Vd (%) represents the volume of distribution of the component.

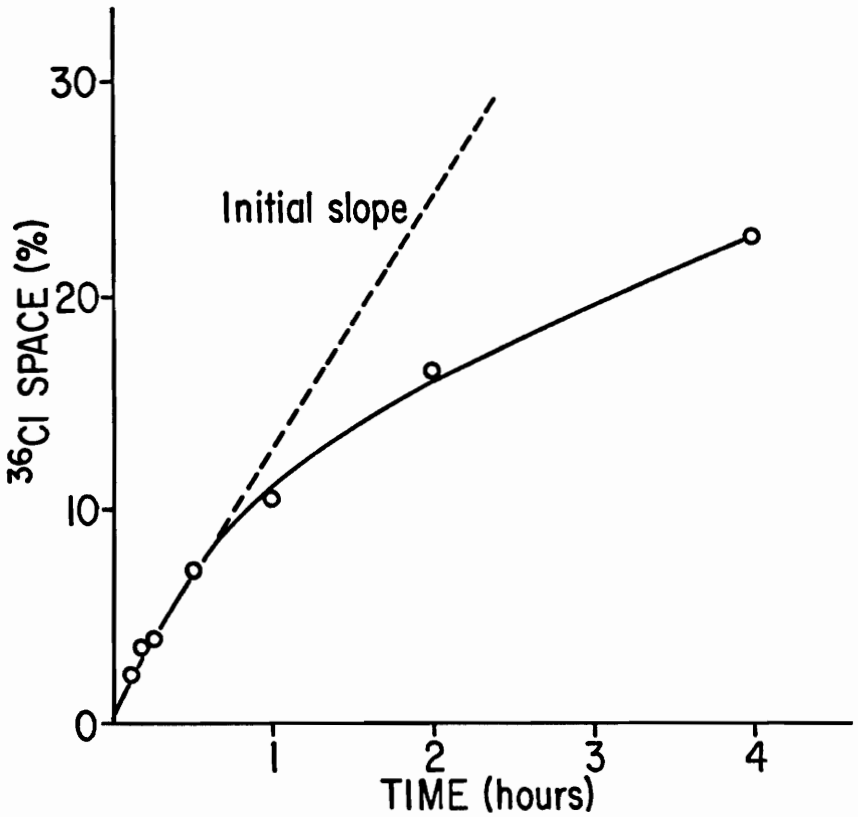
30
20
10
0
Initial slope
^{36}Cl SPACE (%)
1
2
3
4
TIME (hours)

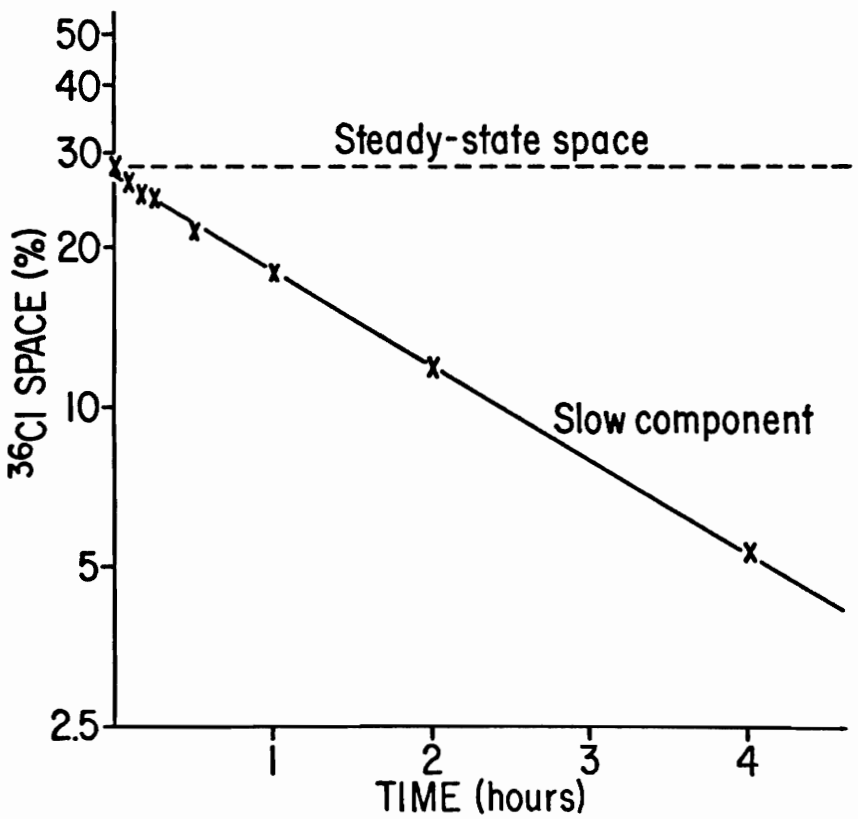
50
40
30
20
10
5
2.5
Steady-state space
Slow component
^{36}Cl SPACE (%)
1
2
3
4
TIME (hours)

for the slow components of the cerebral cortex, cerebellum, and choroid plexus of the lateral as well as the fourth ventricle; PA values for the fast and slow components of radioisotope uptake into the CSF are included for comparison. The unidirectional influx was calculated as the product of the PA and extracellular fluid ion concentration (Table 6). PA values for the cerebral cortex, cerebellum, and choroid plexuses ranged from 0.08 to 0.21 ml/h/g, while the CSF fast component PA was 5-10 times that of the tissue values. Na influx into the CNS was at least a third greater than Cl influx except for the lateral ventricle choroid plexus and CSF slow component. For the CSF fast component, the Cl and Na unidirectional influx were reasonable estimates of the CSF ion concentrations, i.e., $\lceil Cl \rceil = 117$ and $\lceil Na \rceil = 155$ mmol/kg H_2O. For comparison, permeability surface-area products for ^3H-mannitol, as determined from the initial slope of the uptake curves (Fig. 9), were 0.0098 (cerebral cortex), 0.0120 (cerebellum), and 0.0212 (fast component CSF) ml/h/g.

TABLE 6. PERMEABILITY SURFACE-AREA PRODUCT AND UNIDIRECTIONAL INFLUX FOR ^{36}Cl AND ^{22}Na UPTAKE INTO THE CNS

Compartment	^{36}Cl		^{22}Na	
	Permeability surface-area product (ml/h/g)	Unidirectional influx (mmol/h/kg)	Permeability surface-area product (ml/h/g)	Unidirectional influx (mmol/h/kg)
Cerebral cortex	0.111 ± 0.006	12.7	0.139[t] ± 0.009	19.9
Cerebellum	0.161 ± 0.027	18.4	0.196 ± 0.004	28.0
Cerebrospinal fluid (fast component)	0.944 ± 0.202*	107.6	1.150 ± 0.107*	164.5
Cerebrospinal fluid (slow component)	0.597 ± 0.046*	68.1	0.439 ± 0.031[t]	62.8
Lateral ventricle choroid plexus	0.206 ± 0.044*	23.5	0.079 ± 0.009*[t]	11.3
Fourth ventricle choroid plexus	0.164 ± 0.029	18.7	0.213 ± 0.021*	30.5

Component rate constants were converted to permeability surface-area products by the formula: PA = k x Vd/100. Unidirectional influx was determined by multiplying the PA by the ion concentration in the extracellular fluid. For tissues, only data for the slow component is presented. Values represent a mean + S.E.M. *$P < 0.05$ (compartment vs. cerebral cortex for either ^{36}Cl or ^{22}Na). [t]$P < 0.05$ (compartment ^{36}Cl PA vs. ^{22}Na PA).

DISCUSSION

Compartment analysis of isotope uptake into brain tissue and CSF was utilized to determine the rate of exchange across the blood-brain and blood-CSF barriers. Due to the heterogeneity of ^{22}Na penetration into the CNS (LUCIANO, 1968), an analysis by region rather than by whole brain was performed. Furthermore, the uptake of three radioisotopes (^{36}Cl, ^{22}Na, and ^{3}H-mannitol) was examined in order to obtain a comparative indication of influx across the two CNS barriers.

^{36}Cl and ^{22}Na uptake into the cerebral cortex (gray matter) and cerebellum were resolved by graphical analysis into two components. The fast component ($t_{1/2}$ 0.02-0.05 h, fractional volume 0.04-0.08) is comprised of the vascular compartment (~1%) and a small perivascular space (0-2%) (ŠTULC, 1967; LEVIN & PATLAK, 1972). A comparable volume for the total vascular and perivascular space was observed after the 1-h distribution of ^{3}H-inulin in the cerebral cortex (1.6%) and cerebellum (2.0%). The anatomical location of the perivascular space is presently unknown; however, BRADBURY (1979) has proposed that the perivascular space may represent the space between the brain capillary endothelium and the astrocytic lining of the capillary or may represent the capillary endothelium itself.

The slow component ($t_{1/2}$ 1.1-1.7 h, fractional volume 0.92-0.96) represents isotope movement across the blood-brain barrier into the brain

extracellular and cellular compartments. While there is a paucity of data on regional ^{22}Na or ^{36}Cl uptake into the CNS, the 1.6 h ^{22}Na $t_{1/2}$ for the rat cerebral cortex gray matter compares favorably with the corresponding 2.0 h $t_{1/2}$ reported by LEVIN & PATLAK (1972) for the same species. Furthermore, the 1.1-1.7 $t_{1/2}$ for ^{22}Na or ^{36}Cl distribution in the cerebral cortex gray matter and cerebellum are similar to the 1.0-1.5 range of values reported for uptake of the two isotopes in the rat cerebral cortex (REED et al., 1964; VERNADAKIS & WOODBURY, 1965; BUHRLEY & REED, 1972). The observation that both ^{36}Cl and ^{22}Na distribute within the cerebellum in $\sim$2/3 the time necessary for isotope distribution within the cerebral cortex substantiates the autoradiographic evidence of LUCIANO (1968) for significant heterogeneity in brain tissue uptake of ^{22}Na. For both cerebral cortex and cerebellum, the radioisotope steady-state spaces were equivalent to the chemically determined Cl and Na spaces. No evidence was observed for a very slow ($t_{1/2}$ 3–14 h) compartment for either ^{36}Cl or ^{22}Na uptake into the CNS, as was reported previously (REED et al., 1964; VERNADAKIS & WOODBURY, 1965; LEVIN & PATLAK, 1972). Other reports of ^{22}Na uptake into the rat brain have failed to detect a third (very slow) compartment (LUCIANO, 1968; BUHRLEY & REED, 1972). Furthermore, the rapid and complete exchangeability of brain Cl and Na <u>in vitro</u> ($t_{1/2} < 1$ h) would indicate that once the isotope has penetrated the blood-brain barrier <u>in vivo</u>, distribution between the cellular and extracellular compartments proceeds quickly (DAVSON & SPAZIANI, 1959; KEESEY & WALLGREN, 1965; BRADBURY et al., 1968). Many of the studies in which a very slow component ($t_{1/2}$ 3-14 h)

was observed for ^{36}Cl or ^{22}Na uptake into brain tissue utilized 24-h nephrectomy to maintain stable levels of radioisotope in the plasma. The changes in brain tissue, plasma, and CSF electrolyte content (especially K) induced by > 8 h of nephrectomy (HISE & JOHANSON, 1979), may alter significantly ^{36}Cl and ^{22}Na uptake into the CNS. In the present study, 4-h nephrectomy was utilized to minimize induced alterations in tissue and fluid ion content. Thus, the slow component of ^{36}Cl and ^{22}Na uptake into the cerebral cortex and cerebellum reflects the rate-limiting step, movement across the blood-brain barrier.

As reported in the preceding paper (see PART ONE), the uptake of ^{36}Cl and ^{22}Na into the CSF was resolved into two components; a fast component ($t_{1/2}$ 0.18 h, fractional volume 0.26) probably reflecting isotope movement across the choroid plexuses, and a slow component ($t_{1/2}$ 1.2 h, fractional volume 0.74) reflecting primarily brain-CSF isotope exchange. The similarity between the CSF slow component $t_{1/2}$ and the brain tissue slow component $t_{1/2}$ reflects the ease with which ^{22}Na and ^{36}Cl pass through the ventricular ependyma (DAVSON, 1955).

Compartment analysis of ^{36}Cl and ^{22}Na uptake into the CNS failed to determine the in vivo extracellular and cellular fluid volumes of the brain because ion movement across the blood-brain barrier is rate limiting. However, due to the presence of the blood-brain barrier and to the rapid exchange of isotopes between the brain extracellular space and the CSF, the CSF radioisotope activity is a better approximation of the brain extracellular fluid (ECF) activity than is the plasma. Thus, the initial slope of the brain space/CSF

space curve (Fig. 7) provides an estimate of the volume of CSF which would account for the brain tissue radioactivity. Both ^{22}Na and ^{36}Cl determine similar volumes for the extracellular space of the cerebral cortex (average ^{36}Cl and ^{22}Na, 13.4%) and cerebellum (average 13.1%). These values compare favorably with the 13.5-14.5% extracellular space of the rat brain as measured by the brain ^{14}C-inulin space after 6-8 h of simultaneous perfusion of the plasma and ventricular system with ^{14}C-inulin (WOODWARD et al., 1967). Similarly, RAPOPORT (1979), utilizing a kinetic analysis of ^{14}C-sucrose uptake into various regions of the rat CNS, reported a 14% volume of distribution in the cerebral cortex and a 13% volume in the cerebellum. Furthermore, application of the technique for estimating brain ECF volume to infant rats has shown a steady decrease in the extracellular space of the cerebral cortex from 24% (1 wk-old rats), 16% (2 wk), to 13% (5 wk) (unpublished data). A comparable decrease in the brain extracellular space of maturing rats was measured with ^{14}C-inulin by FERGUSON & WOODBURY (1969). Thus, the initial slope of the brain tissue space/CSF space provides a reasonable estimate of the in vivo brain extracellular space without requiring such invasive techniques as subarachnoid or ventriculo-cisternal perfusion.

Calculation of cell electrolyte concentrations in the CNS requires not only the volume of the extracellular space but also the relative volumes of neuronal and glial cells. For the 4 ratios examined (neuronal volume/glial volume 3/1, 2/1, 1/1, and 1/2), glial cell $[Cl]$ was from 2 to 6 times that in neuronal cells based on a passive neuronal Cl distribution and a neuronal resting membrane potential of -70 mV. Whereas BRIZZEE et al. (1964)

measured the numbers of glia/neurons as 1/1 to 3/1 in the rat cerebral cortex, others have estimated that glia outnumber neurons by a factor of about 5 to 10 (HERTZ & SCHOUSBOE, 1975). Considering the small size of glial cells, a neuronal cell volume/glial cell volume of 2/1 is a reasonable estimate of the two compartment volumes (HERTZ, 1977; POPE, 1978). As summarized in Fig. 8, glial cell [Cl] (36-46 mmol/kg cell H_2O) was ~4 times that of neuronal cell [Cl] with a neuronal/glial cell volume of 2/1. Since astrocyte resting membrane potentials of -70 to -90 mV are reported (KATZMAN & PAPPIUS, 1973), a calculated glia cell [Cl] of 5-10 mmol/kg cell H_2O would be predicted for passive distribution. The accumulation of Cl within the glial cell against an electrochemical potential difference represents evidence for active transport of Cl by the glial cell. BOURKE & NELSON (1972) have reported a K-dependent Cl accumulation by glial cells in the in vivo cerebral cortex. A similar process has been observed in in vitro astrocyte tissue cultures (GILL et al., 1974; KIMELBERG et al., 1979).

The relative permeability of the blood-brain and blood-CSF barriers was evaluated by converting component rate constants to permeability surface-area products. The PA can be directly related to permeability if the surface area is known (BRADBURY, 1979). For comparing the rate of uptake of several isotopes into one tissue the relative permeability (PA) is adequate since the area for exchange is presumably the same. As shown in Table 6, the relative permeability to ^{22}Na was slightly greater than that to ^{36}Cl in the cerebral cortex, cerebellum, fourth ventricle choroid plexus, and fast component CSF. The PA to ^{3}H-mannitol was 1/10 that to ^{36}Cl in the cerebral cortex

and cerebellum and 1/5 that to ^{36}Cl in the CSF fast component. Calculation of PA from rate constants reported by REED et al. (1964) confirms the observation that the relative permeability of the rat cerebral hemisphere to ^{22}Na (0.154 ml/h/g) is slightly greater than that to ^{36}Cl (0.135 ml/h/g). In contrast, DAVSON & WELCH (1971) obtained equivalent PA to ^{22}Na and ^{36}Cl in the rabbit brain. The PA of the rat brain to ^{3}H-mannitol (0.01 ml/h/g) as reported by SISSON & OLDENDORF (1971) compares favorably to the values for the cerebral cortex and cerebellum as reported in the present paper. Thus, the permeability surface-area products to ^{36}Cl, ^{22}Na, and ^{3}H-mannitol for the cerebral cortex and cerebellum agree with literature values for the rat brain.

If the surface area for exchange is known, the PA can be converted to permeability (cm/sec). CRONE (1963) calculated 240 cm^2/g for the surface area of the cerebral capillaries. However, BRADBURY (1979) considered 240 cm^2/g an overestimate and proposed a range of 60-140 cm^2/g (average $\sim$100 cm^2/g). Similarly, WELCH & SADLER (1966) calculated the surface area of the rabbit choroid plexus epithelium as 360 cm^2/g. If only the basolateral membrane is considered for exchange (see PART ONE), the choroid epithelial surface area would be only $\sim$1/3 of the total surface area or an average of $\sim$120 cm^2/g (WELCH & SADLER, 1966). With the average estimates of surface area, the permeability of the cerebral cortex and cerebellum capillaries and the choroid plexus epithelium (CSF fast component) to ^{36}Cl was calculated to be 3.1×10^{-7}, 4.5×10^{-7}, and 2.2×10^{-6} cm/sec and to ^{22}Na was 3.9×10^{-7}, 5.4×10^{-7}, and 2.6×10^{-6} cm/sec, respectively.

These values compare favorably with the brain permeability to ^{36}Cl and ^{22}Na (1.6×10^{-7} cm/sec) as estimated by RAPOPORT (1976); the 2-fold lesser PA values obtained by RAPOPORT (1976) were calculated assuming a cerebral capillary surface area of 240 cm^2/g as compared to 100 cm^2/g in the present study. The values for choroid plexus permeability to ^{36}Cl and ^{22}Na are similar to the P_{Cl} of 8×10^{-6} and P_{Na} of 6×10^{-6} cm/sec for the in vitro frog fourth ventricle choroid plexus (WRIGHT, 1972). For ^{3}H-mannitol, the permeability of the cerebral cortex (2.7×10^{-8}), cerebellum (3.3×10^{-8}) and choroid plexus (4.9×10^{-8} cm/sec) was calculated. The greater calculated capillary permeability to ^{36}Cl, ^{22}Na, and ^{3}H-mannitol in the cerebellum than in the cerebral cortex may be due to an underestimation of the cerebellar capillary surface area; the residual erythrocyte content of the cerebellum was 2x that of the cerebral cortex, which may indicate a greater cerebellar vascularity and thus surface area (JOHANSON, 1980). Furthermore, the difference between the choroid plexus epithelium and brain capillary permeability to ^{3}H-manntiol (choroid plexus $\approx$ 2x cerebral cortex) and to ^{36}Cl and ^{22}Na (choroid plexus $\approx$ 7x cerebral cortex) may be due to active transcellular Na and Cl transport by the choroid epithelial cell from plasma to CSF. However, analysis of the uptake of all three radioisotopes (^{36}Cl, ^{22}Na, and ^{3}H-mannitol) indicates that the effective permeability of the choroid epithelium (blood-CSF barrier) is greater than that of the cerebral cortex or cerebellum capillary endothelium (blood-brain barrier).

REFERENCES

BOULDIN T. W. & KRIGMAN M.R. (1975) Differential permeability of cerebral capillary and choroid plexus to lanthanum ion. Brain Res. 99, 444-448.

BOURKE R.S. & NELSON K. M. (1972) Further studies on the K-dependent swelling of primate cerebral cortex in vivo: The enzymatic basis of the K-dependent transport of chloride. J. Neurochem. 19, 663-685.

BRADBURY M. (1979) The Concept of a Blood-Brain Barrier, pp 1-59. Wiley, New York.

BRADBURY M.W.B. & CROWDER J. (1976) Compartments and barriers in the sciatic nerve of the rabbit. Brain Res. 103, 515-526.

BRADBURY M.W.B., VILLAMIN M. & KLEEMAN C.R. (1968) Extracellular fluid, ionic distribution and exchange in isolated frog brain. Am. J. Physiol. 214, 643-651.

BRIGHTMAN M.W. & REESE T.S. (1969) Junctions between intimately apposed cell membranes in the vertebrate brain. J. Cell Biol. 40, 648-677.

BRIZZEE K.R., VOGT J. & KHARETCHKO X. (1964) Postnatal changes in glia/neuron index with a comparison of methods of cell enumeration in the white rat, in Progress in Brain Research (PURPURA D.P. & SCHADE J.D., eds.), Vol. 4, pp. 136-149. Elsevier Publishing Co., Amsterdam.

BUHRLEY L.E. & REED D.J. (1972) The effect of furosemide on sodium-22 uptake into cerebrospinal fluid and brain. Exp. Brain Res. 14, 503-510.

DAVSON H. (1955) A comparative study of the aqueous humor and cerebrospinal fluid in the rabbit. J. Physiol., Lond. 129, 111-133.

DAVSON H. & SPAZIANI E. (1959) The blood-brain barrier and the extracellular space of brain. J. Physiol., Lond. 149, 135-143.

DAVSON H. & WELCH K. (1971) The permeation of several materials into fluids of the rabbit's brain. J. Physiol., Lond. 218, 337-351.

EISENBERG H.M. & SUDDITH R.L. (1979) Cerebral vessels have the capacity to transport sodium and potassium. Science, N.Y. 206, 1083-1085.

FENSTERMACHER J.D. (1975) Mechanisms of ion distribution between blood and brain, in The Nervous System (TOWER D.B., ed.), pp. 299-311. Raven Press, New York.

FERGUSON R.K. & WOODBURY D.M. (1969) Penetration of ^{14}C-inulin and ^{14}C-sucrose into brain, cerebrospinal fluid, and skeletal muscle of developing rats. Exp. Brain Res. 7, 181-194.

GILL T.H., YOUNG O.M. & TOWER D.B. (1974) The uptake of ^{36}Cl into astrocytes in tissue culture by a potassium-dependent saturable process. J. Neurochem. 23, 1011-1018.

HERTZ L. & SCHOUSBOE A. (1975) Ion and energy metabolism of the brain at the cellular level, in Int. Rev. Neurobiology (PFEIFFER C. & SMYTHIES J., eds.), Vol. 18, pp. 141-211. Academic Press, New York.

HERTZ L. (1977) Drug-induced alterations of ion distribution at the cellular level of the central nervous system. Pharmac. Rev. 29, 35-65.

HISE M.A. & JOHANSON C.E. (1979) The sink action of cerebrospinal fluid in uremia. Eur. Neurol. 18, 328-337.

JOHANSON C.E. (1980) Permeability and vascularity of the developing brain: Cerebellum vs. cerebral cortex. Brain Res. 190, 3-16.

JOHANSON C.E. & WOODBURY D.M. (1978) Uptake of [^{14}C] urea by the in vivo choroid plexus-cerebrospinal fluid-brain system: Identification of sites of molecular sieving. J. Physiol., Lond. 275, 167-176.

KATZMAN R. & PAPPIUS H.M. (1973) Brain Electrolytes and Fluid Metabolism, pp. 149-187. Williams & Wilkins, Baltimore.

KEESEY J.C. & WALLGREN H. (1965) Movements of radioactive sodium in cerebral cortex slices in response to electrical stimulation. Biochem. J. 95, 301-310.

KIMELBERG H.K., BIDDLECOME S. & BOURKE R.S. (1979) SITS - inhibitable Cl transport and Na-dependent H production in primary astroglial cultures. Brain Res. 173, 111-124.

LEVIN V. & PATLAK C. S. (1972) A compartmental analysis of ^{24}Na kinetics in rat cerebrum, sciatic nerve and cerebrospinal fluid. J. Physiol., Lond. 224, 559-561.

LUCIANO D.S. (1968) Sodium movement across the blood-brain barrier in newborn and adult rats and its autoradiographic localization. Brain Res. 9, 334-350.

MANERY J.F. & BALE W.F. (1941) The penetration of radioactive sodium and phosphorus into the extra and intracellular phases of tissues. Am. J. Physiol. 132, 215-230.

MANERY J.F. & HAEGE L.F. (1941) The extent to which radioactive chloride penetrates tissues, and its significance. Am. J. Physiol. 134, 83-93.

POPE A. (1978) Neuroglia: quantitative aspects, in Dynamic Properties of Glia Cells (SCHOFFENIELS E., FRANCK G., HERTZ L. & TOWER D., eds.), pp. 13-20. Pergamon Press, Oxford.

RAPOPORT S. I. (1976) Blood-Brain Barrier in Physiology and Medicine, pp. 87-100. Raven Press, New York.

RAPOPORT S.I., OHNO K. & PETTIGREW K.D. (1979) Blood-brain barrier permeability in senescent rats. J. Gerontol. 34, 162-169.

REED D.J., WOODBURY D.M. & HOLTZER R.L. (1964) Brain edema, electrolytes, and extracellular space. Archs. Neurol. 10, 604-616.

SISSON W.B. & OLDENDORF W. H. (1971) Brain distribution spaces of mannitol-^{3}H, inulin-^{14}C, and dextran-^{14}C in the rat. Am. J. Physiol. 221, 214-217.

SOLOMON A.K. (1949) Equations for tracer experiments. J. Clin. Invest. 28, 1297-1307.

STULC J. (1967) The permeability of mouse cerebral capillaries to sodium. Life Sci. 6, 1837-1846.

VERNADAKIS A. & WOODBURY D.M. (1965) Cellular and extracellular spaces in developing rat brain. Archs Neurol. 12, 284-293.

WELCH K. & SADLER K. (1966) Permeability of the choroid plexus of the rabbit to several solutes. Am. J. Physiol. 210, 652-660.

WOODBURY D.M. (1967) Distribution of nonelectrolytes and electrolytes in the brain as affected by alterations in cerebrospinal fluid secretion, in Progress in Brain Research (LAJTHA A. & FORD D.H., eds.), Vol. 29, pp. 297-313. Elsevier Publ. Co., Amsterdam.

WOODWARD D.L., REED D.J. & WOODBURY D.M. (1967) Extracellular spaces of rat cerebral cortex. Am. J. Physiol. 212, 367-370.

WRIGHT E.M. (1972) Mechanisms of ion transport across the choroid plexus. J. Physiol., Lond. 226, 545-571.

PART THREE

KINETIC ANALYSIS OF CHLORIDE-36 AND SODIUM-22 UPTAKE INTO THE IN VIVO CHOROID PLEXUS-CEREBROSPINAL FLUID-BRAIN SYSTEM: ONTOGENY OF THE BLOOD-BRAIN AND BLOOD-CSF BARRIERS

INTRODUCTION

There are a number of observations which indicate the absence or decreased effectiveness of the blood-brain and blood-CSF barriers in embryonic and infant animals (WOODBURY, 1974; SAUNDERS, 1977; BRADBURY, 1979). The rat blood-brain barrier decreases in permeability to hydrophilic solutes between birth and adulthood (FERGUSON & WOODBURY, 1969; PARANDOOSH & JOHANSON, 1979; JOHANSON, 1980). Furthermore, active transport systems in the rat brain capillaries develop during the first 5 wk of postnatal life (BASS & LUNDBORG, 1973b; CREMER et al., 1976). Similarly, there is a reduction in the permeability of the rat choroidal ependyma (blood-CSF barrier) (RAMEY & BIRGE, 1979), and an increase in choroidal epithelial cell transport capability and fluid production (BIERER & HEISEY, 1972; JOHANSON & WOODBURY, 1974).

The slow movement ($t_{1/2}$ >1 h) of ^{36}Cl and ^{22}Na from the plasma into the CNS is a result of the blood-brain and blood-CSF barriers. While the kinetics of ^{36}Cl and ^{22}Na uptake into brain tissue and CSF have been analyzed for the adult animal (DAVSON, 1955; REED et al., 1964; LEVIN & PATLAK, 1972; also see PART ONE), apparently only two literature reports have compared ^{36}Cl (VERNADAKIS & WOODBURY, 1965) or ^{22}Na (LUCIANO, 1968) movement across the blood-brain barrier of newborn and adult animals. Also, few studies have examined regional differences in

blood-brain barrier permeability to these isotopes, and age-related changes in the regional permeability differences (LUCIANO, 1968). Lastly, reports have indicated that the relative permeability of the adult choroidal ependyma is significantly greater than the endothelial cells of the cerebral capillaries (BOULDIN & KRIGMAN, 1975; RAPOPORT, 1976); the choroid plexus has been classified as a "leaky" epithelium and the cerebral capillaries as a "tight" barrier (BRADBURY, 1979). Only one report has simultaneously compared developmental changes in blood-brain and blood-CSF barrier permeability (PARANDOOSH & JOHANSON, 1979). Thus, to understand better the transport and permeability properties of the developing blood-brain and blood-CSF barriers, we have analyzed ^{36}Cl and ^{22}Na uptake into the cerebral cortex, cerebellum, cisternal CSF, and the choroid plexuses of the lateral and fourth ventricles of the postnatal rat. The short-term uptake of ^{3}H-mannitol was examined in 3 age groups for comparison with the two electrolytes. The results of the present study indicate that the adult choroid plexus can actively transport Cl and Na; developmental changes in plexus ^{36}Cl and ^{22}Na uptake are related to the onset of CSF production. The effective permeability of the blood-brain and blood-CSF barriers to ^{3}H-mannitol decreased with age (barrier "tightening"); due to the maturation of Na and possibly Cl transport systems at the two barriers (WRIGHT, 1978a; EISENBERG & SUDDITH, 1979), the effective permeability of the blood-brain barrier to ^{36}Cl and ^{22}Na decreased markedly less than to ^{3}H-mannitol, and that of the blood-CSF barrier increased $\sim$10-fold between 1 wk and 5 wk of age.

MATERIALS AND METHODS

Animals and experimental procedure

Sprague-Dawley rats of 1 week (19 ± 1 (S.E.M.) g), 2 weeks (36 ± 2 g), and 5 weeks (108 ± 2 g) postnatal age were utilized for measurement of radioisotope uptake into various regions of the CNS. A total of 189 rats was separated into 3 groups as follows: i) ^{36}Cl uptake was determined in 27 animals of each age group (total 81); ii) ^{22}Na uptake was examined in 24 rats of 1, 2, or 5 weeks of age (total 72); and iii) the initial distribution of ^{3}H-mannitol was analyzed in 12 rats from each of the three age groups (total 36).

Treatment

Eight h prior to sacrifice, each rat was taken from the litter and placed in a light-heated (38° C) environment for the remainder of the treatment period (neonatal rats were not reunited with their mothers due to the high incidence of maternal cannibalism after human contact). ^{36}Cl (0.1 μCi/g) was injected intraperitoneally at 1/12, 1/6, 1/4, 1/2, 1, 2, 4, and 8 h before death. ^{3}H-mannitol (0.5 μCi/g) was injected i.p. at 1/12, 1/6, 1/4, and 1 h before death. All radioisotope solutions were adjusted with 0.9% NaCl so that the final injected volume was 0.01 ml/g. To ensure a stable level of radioisotope in the plasma, all animals were briefly anesthetized with ether and bilaterally nephrectomized by ligation of the renal pedi-

cles 4 h prior to sacrifice.

Sampling and analysis of tissues and fluids

At the time of sacrifice, animals were anesthetized with ether and an arterial blood sample was taken from the abdominal aorta with a heparinized syringe. CSF was sampled from the cisterna magna immediately thereafter with a glass micropipet. The lateral and fourth ventricle choroid plexuses were obtained with the aid of a dissecting microscope and ophthalmologic forceps within 2-3 min after death. A slice (~1 mm) of cerebral cortex gray matter was taken from the parietal lobe; the cerebellar hemispheres were also removed for analysis. Brain tissue was blotted on filter paper to remove any excess blood and the meninges.

Specimens, other than the choroid plexuses, were placed in tared vials and weighed on a Sartorius balance. The choroid plexuses, which were placed on tared aluminum pans (~1 mg), were analyzed for wet tissue weight by the method previously described (JOHANSON et al., 1976). ^{36}Cl and ^{3}H activity were assayed by liquid scintillation counting (Nuclear Chicago Isocap 300) after sample digestion with 1 M piperidine. ^{22}Na activity was assayed by gamma counting (Beckman Biogamma) without further preparation. Extracellular fluid (plasma H_2O x D.F.) [Cl] and [Na] were determined by amperometric titration of Ag and by flame photometry, respectively (see PART ONE).

Calculations and statistical analyses

Tissue or fluid radioactivity was expressed as a volume of distribution

or space (%) = 100 x (dpm/g tissue or fluid)/(dpm/g plasma H_2O x D.F.) where D.F. is the appropriate Donnan factor. Uptake curves were resolved into components by the graphical analysis method (see PART ONE and Fig. 11). Components were described by linear regression analysis (ln space vs. time). The slope, which is equivalent to the component rate constant (k), was converted to a half-time ($t_{1/2}$) by the formula: $t_{1/2} = (\ln 2)/k$. The component volume of distribution was obtained as the exp (y-intercept of the line). 95% confidence limits are listed for $t_{1/2}$ and Vd, because on conversion from k and ln Vd, respectively, the S.E.M. were no longer symmetrical. Parenchymal cell concentrations of Cl or Na were determined by subtracting non-parenchymal cell (extracellular, erythrocyte) contributions from tissue electrolyte and water content: $[X]cell = \frac{(X)tissue - (X)e - (X)r}{Vtissue - Ve - Vr}$ where (X) = Na or Cl content (mmol/kg wet weight), V = fractional volume of water, e = extracellular fluid, and r = residual erythrocytes. In the choroid plexuses, the extracellular space was obtained as the 1-h tissue space of ^{3}H-mannitol. The extracellular space of the cerebral cortex and cerebellum was estimated as the initial slope of the brain tissue activity vs. CSF activity curve (see PART TWO). Permeability surface-area products, as a measure of barrier permeability (BRADBURY, 1979), were calculated for ^{36}Cl and ^{22}Na as PA (ml/h/g) = k x Vd/100. Because ^{3}H-mannitol uptake into the CNS was not followed to steady state, the PA for ^{3}H-mannitol was determined as the initial slope of the tissue space vs. time curve (BRADBURY, 1979). One-way analysis of variance was used to test for the statistical significance of differ-

ences among the 3 age groups. When differences were noted at the 5% level, the Tukey version of the multiple-range test was employed to compare the various groups.

Materials

^{22}Na-NaCl (carrier-free) and ^{3}H-mannitol (0.123 mCi/g) were obtained from New England Nuclear; ^{36}Cl-NaCl (12.7 mCi/mg) was purchased from ICN Chemical and Radioisotope Division. Radiochemical and chemical purity were reported as > 99% by both companies.

RESULTS

Stable radioisotope levels were maintained in the plasma from 1/12 to 8 h by prevention of renal isotope excretion (4-h bilateral nephrectomy). Regression analysis of plasma ^{36}Cl, ^{22}Na, or ^{3}H-mannitol activity as a function of time yielded slopes not significantly different from 0 for 1-, 2-, and 5-wk-postnatal rats. Furthermore, the standard deviation of the plasma radioisotope activity was from 3-9% of the mean activity for all 3 age groups. Thus, the analysis and interpretation of the uptake curves of tissue and CSF were based on a constant plasma radioactivity.

Chemical analysis of extracellular fluid (plasma H_2O x D.F.) [Cl] and [Na] revealed small changes in concentration during development. The extracellular fluid [Cl] significantly decreased from 121 $\pm$ 2 mmol/kg H_2O for the 1-wk rat to 114 $\pm$ 1 for the 5-wk animal. In contrast, an increase of 12.5 mmol/kg H_2O was observed in extracellular fluid [Na] between 1 and 5 wk of age ($P < 0.05$).

LVCP uptake by 1-wk- and 2-wk-old rats is shown for ^{36}Cl and for ^{22}Na in Fig. 10. The LVCP ^{36}Cl steady-state space at 1 wk of age (63.0 $\pm$ 1.5%) was significantly greater than the 2-wk space (56.9 $\pm$ 1.2%). Similarly, the LVCP ^{22}Na steady-state space at 1 wk (44.6 $\pm$ 2.7%) decreased to 34.1 $\pm$ 0.8% by the second wk ($P < 0.05$). In comparison, while the 4VCP ^{22}Na steady-state space decreased from 46.8 $\pm$ 2.6 at 1 week to 37.8 $\pm$ 0.7%

Fig. 10. The uptake of ^{36}Cl and ^{22}Na into the LVCP of 1-wk and 2-wk rats as a function of time after administration. The left-hand portion of the figure represents the uptake of ^{36}Cl and the right-hand portion that of ^{22}Na. Either ^{36}Cl or ^{22}Na (0.1 μCi/g) was injected at various times prior to sacrifice into 4-h nephrectomized rats. Tissue radioactivity was expressed as a space (%) = 100 x (dpm/g tissue)/(dpm/g extracellular fluid). Values are means $\pm$ S.E.M. for 3 animals.

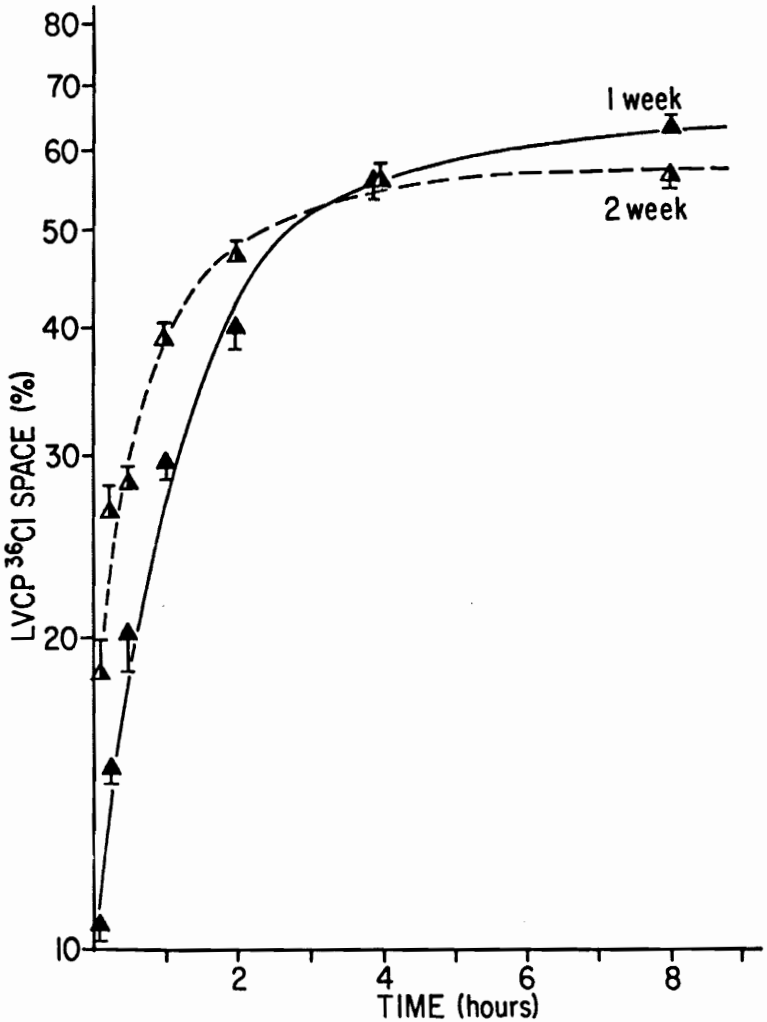
80
70
60
50
40
30
20
10
LVCP ^{36}Cl SPACE (%)
1 week
2 week
2
4
6
8
TIME (hours)

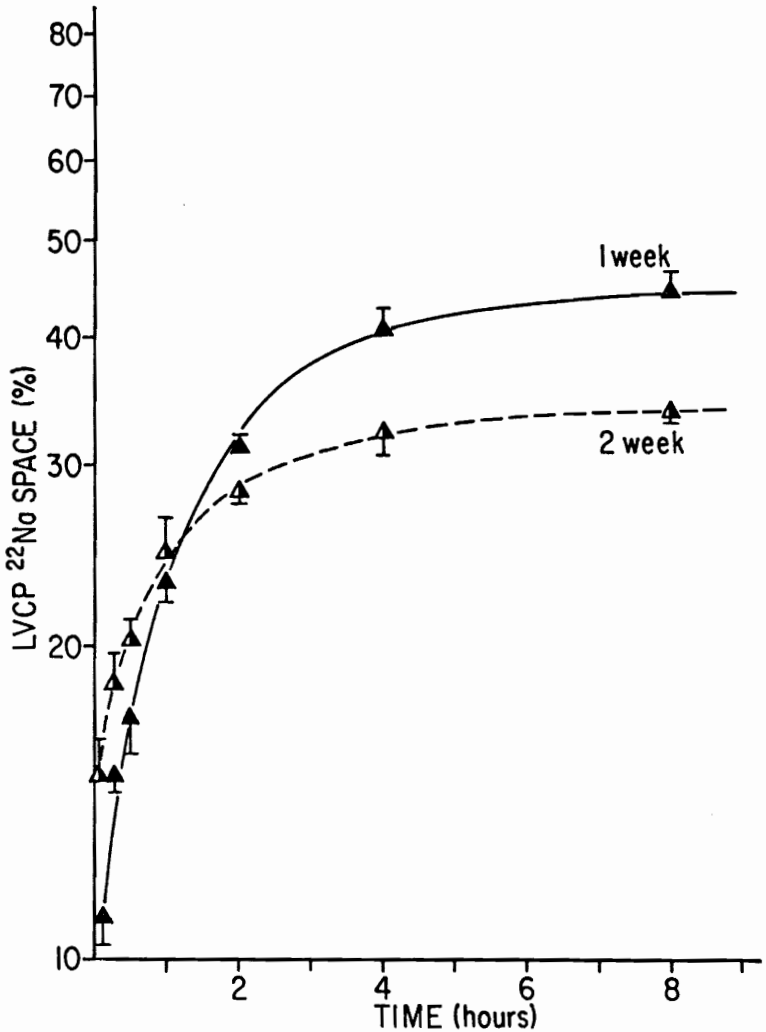
80
70
60
50
40
30
20
10
LVCP ^{22}Na SPACE (%)
1 week
2 week
2
4
6
8
TIME (hours)

at 2 wk ($P < 0.05$), the 4VCP ^{36}Cl space did not change significantly from 1 wk (59.4 ± 2.3%) to 2 wk (58.9 ± 2.1%) of age. Neither the ^{36}Cl nor the ^{22}Na steady-state spaces differed between the 2-wk and 5-wk animals in either the LVCP or 4VCP. As shown in Fig. 10, the early time period uptake of ^{36}Cl or ^{22}Na by the LVCP was considerably less in the 1-wk than in the 2-wk rat. ^{36}Cl and ^{22}Na uptake into the 5-wk LVCP and 4VCP are similar to that of the 2-wk-old rat.

^{36}Cl and ^{22}Na uptake curves for the LVCP and 4VCP were resolved into components by a modification of the graphical analysis method. For all 3 age groups, radioisotope uptake resolved into 2 components which differed in rate by a factor of 10 or more. In Table 7, component half-time ($t_{1/2}$) and volume of distribution (Vd) are summarized for the developing choroid plexuses. Both radioisotopes distributed rapidly in the fast component volume ($t_{1/2}$ 0.02-0.12 h); however, ^{22}Na uptake into the 1-wk LVCP and 4VCP fast component ($t_{1/2}$ 0.08-0.12 h) was distinctly slower than ^{36}Cl or ^{22}Na distribution within the LVCP and 4VCP fast components of other ages ($t_{1/2}$ 0.02-0.05). Comparable ^{22}Na fast component Vd were obtained for each age group in both the LVCP and 4VCP. In contrast, both LVCP and 4VCP ^{36}Cl fast component Vd increased from 9-10% at 1 wk to 25% at 5 wk. Choroid plexus slow component $t_{1/2}$ ranged from 0.8 to 1.9 h for ^{36}Cl and ^{22}Na. Both LVCP ^{22}Na and 4VCP ^{36}Cl slow component $t_{1/2}$ increased with age while LVCP ^{36}Cl and 4VCP ^{22}Na $t_{1/2}$ decreased with age. ^{36}Cl slow component Vd declined steadily from 1 to 5 wk of age in the choroid plexuses. A significant decrease in ^{22}Na slow component Vd of the LVCP and 4VCP was

TABLE 7. ANALYSIS OF COMPONENTS OF ^{36}Cl AND ^{22}Na UPTAKE INTO THE LATERAL AND FOURTH VENTRICLE CHOROID PLEXUSES OF DEVELOPING RATS

	Fast component		Slow component	
Compartment	$t_{1/2}$ (h)	Vd (%)	$t_{1/2}$ (h)	Vd (%)
A. Chloride-36				
Lateral ventricle choroid plexus				
1 week	0.03	10	1.6(1.4-1.9)	53(49-57)
2 week	0.05	18	1.0(0.9-1.1)	39(36-43)
5 week	0.03	25	1.0(0.7-1.6)	30(22-40)
Fourth ventricle choroid plexus				
1 week	0.03	9	0.9(0.8-1.2)	50(43-58)
2 week	0.05	21	1.3(1.2-1.5)	38(36-40)
5 week	0.05	25	1.3(1.0-1.8)	31(27-36)
B. Sodium-22				
Lateral ventricle choroid plexus				
1 week	0.08	12	1.4(1.1-2.1)	33(28-40)
2 week	0.03	15	1.2(0.9-1.5)	19(17-22)
5 week	0.02	14	1.9(1.7-2.3)	22(21-23)
Fourth ventricle choroid plexus				
1 week	0.12	17	1.2(0.9-1.8)	30(24-37)
2 week	0.03	17	0.8(0.7-0.9)	26(23-30)
5 week	0.02	13	0.9(0.7-1.0)	26(23-30)

Radioisotope uptake curves were resolved into components by the method of graphical analysis (see Fig. 2) and fitted to straight lines (ln space vs. time) by linear regression. The half-time ($t_{1/2}$) was obtained by dividing ln 2 by the slope (k) of the regression line. The volume of distribution (Vd) was calculated as exp (y-intercept of the regression line). Values in parentheses are the 95% confidence limits for the parameter.

seen only between 1 and 2 wk of age; the ^{22}Na Vd of the 5-wk rat tended to be equal or greater than that of the 2-wk rat.

^{36}Cl uptake into the CSF is shown in Fig. 11 for 1-wk and 5-wk rats. While no significant changes were detected in the CSF steady-state space for ^{36}Cl (116.7 $\pm$ 0.9%) or ^{22}Na (111.8 $\pm$ 0.9%) between 1 and 5 wk of age, both radioisotope spaces tended to increase between 2 and 5 wk. As for the choroid plexuses, early time period CSF spaces (1/12-1/2 h) for ^{36}Cl and ^{22}Na were significantly less in the 1-wk than in the 5-wk animals. As shown in Fig. 11, resolution of CSF uptake curves into components yielded only 1 statistically significant component in the 1-wk-old rats. In contrast, the CSF uptake curve of 5-wk-old rats resolved into 2 components: a fast component which contributed $\sim$1/4 of the steady-state space and a slow component which contributed $\sim$3/4 of the space. Similar kinetics were observed for CSF ^{22}Na uptake at the 2 ages. Table 8 summarizes the CSF component $t_{1/2}$ and Vd for the 3 age groups. Fast component $t_{1/2}$ for ^{36}Cl and ^{22}Na were comparable throughout development ($t_{1/2}$ 0.10-0.19 h). An $\sim$10-fold increase with age was noted in CSF fast component Vd for both radioisotopes. The CSF slow component $t_{1/2}$ for ^{36}Cl was slower (by 0.2-0.3 h) than for ^{22}Na in 1-wk and 2-wk animals. By 5 wk of age, the ^{22}Na slow component $t_{1/2}$ increased by 0.5-0.6 h, becoming greater than the ^{36}Cl $t_{1/2}$ by 0.2 h. Reflecting the increase in fast component Vd, CSF slow component Vd declined between 1 and 5 wk.

The uptake of ^{36}Cl and ^{22}Na into the cerebral cortex and cerebellum of developing rats is shown in Fig. 12. The ^{36}Cl steady-state space of the

Fig. 11. The uptake of ^{22}Na into the CSF of 1-wk and 5-wk rats as a function of time after administration. The left-hand portion of the figure represents ^{22}Na uptake into the CSF at 1 wk of age and the right-hand portion that at 5 wk of age. ^{22}Na (0.1 μCi/g) was injected at various times prior to sacrifice into 4-h nephrectomized rats. CSF radioactivity (□—□) was expressed as a space (%) = 100 x (dpm/g CSF)/(dpm/g extracellular fluid). The CSF uptake of ^{22}Na was resolved into a slow component by subtracting the observed spaces from the steady-state space and plotting the difference (X---X) as a function of time. The slope and y-intercept were obtained by fitting the linear portion of the graph to a straight line by the least squares method. The fast component of 5-wk rats was resolved by subtracting the spaces predicted by the extrapolated slow component line from the spaces which were not fitted to the slow component line (T = 0, 1/12, 1/6, and 1/4), and plotting the difference (X---X) versus time. Again, a slope and y-intercept were obtained from linear regression. The fractional volume represents the ratio of the component volume and the steady-state space. Each point represents a mean for 3 animals. Standard errors are generally < 5% of the respective means.

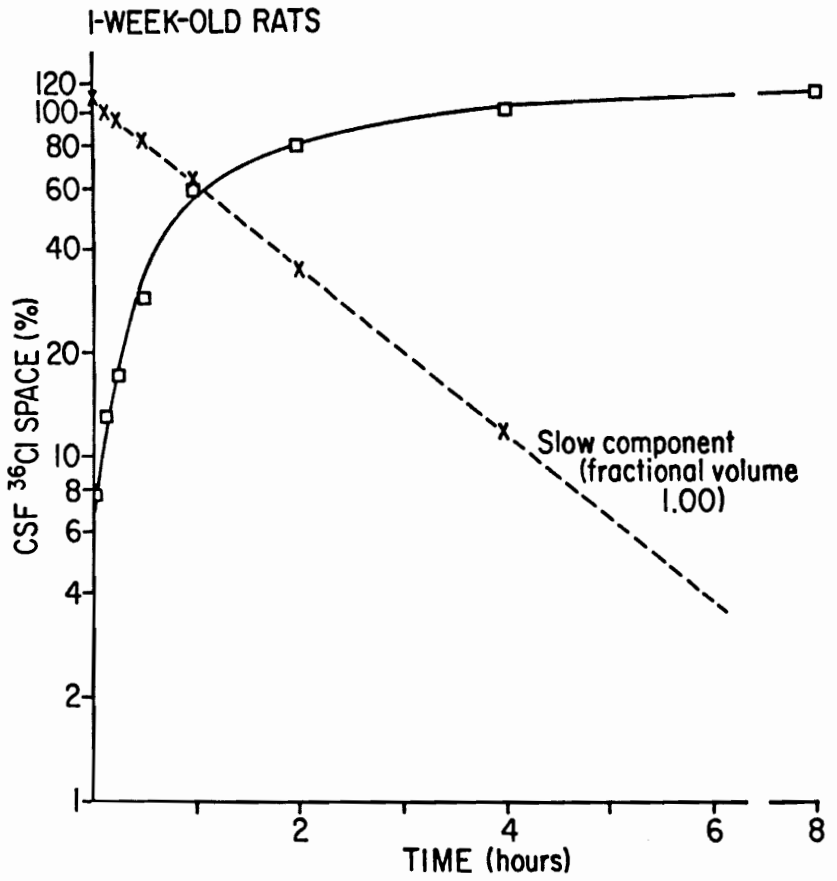
1-WEEK-OLD RATS
CSF ^{36}Cl SPACE (%)
120
100
80
60
40
20
10
8
6
4
2
1
2
4
6
8
TIME (hours)
Slow component
(fractional volume
1.00)

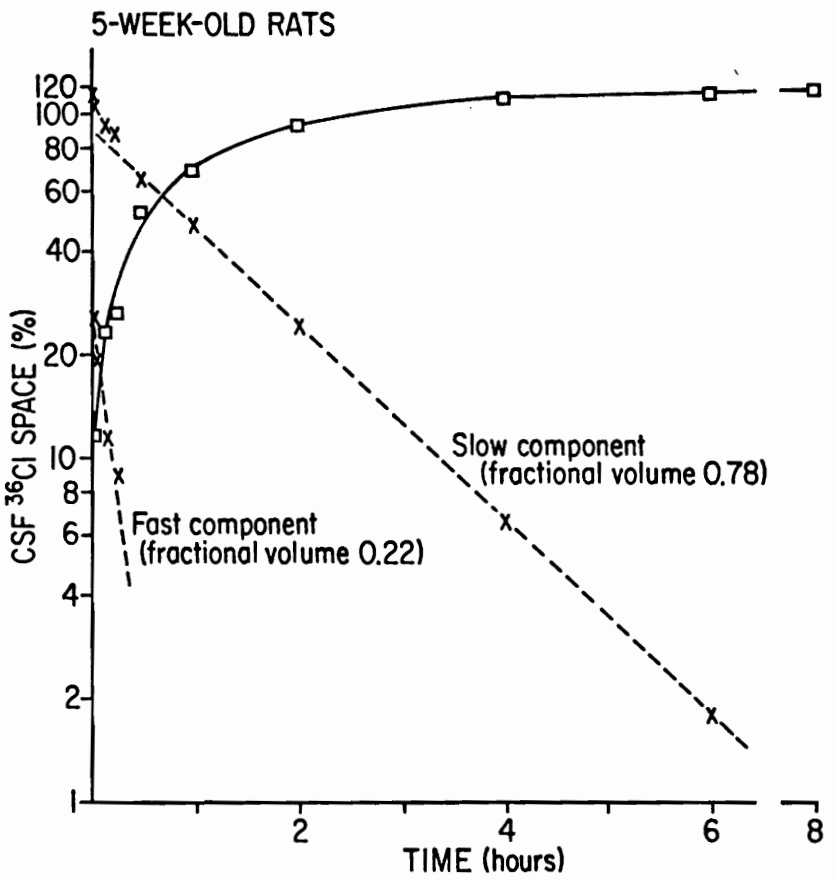
5-WEEK-OLD RATS
CSF ^{36}Cl SPACE (%)
120
100
80
60
40
20
10
8
6
4
2
1
2
4
6
8
TIME (hours)
Slow component
(fractional volume 0.78)
Fast component
(fractional volume 0.22)

TABLE 8. ANALYSIS OF COMPONENTS OF ^{36}Cl AND ^{22}Na UPTAKE INTO THE CSF OF DEVELOPING RATS

	Fast component		Slow component	
Isotope	$t_{1/2}$ (h)	Vd (%)	$t_{1/2}$ (h)	Vd (%)
Chloride-36				
1 week	0.11(0.04-0.35)	3(1- 6)	1.1(1.0-1.3)	111(105-118)
2 week	0.10(0.07-0.21)	16(11-21)	0.9(0.8-1.0)	100(94-107)
5 week	0.19(0.11-0.40)	26(17-37)	1.1(0.9-1.2)	91(74-113)
Sodium-22				
1 week	0.18(0.08-0.46)	2(1- 7)	0.8(0.7-0.9)	106(100-112)
2 week	0.16(0.04-0.57)	2(1- 4)	0.7(0.7-0.8)	104(101-107)
5 week	0.18(0.15-0.21)	29(26-33)	1.3(1.2-1.5)	83(66-105)

Values in parentheses are 95% confidence limits for the parameter. See Table 1 for other details.

Fig. 12. The uptake of ^{36}Cl and ^{22}Na into the cerebral cortex and cerebellum of 1-wk, 2-wk, and 5-wk rats as a function of time after administration. The upper-half of the figure represents isotope uptake into the cerebral cortex and the lower-half that into the cerebellum. For both tissues, ^{36}Cl uptake is shown in the left-hand portion and ^{22}Na uptake in the right-hand portion of the figure. See Fig. 1 for details.

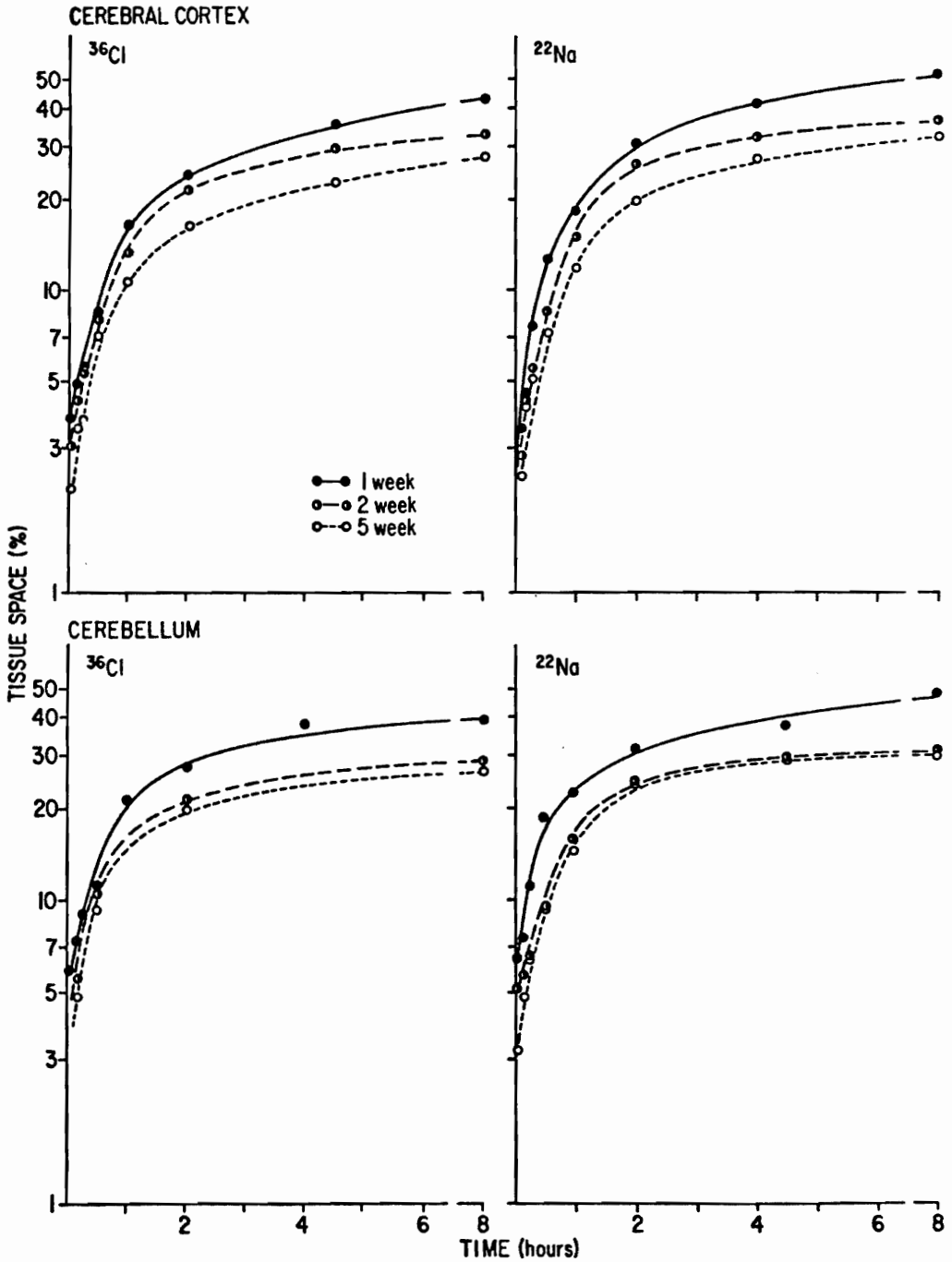
CEREBRAL CORTEX
^{36}Cl
^{22}Na
CEREBELLUM
^{36}Cl
^{22}Na
1 week
2 week
5 week
TISSUE SPACE (%)
TIME (hours)
50
40
30
20
10
7
5
3
1
2
4
6
8

cerebral cortex decreased steadily with age from 42.0 ± 1.0% at 1 wk to 32.9 ± 1.0% at 2 wk and to 28.0 ± 0.3% at 5 wk of age. Similarly, the ^{22}Na steady-state space of the cerebral cortex decreased from 50.7 ± 1.2% at 1 wk to 36.2 ± 0.3% at 2 wk and to 32.4 ± 0.5% at 5 wk. In the cerebellum, as in the cerebral cortex, a marked decline of 10% and 16% was observed in the steady-state ^{36}Cl and ^{22}Na spaces, respectively, between the ages of 1 and 2 wk. However, unlike the cerebral cortex, only a small decrease was detected between the 2 and 5 wk cerebellum ^{36}Cl or ^{22}Na spaces (Fig. 12). Resolution of the uptake curves yielded, as for the choroid plexuses, a fast and a slow component (Table 9). In general, the fast component filled at a rate at least 30 times that of the slow component and represented less than 1/7 of the total tissue isotope space. The fast component Vd of the cerebellum tended to decrease with age for both ^{36}Cl and ^{22}Na. The slow component Vd of the cerebral cortex declined in magnitude with age, reflecting the decreased steady-state volume. However, neither the ^{36}Cl nor the ^{22}Na Vd of the cerebellar slow component changed significantly between 2 and 5 wk of age. As for the slow component $t_{1/2}$ of the CSF, the $t_{1/2}$ of both the cerebral cortex and cerebellum slow components tended to be less at 2 wk than at 1 or 5 wk. At all 3 ages, the ^{36}Cl and ^{22}Na $t_{1/2}$ for the cerebellum slow component were less than the corresponding $t_{1/2}$ for the cerebral cortex.

Unlike ^{36}Cl or ^{22}Na, ^{3}H-mannitol achieved a steady-state distribution within the LVCP or 4VCP by ~15 min. As shown in Fig. 13 for the 1-wk LVCP, the 1/4 and 1 h ^{3}H-mannitol Vd were not significantly different for any of the 3 age groups. A small decline was detected in the LVCP (Δ2.7%)

TABLE 9. ANALYSIS OF COMPONENTS OF ^{36}Cl AND ^{22}Na UPTAKE INTO CEREBRAL CORTEX AND CEREBELLUM OF DEVELOPING RATS

	Fast component		Slow component	
Compartment	$t_{1/2}$ (h)	Vd (%)	$t_{1/2}$ (h)	Vd (%)
A. Chloride-36				
Cerebral cortex				
1 week	0.02	1	1.6(1.5-1.7)	41(40-42)
2 week	0.03	2	1.5(1.4-1.6)	31(30-32)
5 week	0.03	1	1.7(1.4-2.0)	27(25-29)
Cerebellum				
1 week	0.03	5	1.2(1.1-1.3)	34(33-35)
2 week	0.02	4	1.1(1.0-1.2)	25(24-26)
5 week	0.05	2	1.2(0.8-1.6)	24(19-32)
B. Sodium-22				
Cerebral cortex				
1 week	0.02	2	1.5(1.4-1.6)	49(48-51)
2 week	0.02	1	1.1(1.0-1.2)	35(34-37)
5 week	0.02	1	1.5(1.3-1.8)	31(29-33)
Cerebellum				
1 week	0.03	6	1.2(1.1-1.4)	42(40-44)
2 week	0.02	3	0.8(0.7-0.9)	29(28-30)
5 week	0.02	2	1.1(1.0-1.2)	31(30-32)

Values in parentheses are 95% confidence limits for the parameter. See Table 1 for other details.

Fig. 13. The uptake of ^{3}H-mannitol by the LVCP of 1-wk rats as a function of time after administration. ^{3}H-mannitol (0.5 μCi/g) was injected at various times prior to sacrifice into 4-h nephrectomized rats. LVCP radioactivity (▲—▲) was expressed as a space (%) = 100 x (dpm/g tissue)/(dpm/g plasma H_2O). The uptake of ^{3}H-mannitol was resolved into 1 component by subtracting the 0, 5, 10 and 15 min spaces from the steady-state space and plotting the difference (X---X). Each point represents a mean $\pm$ S.E.M. for 3 animals.

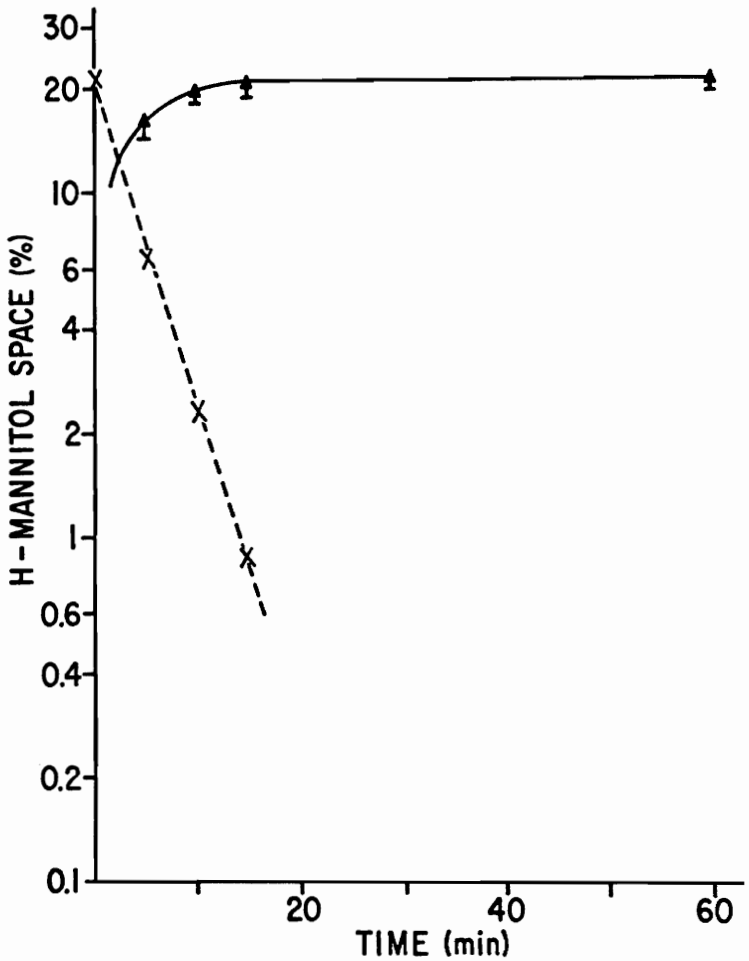
30
20
10
6
4
2
1
0.6
0.4
0.2
0.1
H-MANNITOL SPACE (%)
20
40
60
TIME (min)

and 4VCP (Δ1.7%) ^{3}H-mannitol Vd between the 1-wk and 5-wk rats. A similar decrease was noted in the LVCP and 4VCP tissue water content with age. Graphical analysis of the choroid plexus uptake of ^{3}H-mannitol yielded only 1 component with a $t_{1/2}$ of 0.04-0.06 h which did not change significantly with development (Fig. 13).

Steady-state spaces of ^{36}Cl and ^{22}Na in the choroid plexuses were converted to epithelial cell [Cl] and [Na] by subtracting extracellular fluid and erythrocyte contributions from the tissue ion and water contents (see Methods). As shown in Fig. 14, LVCP and 4VCP cell [Cl] decreased by 14 and 9 mmol/kg cell H_2O, respectively, between 1 and 5 wk of age. Developmental differences between the 2 choroid plexuses were detected in that LVCP cell [Cl] fell by 8 mmol/kg H_2O between 1 wk and 2 wk, however 4VCP [Cl] did not change significantly (1 mmol/kg H_2O) during that period. As for choroid plexus [Cl], both LVCP and 4VCP cell [Na] decreased during the 1 to 5 wk period. Yet, LVCP [Na] fell between 1 and 2 wk of age and then remained constant from 2 to 5 wk, whereas 4VCP [Na] decreased between the first and second wk and then increased by 8 mmol/kg H_2O by the fifth wk of postnatal age.

By analyzing ^{36}Cl and ^{22}Na uptake into both brain tissue and CSF, the extracellular space of the brain can be estimated (see PART TWO). Because the CSF activity represents a better estimate of the radioisotope level in the brain extracellular fluid than does the plasma, the initial slope (when the majority of the isotope in the brain tissue is contained within the brain extracellular fluid) of the brain space versus CSF space curve provides a

Fig. 14. Calculated LVCP and 4VCP cell [Cl] and [Na] of 1-wk, 2-wk, and 5-wk rats. The upper-half of the figure represents cell [Cl] and the lower-half represents cell [Na] for the 3 age groups. See Materials and Methods for the details of the calculation. Each bar graph represents the mean $\pm$ S.E.M. for at least 6 rats.

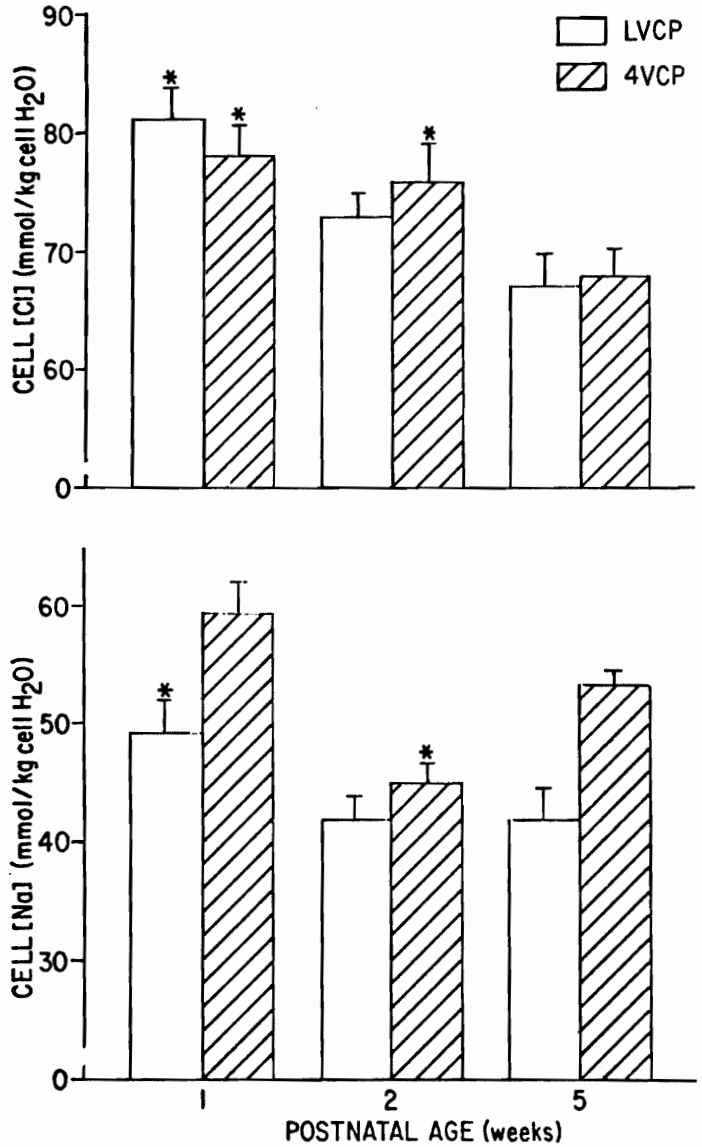
LVCP
4VCP
CELL [Cl] (mmol/kg cell H_2O)
90
80
70
60
0
CELL [Na] (mmol/kg cell H_2O)
60
50
40
30
0
1
2
5
POSTNATAL AGE (weeks)

measurement of the volume of CSF which would account for the brain radioactivity (extracellular space). Fig. 15 summarizes the cerebral cortex and cerebellum extracellular spaces, which were obtained from ^{36}Cl and ^{22}Na uptake analysis, as a function of postnatal age. A steady decline in extracellular fluid volume was detected in both brain regions as the animals matured. On average, the extracellular fluid volume of the 5-wk-old rats was ~45% of that of 1-wk-old rats. The ^{22}Na distribution consistently estimated a slightly larger volume for the cerebral cortex or cerebellum extracellular space than did ^{36}Cl.

With the above measurements of extracellular volume, an average cell [Cl] or [Na] was calculated for the cerebral cortex and cerebellum. While cell [Na] fell significantly by 15 and 5 mmol/kg H_2O in both the cerebral cortex and cerebellum, respectively, between 1 and 2 wk of age, the cell [Na] remained unaltered at 34 mmol/kg H_2O from 2 wk to 5 wk in both brain regions. In contrast, cerebral cortex cell [Cl] tended to decrease by 5 mmol/kg H_2O from 1 wk to 5 wk, and cerebellum cell [Cl] tended to increase by 5 mmol/kg H_2O over that period. Again, like cell [Na], the cerebral cortex and cerebellum cell [Cl] approached a common value of ~20 mmol/kg H_2O during development.

The permeability of the developing blood-brain and blood-CSF barriers to ^{36}Cl and ^{22}Na was evaluated by calculating permeability surface-area products (PA). The PA can be converted to permeability if the surface-area for exchange is known. Though the surface area of the two CNS barriers undoubtedly changes during the first few weeks of postnatal life, the PA is, at

Fig. 15. Cerebral cortex and cerebellum extracellular space as determined by ^{36}Cl and ^{22}Na for 1-wk, 2-wk, and 5-wk rats. The upper-half of the figure represents the extracellular space of the cerebral cortex and the lower-half that of the cerebellum. The extracellular space at each age was calculated for ^{36}Cl or ^{22}Na as the initial slope of the tissue space/CSF space curve. Each bar graph represents a mean $\pm$ S.E.M. of the slope.

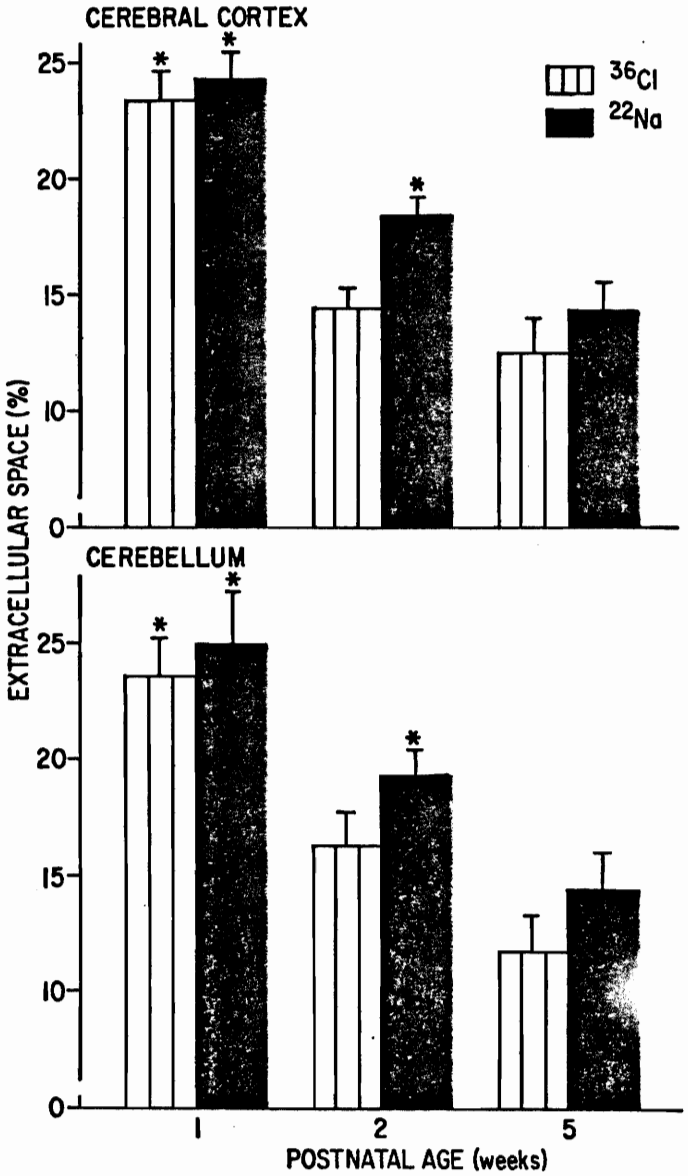
CEREBRAL CORTEX
CEREBELLUM
^{36}Cl
^{22}Na
EXTRACELLULAR SPACE (%)
0
10
15
20
25
1
2
5
POSTNATAL AGE (weeks)

minimum, a valid indication of the relative permeability for an age group in which several isotopes (^{36}Cl, ^{22}Na, or ^{3}H-mannitol) are compared. In Table 10, the PA for several regions of the CNS to ^{36}Cl and ^{22}Na are listed as a function of age. For both radioisotopes, cerebral cortex and cerebellum PA decreased on average 1/3 over the postnatal period of 1 to 5 wk. Similarly, CSF (slow component) PA fell significantly for both ^{36}Cl and ^{22}Na during the first 5 wk of postnatal life. CSF (fast component) PA increased at least 5-fold for both ^{36}Cl and ^{22}Na between 1 and 5 wk. Whereas 4VCP PA for ^{36}Cl and LVCP PA for ^{22}Na both fell by ~50-60% during the interval of 1-5 wk, LVCP PA for ^{36}Cl and 4VCP PA for ^{22}Na showed no significant trend during development. Except for the choroid plexuses, the PA for ^{22}Na of the cerebral cortex, cerebellum, and CSF were generally greater than the corresponding PA for ^{36}Cl at each stage of development.

Permeability surface-area products were calculated for ^{3}H-mannitol uptake into the cerebral cortex, cerebellum, and CSF (fast component) by determining the initial slope of the curve of ^{3}H-mannitol space versus time. Table 11 summarizes the PA for ^{3}H-mannitol in the developing rat CNS. As for ^{36}Cl and ^{22}Na, the cerebral cortex and cerebellum PA for ^{3}H-mannitol decreased ~80% during the first 5 wk of postnatal life. Cerebrospinal fluid (fast component) PA for ^{3}H-mannitol also fell by 82% from 1 wk to 5 wk. The cerebellum PA for ^{3}H-mannitol was always greater than the corresponding cerebral cortex PA, as was the case for both ^{36}Cl and ^{22}Na. Lastly, whereas the relative magnitude of cerebral cortex and cerebellum PA was $^{22}Na > {}^{36}Cl > {}^{3}H$-mannitol at each age group, the CSF PA for the 3 isotopes were

TABLE 10. PERMEABILITY SURFACE-AREA PRODUCTS FOR ^{36}Cl AND ^{22}Na UPTAKE INTO THE DEVELOPING RAT CNS

	PA (ml/h/g) for ^{36}Cl			PA (ml/h/g) for ^{22}Na		
Compartment	1 week	2 week	5 week	1 week	2 week	5 week
Lateral ventricle choroid plexus	0.230 ± 0.014	0.270 ± 0.019	0.208 ± 0.044	0.163*† ± 0.017	0.110 ± 0.015	0.080 ± 0.009
Fourth ventricle choroid plexus	0.385*† ± 0.032	0.203 ± 0.013	0.165 ± 0.029	0.173 ± 0.030	0.182 ± 0.018	0.200 ± 0.021
Cerebrospinal fluid						
Fast component	0.189*† ± 0.331	1.109 ± 0.248	0.949 ± 0.202	0.077* ± 0.333	0.087* ± 0.325	1.117 ± 0.107
Slow component	0.699* ± 0.031	0.770* ± 0.038	0.573 ± 0.046	0.918* ± 0.058	1.030* ± 0.017	0.443 ± 0.031
Cerebral cortex	0.178*† ± 0.005	0.143* ± 0.005	0.110 ± 0.006	0.226* ± 0.007	0.221* ± 0.004	0.143 ± 0.009
Cerebellum	0.196*† ± 0.006	0.158 ± 0.006	0.139 ± 0.027	0.243* ± 0.011	0.251* ± 0.009	0.195 ± 0.004

Component rate constants (k) were converted to permeability surface-area products with the formula: PA = k x Vd/100. For tissues only data for the slow component is presented. Values represent a mean ± S.E.M. *$P < 0.05$ (1 or 2 week vs. 5 week) by multiple range test. †$P < 0.05$ (1 week vs. 2 week) by multiple range test.

TABLE 11. PERMEABILITY SURFACE-AREA PRODUCTS FOR ^{3}H-MANNITOL UPTAKE INTO THE DEVELOPING RAT CNS

	PA (ml/h/g) for ^{3}H-mannitol		
Compartment	1 week	2 week	5 week
Cerebral cortex	0.0447* ± 0.0023	0.0327* ± 0.0052	0.0098 ± 0.0074
Cerebellum	0.0709*^{t} ± 0.0031	0.0338* ± 0.0046	0.0120 ± 0.0088
Cerebrospinal fluid	0.1211* ± 0.0088	0.1015* ± 0.0026	0.0212 ± 0.0080

Permeability surface-area products were determined as the initial slope of the ^{3}H-mannitol space vs. time curve. Values represent a mean ± S.E.M. *$P < 0.05$ (1 week or 2 week vs. 5 week) by multiple range test. $^{t}P < 0.05$ (1 week vs. 2 week) by multiple range test.

comparable at 1 wk ($P > 0.05$) and diverged (PA for ^{36}Cl and ^{22}Na increased and PA for ^{3}H-mannitol decreased) with age.

DISCUSSION

The choroid plexuses are convenient tissues for the utilization of the compartmentation technique to monitor the maturation of Cl and Na transport into the CNS. With measurements of tissue extracellular space, residual erythrocyte volume, and exchangeable ion content, tissue Cl and Na content can be converted to epithelial cell [Cl] and [Na]. Due to the homogeneous epithelial cell population of the choroid plexuses, the calculated cell [Cl] or [Na] represents a reasonable estimation of the in vivo ion concentration. Furthermore, the parameters necessary for cell concentration calculations can be obtained readily for the LVCP and 4VCP of developing rats. Thus, by monitoring changes in choroidal epithelial cell [Cl] and [Na] with age, the relationship between ion transport and CSF production was examined.

The tissue extracellular volume, as measured by the 1-h ^{3}H-mannitol space, decreased slightly with age for the LVCP (from 21% at 1 wk to 19% at 5 wk) and the 4VCP (from 19% at 1 wk to 17% at 5 wk). JOHANSON et al. (1976) obtained a qualitatively similar reduction in LVCP extracellular volume, as estimated by the 1-h ^{3}H-inulin space, with maturation. Uptake of ^{3}H-mannitol into the choroid plexus of each age group was rapid and resolved into a single component with a $t_{1/2}$ of 0.04-0.05 h. The fast components of ^{36}Cl and ^{22}Na uptake into the choroid plexuses had comparable $t_{1/2}$ to that of ^{3}H-mannitol. However, the fast component Vd for ^{36}Cl or ^{22}Na generally

differed from the corresponding ^{3}H-mannitol space; both LVCP and 4VCP ^{36}Cl Vd for the fast component increased by 15-16% (from 9-10% to 25%) with age while the ^{22}Na Vd (fast component) were 1-6% less than the ^{3}H-mannitol space at each age. If a correction for residual erythrocyte ^{36}Cl content (1-2% at 1-2 wk and 5-6% at 5 wk) is subtracted from the ^{36}Cl fast component Vd of the choroid plexuses, values not significantly different from the ^{3}H-mannitol spaces are obtained for 2-wk and 5-wk rats; the corrected ^{36}Cl Vd of the fast component at 1 wk of age was $\sim 1/2$ of the ^{3}H-mannitol space. Correction of the choroid plexus ^{22}Na Vd (fast component) by subtraction of the residual erythrocyte ^{22}Na content did not significantly alter the fast component Vd for any of the three age groups. Thus, for the 2-wk and 5-wk rats, both the ^{36}Cl fast component Vd and the ^{3}H-mannitol space determined similar extracellular volumes for the LVCP and 4VCP (17-20%). The ^{22}Na Vd of the fast component determined a slightly lower value for the LVCP (14-15%) and 4VCP (13-17%) extracellular space of 2-wk and 5-wk rats.

While the 2-wk rat ^{3}H-mannitol space and ^{36}Cl fast component Vd estimated similar volumes for the choroid plexus extracellular space, the ^{36}Cl fast component Vd at 1 wk was $\sim 1/2$ that of the corresponding ^{3}H-mannitol space. The ^{22}Na fast component Vd (12-17%) at 1 wk was intermediate between the ^{36}Cl fast component Vd (9-10%) and the ^{3}H-mannitol space (19-21%) for both the LVCP and 4VCP; however, the fast component $t_{1/2}$ for ^{22}Na (0.08-0.12 h) was $\sim$3-4 times slower than the ^{36}Cl $t_{1/2}$ (0.03 h). The differences in radioisotope distribution between the 1-wk and 2-wk

choroid plexus may reflect developmental changes in LVCP and 4VCP stromal space. During postnatal maturation the basement membrane and connective tissue of the rat choroid plexus enlarge until ~4 wk post partum (CANCILLA et al., 1966); the stroma of gelatinous connective tissue is replaced by a dense fibrous connective tissue (KAPPERS, 1958). The interstitial connective tissue of the 1-wk rat choroid plexus may be penetrated poorly by ^{36}Cl (small fast component Vd) and ^{22}Na (long $t_{1/2}$). As the choroid plexuses mature, the stromal material may change to allow full ^{36}Cl penetration (^{3}H-mannitol space = ^{36}Cl fast component Vd) and yet exclude ^{22}Na (^{3}H-mannitol space > ^{22}Na fast component Vd) by 2 and 5 wk of age. A comparable ionic exclusion and accumulation due possibly to fixed charges in the interstitial compartment has been reported for ^{35}S-sulfate (as compared to ^{3}H-sucrose) in the rat skeletal muscle and cardiac muscle, respectively (MACCHIA et al., 1979). Thus, the differences with age between the choroid plexus ^{3}H-mannitol space, ^{36}Cl fast component Vd (corrected for erythrocyte ^{36}Cl), and ^{22}Na fast component Vd may reflect developmental changes in the plexus interstitial matrix. Furthermore, the small yet significant differences in volume amongst the 3 radioisotopes emphasize the problems of estimating tissue extracellular space solely on the basis of the distribution of one marker.

With measurements of rat choroid plexus residual erythrocyte volume (JOHANSON et al., 1976) and with ^{3}H-mannitol estimates of plexus extracellular space, tissue ^{36}Cl and ^{22}Na steady-state spaces were converted to LVCP and 4VCP cell $[Cl]$ and $[Na]$ for each age group. As detected by PERSHING & JOHANSON (1979), both LVCP and 4VCP cell $[Na]$ decreased

between 1 and 5 wk of age. Similarly, choroid plexus cell [Cl] fell in magnitude during the first 5 wk of postnatal life. Calculated passive membrane potentials for Cl, as obtained from the Nernst equation (reference: extracellular fluid), decreased slightly from -11 to -14 mV for both the LVCP and 4VCP between 1 and 5 wk of age. Though measurements of infant choroid plexus membrane potential have not been reported, WELCH & SADLER (1965) and WRIGHT (1978) have measured adult rabbit and bullfrog choroid plexus membrane potential, respectively, as -50 to -60 mV. Since the K passive membrane potential for the choroid plexus decreases with age by less than -9 mV (JOHANSON et al., 1976; PERSHING & JOHANSON, 1979), it may be reasonable to assume that the choroid plexus membrane potential of a 1-wk or 2-wk rat differs, at most, from the adult (5 wk) by less than -15 to -20 mV. Thus, the electrochemical potential difference for Cl ranged from a minimum of -19 mV at 1 wk to a maximum of -46 mV at 5 wk, which provides evidence for the active accumulation of Cl by the choroid plexus as early as 1 wk post partum.

The decline in LVCP and 4VCP cell [Cl] with age, though at first surprising, may provide an insight into the mechanism of choroidal Cl transport. FRIZZELL et al. (1979) have postulated that intracellular Cl accumulation in epithelial tissues is mediated via a Na-coupled Cl mechanism; the energy necessary for the active transport of Cl is derived from coupling to the Na electrochemical potential difference. Na-coupled Cl transport by the choroid plexus may be possible because the Na electrochemical potential difference across the choroidal basolateral membrane was 2-3 times that for Cl at

each age. If Cl were transported into the choroidal ependyma across the basolateral membrane via a Na-coupled mechanism, Cl exit from the cell into the CSF (down an electrochemical potential gradient) could be controlled by regulating the movement of Cl across the apical membrane. The 1-wk rat choroid plexus may have the Na-coupled Cl transport mechanism at the basolateral membrane, yet lack the apical membrane Na-K pump capacity (STASTNY et al., 1978) and permeability regulation to Cl to move Cl out of the cell and into the CSF. Thus, at 1 wk, epithelial cell [Cl] and [Na] were greater than at 2 or 5 wk because ion transport into the choroidal cell across the basolateral membrane was not coupled with ion movement into the CSF. As the apical membrane Na-K pump increased in capacity (2-5 wk), cell [Cl] and [Na] would be expected to decrease as Na and Cl more readily move across the apical membrane into the CSF.

The significant increase in 4VCP cell [Na] between 2 and 5 wk may represent the maturation of Na-coupled transport systems other than that for Cl. In vitro LVCP and 4VCP have been found to accumulate actively organic (5-hydroxyindoleacetic acid) and inorganic (iodide, sulfate) anions (WELCH, 1962; CSERR & VAN DYKE, 1971; SAMPATH & NEFF, 1974; WRIGHT, 1978b); amino acids (COBEN et al., 1971), and sugars (CSAKY & RIGOR, 1964). Evidence suggests that many of these transport systems are Na dependent (CSAKY & RIGOR, 1964; COBEN et al., 1971; WRIGHT, 1978b); similar to Na-coupled Cl cotransport, active transport of amino acids and sugars may be driven by the sodium electrochemical potential gradient. Furthermore, a greater transport capacity (up to 2x) generally has been observed

in the 4VCP than in the LVCP (WELCH, 1962; CSERR & VAN DYKE, 1971). Lastly, BIERER & HEISEY (1972) found a significant increase in organic anion transport in the LVCP and 4VCP with postnatal age. Thus, maturation of Na-dependent transport systems (which allow Na to enter the cell) in the 4VCP between 2 and 5 wk of age may contribute to the increase in 4VCP cell [Na] during that period.

As for the choroid plexuses, radioisotope uptake into the CSF changed markedly during maturation. Whereas only one significant component (slow) was resolved from the CSF ^{36}Cl or ^{22}Na curves of 1-wk rats, 2 components (fast and slow) were obtained by 5 wk of age. As suggested by LEVIN & PATLAK (1972), the fast component probably represents ^{36}Cl or ^{22}Na movement across the blood-CSF barrier (choroidal ependyma). First, the ~10-fold increase in fast component volume during the first 5 wk of postnatal life corresponds to the onset of rat CSF production (BASS & LUNDBORG, 1973a; JOHANSON & WOODBURY, 1974). Second, the ~33% decrease in CSF secretion after choroid plexectomy (MILHORAT et al., 1971) compares favorably to the fractional volume (^{36}Cl or ^{22}Na) of the CSF fast component (22-26%). JOHANSON & WOODBURY (1978) obtained a CSF fast component (fractional volume 0.21) by graphical analysis of the uptake of a nonelectrolyte, ^{14}C-urea, into the CSF. Lastly, acetazolamide treatment (20 mg/kg), which inhibits choroid plexus fluid production by > 95% (MELBY & REED, 1978) eliminates the fast component of ^{36}Cl uptake into the 5-wk rat CSF (unpublished data). The onset of choroid plexus fluid secretion (~2 wk), as indicated by the volume of the CSF fast component, corresponds to the

decrease in choroid plexus cell [Cl] and [Na] between 1 and 2 wk of postnatal age.

A schematic model of the developmental changes in choroid plexus Cl and Na transport, and fluid production is shown in Fig. 16. In the 1-wk-old rat, Cl is transported across the basolateral membrane by Na-dependent Cl cotransport. It is postulated that high cell concentrations of Cl and Na result from a low level of active Na transport at the apical membrane, and possibly from a low apical membrane permeability to Cl. As a result, fluid production by the 1-wk plexus is negligible. As the choroid plexus matures, increased Na-K pump activity actively transports more Na into the CSF across the apical membrane and thus cell [Na] falls in magnitude. Cl and H_2O move into the CSF down the electrical and osmotic gradients, respectively, generated by active Na transport. By 5 wk of postnatal age, choroidal cell [Cl] is significantly less than in the 1-wk rat and plexus fluid production accounts for $\sim$1/4 of the CSF secretion (CSF fast component Vd).

The cerebral cortex and cerebellum steady-state spaces of ^{36}Cl and ^{22}Na decreased with postnatal age (Fig. 12). A similar trend for the rat cerebral cortex was obtained by analysis of the chemical Cl and Na space (VERNADAKIS & WOODBURY, 1962). Likewise, VERNADAKIS & WOODBURY (1965) and LUCIANO (1968) observed a decline in magnitude in the rat cerebral cortex ^{36}Cl and ^{22}Na spaces, respectively, with postnatal age. Because the rate-limiting step of radioisotope uptake into the brain is movement across the capillary endothelium (blood-brain barrier), in vivo extracellular and cellular spaces of the brain could not be determined by graphical

Fig. 16. A schematic representation of ion and water transport across the choroidal epithelium of 1-wk and 5-wk rats. The magnitude of the flux is indicated by the width of the arrow. Similarly, the magnitude of cell $\lceil Cl \rceil$ and $\lceil Na \rceil$ is indicated by the size of the lettering within the brackets. Cl is postulated to enter the epithelial cell from the stromal interstitail fluid by a Na-dependent Cl cotransport mechanism on the basolateral membrane. Na is actively extruded from the cell into the CSF by an apical membrane Na-K pump. Water secretion arises from the osmotic gradients generated by Na and Cl transport.

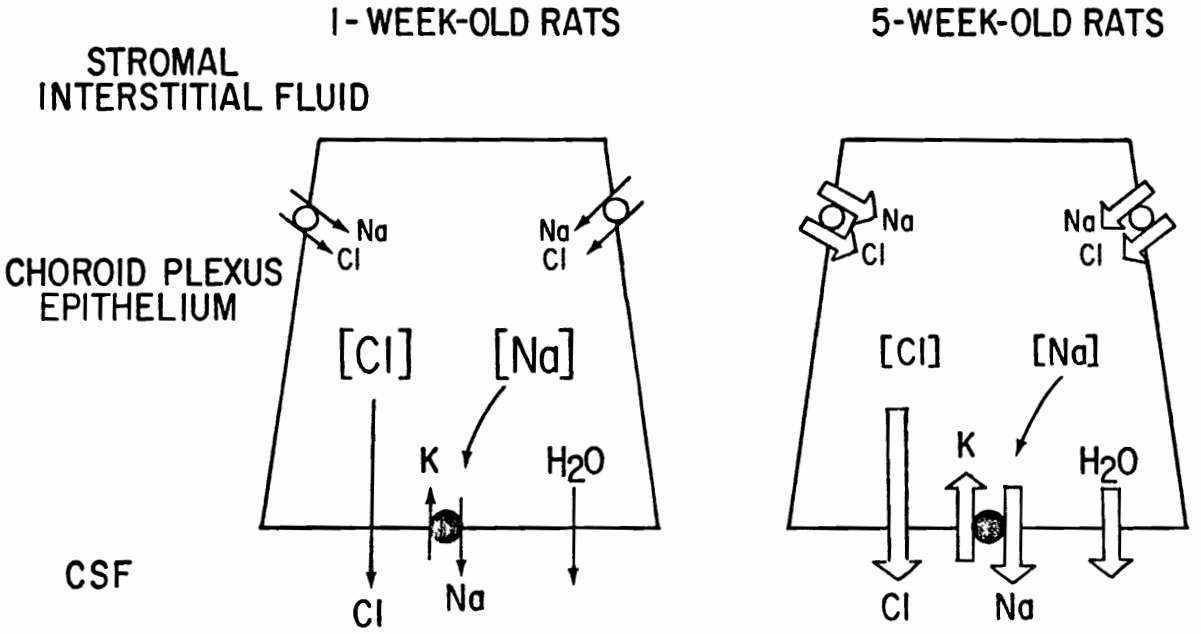
1-WEEK-OLD RATS
5-WEEK-OLD RATS
STROMAL
INTERSTITIAL FLUID
CHOROID PLEXUS
EPITHELIUM
CSF
Na
Cl
[Cl]
[Na]
K
H2O
Cl
Na

analysis (see PART TWO). However, estimation of the brain extracellular volume from the initial slope of the brain space versus CSF space curve revealed a decrease of ~1/2 in volume between 1 and 5 wk. A qualitatively similar trend in brain extracellular space with age was obtained by analysis of brain/CSF concentration ratio for inulin in young rats (FERGUSON & WOODBURY, 1969), and by analysis of electron micrographs in young rats (CALEY & MAXWELL, 1970). The marked reduction in extracellular space with age is a result of glial cell and neuronal process proliferation (WOODBURY et al., 1974; HERTZ & SCHOUSBOE, 1975). For example, BRIZZEE et al. (1964) measured a 2.5-fold increase in the number of glial/neuronal cells in the rat cerebral cortex between 1 and 7 wk. Furthermore, carbonic anhydrase, a glial cell marker, increases in activity by 6x in the rat brain between 1 and 4 wk post partum (WOODBURY et al., 1974). The reduction in the brain volume of extracellular fluid, which has high [Cl] and [Na] compared to cellular fluid, and the rise in volume of the brain cellular compartment with age are consistent with the fall in magnitude of cerebral cortex and cerebellum ^{36}Cl and ^{22}Na spaces.

Calculated cell [Cl] for the cerebral cortex and cerebellum did not change significantly while cell [Na] decreased between 1 and 5 wk. Because the brain glial cell volume, which is thought to be relatively high in [Na] and [Cl] compared to neurons (HERTZ & SCHOUSBOE, 1975), increases with postnatal age, a greater brain cell [Cl] and [Na] might be expected for adult as compared to infant rats. The lack of such an increase in brain cell [Cl] and [Na] with age may indicate that the extracellular spaces of the

1-wk and 2-wk rats were underestimated; FERGUSON & WOODBURY (1969) obtained significantly greater brain extracellular spaces for infant rats from the uptake of ^{14}C-inulin. Similarly, the lack of an increase in calculated cell [Cl] and [Na] with age may result from changes in the neuronal cell compartment as well as from the glial cell compartment. The Na-K ATPase activity of the rat brain increases 5- to 10-fold during the first 7 wk of postnatal life (SAMSON et al., 1964; SAMSON & QUINN, 1967); during the same period, there is a sharp rise in the electrical activity of the rat cerebral cortex (CRAIN, 1952). The increase in neuronal cell volume (CALEY & MAXWELL, 1971) and a possible increase in the resting membrane potential of cerebral cortex and cerebellar neurons (BOETHIUS, 1972), both of which would tend to lower brain Cl and Na content, may balance the rise in the brain content of Cl and Na due to glial cell proliferation.

The $t_{1/2}$ for ^{36}Cl, ^{22}Na, and ^{3}H-mannitol uptake into the CNS were converted to permeability surface-area products (PA) to evaluate the relative permeability of the developing blood-brain and blood-CSF barriers. The rate-limiting step for radioisotope movement into the brain is transfer across the brain capillaries (blood-brain barrier) (BRADBURY, 1979). As noted by VERNADAKIS & WOODBURY (1965) for ^{36}Cl and LUCIANO (1968) for ^{22}Na, the relative permeability of the cerebral capillaries to both radioisotopes was found to decrease with postnatal age in the present study. Similarly, the PA of the cerebellum to ^{36}Cl and ^{22}Na fell in magnitude between 1 and 5 wk. As for ^{14}C-sucrose and ^{14}C-inulin (FERGUSON & WOODBURY, 1969), the PA of both cerebral cortex and cerebellum to ^{3}H-

mannitol fell in magnitude 5- to 6-fold with maturation (JOHANSON, 1980); the decreases in PA to ^{36}Cl and ^{22}Na were ~1.2 to 1.6x among the three age groups. CALEY & MAXWELL (1970) observed a marked increase in the blood vessel density of the rat cerebral cortex after the first week of postnatal life; a greater surface area of cerebral capillaries would be expected in the adult rat than in the infant. The PA differences with age for both tissues probably represent an underestimation of the actual reduction in blood-brain barrier permeability. The greater decrease in brain PA to ^{3}H-mannitol than to ^{36}Cl or ^{22}Na may reflect the maturation of Na and possibly Cl transport by the cerebral capillaries (EISENBERG & SUDDITH, 1979). Lastly, the PA for the cerebellum to all three radioisotopes was found to be slightly greater than that of the cerebral cortex. The difference in PA may represent a regional variation in blood-brain barrier permeability or may reflect a greater capillary surface area in the cerebellum than in the cerebral cortex (JOHANSON, 1980). Thus, between 1 wk and 5 wk of age, the blood-brain barrier of the rat cerebral cortex and cerebellum was found to decrease in relative permeability to three separate isotopes.

The capillaries supplying the choroid plexus differ from the cerebral capillaries in that they are fenestrated and thus allow the penetration of large molecules into the stromal space. The site of the blood-CSF barrier is the basolateral membrane of the choroid epithelium; the choroid plexus cells are held together by zonulae occludentes (CANCILLA et al., 1966). As for the blood-brain barrier, the PA for the choroidal ependyma (CSF fast component) to ^{3}H-mannitol fell in magnitude ~6-fold between 1 and 5 wk. In

contrast, the PA to ^{36}Cl and ^{22}Na increased ~10x with postnatal age. A greater surface area of the choroid plexus basolateral membrane was found by CANCILLA et al. (1966) as the postnatal choroid ependyma matured; the differences in PA for the blood-CSF barrier probably represent an underestimate of the postnatal change in permeability, as was noted for the blood-brain barrier. The decrease in blood-CSF barrier PA to ^{3}H-mannitol with age probably represents a tightening of the barrier (RAMEY & BIRGE, 1979). The increase in barrier PA to ^{36}Cl and ^{22}Na between 1 and 5 wk reflects the onset of Na and Cl transepithelial transport, and thus fluid secretion (BASS & LUNDBORG, 1976; JOHANSON & WOODBURY, 1974).

REFERENCES

BASS N.H. & LUNDBORG P. (1973a) Postnatal development of bulk flow in the cerebrospinal fluid system of the albino rat: Clearance of carboxyl-[^{14}C]inulin after intrathecal infusion. Brain Res. 52, 323-332.

BASS N.H. & LUNDBORG P. (1973b) Postnatal development of mechanisms for the elimination of organic acids from the brain and cerebrospinal fluid system of the rat: Rapid efflux of [^{3}H]para-aminohippuric acid following intrathecal infusion. Brain Res. 56, 285-298.

BIERER D.W. & HEISEY S.R. (1972) Organic anion transport in the maturing dog choroid plexus. Brain Res. 46, 113-119.

BÖETHIUS J. (1972) Membrane potential in muscle cells of developing chicks and rats, in Foetal and Neonatal Physiology (COMLINE K.S., CROSS K.W., DAWES G.S. & NATHANIELS Z.P.W., eds.), pp. 82-87. Cambridge Univ. Press, Cambridge.

BOULDIN T.W. & KRIGMAN M.R. (1975) Differential permeability of cerebral capillary and choroid plexus to lanthanum ion. Brain Res. 99, 444-448.

BRADBURY M. (1979) The Concept of a Blood-Brain Barrier, pp. 1-59, 289-322. Wiley, New York.

BRIZZEE K.R., VOGT J. & KHARETCHKO X. (1964) Postnatal changes in glia/neuron index with a comparison of methods of cell enumeration in the white rat, in Progress in Brain Research (PURPURA D.P. & SCHADE J.D., eds.), Vol. 4, pp. 136-149. Elsevier Pub. Co., Amsterdam.

CALEY D.W. & MAXWELL D.S. (1970) Development of the blood vessels and extracellular spaces during postnatal maturation of rat cerebral cortex. J. Comp. Neur. 138, 31-48.

CALEY D.W. & MAXWELL D.S. (1971) Ultrastructure of the developing cerebral cortex in the rat, in Brain Development and Behavior (STERMAN M.B., McGINTY D.J. & ADINOLFI A.M., eds.), pp. 91-107. Academic Press, New York.

CANCILLA P.A., ZIMMERMAN H.M. & BECKER N.W. (1966) A histochemical and fine structure study of the developing rat choroid plexus. Acta Neuropath. 6, 188-200.

COBEN L.A., COTLIER E., BEATY C. & BECKER B. (1971) Transport of amino acids by rabbit choroid plexus in vitro. Brain Res. 30, 67-82.

CRAIN S.M. (1952) Development of electrical activity in the cerebral cortex of the albino rat. Proc. Soc. exp. Biol. Med. 81, 49-51.

CREMER J.E., BRAUN L.D. & OLDENDORF W.H. (1976) Changes during development in transport processes of the blood-brain barrier. Biochim. Biophys. Acta 448, 633-637.

CSAKY T.Z. & RIGOR B.M. (1968) The choroid plexus as a glucose barrier, in Progress in Brain Research (LAJTHA A. & FORD D.H., eds.), Vol. 29, pp. 147-153. Elsevier Pub. Co., Amsterdam.

CSERR H.F. & VAN DYKE D.H. (1971) 5-Hydroxyindoleacetic acid accumulation by isolated choroid plexus. Am. J. Physiol. 220, 718-723.

DAVSON H. (1955) A comparative study of the aqueous humor and cerebrospinal fluid in the rabbit. J. Physiol., Lond. 129, 111-133.

EISENBERG H.M. & SUDDITH R.L. (1979) Cerebral vessels have the capacity to transport sodium and potassium. Science, N.Y. 206, 1083-1085.

FERGUSON R.K. & WOODBURY D.M. (1969) Penetration of ^{14}C-inulin and ^{14}C-sucrose into brain, cerebrospinal fluid, and skeletal muscle of developing rats. Exp. Brain Res. 7, 181-194.

FRIZZELL R.A., FIELD M. & SCHULTZ S.G. (1979) Sodium-coupled chloride transport by epithelial tissues. Am. J. Physiol. 236, F1-F8.

HERTZ L. & SCHOUSBOE A. (1975) Ion and energy metabolism of the brain at the cellular level, in Int. Rev. Neurobiology (PFEIFFER C. & SMYTHIES J., eds.), Vol. 18, pp. 141-211. Academic Press, New York.

JOHANSON C. (1980) Permeability and vascularity of the developing brain: Cerebellum vs. cerebral cortex. Brain Res. 190, 3-16.

JOHANSON C.E., REED D.J. & WOODBURY D.M. (1976) Developmental studies of the compartmentalization of water and electrolytes in the choroid plexus of the neonatal rat brain. Brain Res. 116, 35-48.

JOHANSON C.E. & WOODBURY D.M. (1974) Changes in CSF flow and extracellular space in the developing brain, in Drugs and the Developing Brain (VERNADAKIS A. & WEINER N., eds.), pp. 281-287. Plenum, New York.

JOHANSON C.E. & WOODBURY D.M. (1978) Uptake of [^{14}C]urea by the in vivo choroid plexus-cerebrospinal fluid-brain system: Identification of sites of molecular sieving. J. Physiol., Lond. 275, 167-176.

KAPPERS J.A. (1958) Structural and functional changes in the telencephalic choroid plexus during human ontogenesis, in Ciba Foundation Symposium on the Cerebrospinal Fluid (WOLSTENHOLME G.E.W. & O'CONNER C.M., eds.), pp. 3-31. Little Brown, Boston.

LEVIN V. & PATLAK C.S. (1972) A compartmental analysis of ^{24}Na kinetics in rat cerebrum, sciatic nerve and cerebrospinal fluid. J. Physiol., Lond. 224, 559-561.

LUCIANO D.S. (1968) Sodium movement across the blood-brain barrier in newborn and adult rats and its autoradiographic localization. Brain Res. 9, 334-350.

MACCHIA D.D., PAGE E. & POLIMENI P.I. (1979) Interstitial anion distribution in striated muscle determined with [^{35}S]sulfate and [^{3}H]sucrose. Am. J. Physiol. 237, C125-C130.

MELBY J. & REED D.J. (1978) Effect of acetazolamide and furosemide on CSF production by cat choroid plexus in situ. Soc. Neurosci. Abstracts 7, 246.

MILHORAT T.H., HAMMOCK M.K., FENSTERMACHER J.D., RALL D.P. & LEVIN V.A. (1971) Cerebrospinal fluid production by the choroid plexus and brain. Science, N.Y. 173, 330-332.

PARANDOOSH Z. & JOHANSON C.E. (1979) Ontogenic changes in the movement of ^{14}C-urea across the blood-brain and blood-CSF barriers. Fed. Proc. (Abstracts) 83, 779.

PERSHING L.K. & JOHANSON C.E. (1979) Effect of acute metabolic acid-base distortions on choroid plexus Na and K in the developing postnatal rat. Fed. Proc. (Abstracts) 83, 778.

RAMEY B.A. & BIRGE W.J. (1979) Development of cerebrospinal fluid and the blood-cerebrospinal fluid barrier in rabbits. Develop. Biol. 68, 292-298.

RAPOPORT S.I. (1976) Blood-Brain Barrier in Physiology and Medicine, pp. 93-101. Raven Press, New York.

REED D.J., WOODBURY D.M. & HOLTZER R.L. (1964) Brain edema, electrolytes, and extracellular space. Archs Neurol. 10, 604-616.

SAMPATH S.S. & NEFF N.H. (1974) The elimination of 5-hydroxyindole-acetic acid from cerebrospinal fluid: Characteristics of the acid transport system of the choroid plexus. J. Pharmacol. exp. Ther. 188, 410-414.

SAMSON F.E., DICK H.C. & BALFOUR W.M. (1964) Na-K stimulated ATPase in brain during neonatal maturation. Life Sci. 3, 511-515.

SAMSON F.E. & QUINN D.J. (1967) Na-K-activated ATPase in rat brain development. J. Neurochem. 14, 421-427.

SAUNDERS N.R. (1977) Ontogeny of the blood-brain barrier. Exp. Eye Res., Suppl. 523-550.

STASTNY F., RYCHTER Z. & JELINEK R. (1978) Cortisol regulation of choroid plexus Na-K-ATPase activity and cisternal cerebrospinal fluid pressure in chick embryo, in Hormones and Brain Development (DORNER G. & KAWAKAMI M., eds.), pp. 265-270. Elsevier/North-Holland Biomed Press, Amsterdam.

VERNADAKIS A. & WOODBURY D.M. (1962) Electrolyte and amino acid changes in rat brain during maturation. Am. J. Physiol. 203, 748-752.

VERNADAKIS A. & WOODBURY D.M. (1965) Cellular and extracellular spaces in developing rat brain. Archs Neurol. 12, 284-293.

WELCH K. (1962) Active transport of iodide by choroid plexus of the rabbit in vitro. Am. J. Physiol. 202, 757-760.

WELCH K. & SADLER K. (1965) Electrical potentials of choroid plexus of the rabbit. J. Neurosurg. 22, 344-351.

WOODBURY D.M., JOHANSON C. & BRØNDSTED H. (1974) Maturation of the blood-brain and blood-cerebrospinal fluid barriers and transport systems, in Narcotics and the Hypothalamus (ZIMMERMANN E. & GEORGE R., eds.), pp. 225-250. Raven Press, New York.

WRIGHT E.M. (1978a) Transport processes in the formation of the cerebrospinal fluid. Rev. Physiol. Biochem. Pharmacol. 83, 1-34.

WRIGHT E.M. (1978b) Anion transport by choroid plexus epithelium, in Membrane Transport Processes (HOFFMAN J.F., ed.), pp. 293-307. Raven Press, New York.

VITA

Name	Quentin Roberts Smith
Birthdate	August 4, 1954
Birthplace	Ogden, Utah
High School	Phillips Andover Academy Andover, Massachusetts
College 1972-1976	Oberlin College Oberlin, Ohio
University 1976-1980	University of Utah Salt Lake City, Utah
Degree 1976	B.A., Oberlin College Oberlin, Ohio
Honors	Graduation with honors Oberlin College NIH Predoctoral Trainee University of Utah
Professional Organizations	Sigma Xi, Society for Neuroscience, American Chemical Society, American Association for the Advancement of Science

Publications

FUCHSMAN W.H., SMITH Q.R. & STEIN M.R. (1977) Direct Raman evidence for resonance interactions between the porphyrin ring system and ring-conjugated substituents in porphyrins, porphyrin dications, and metalloporphyrins. J. Am. Chem. Soc. 99, 4190.

FUCHSMAN W.H., GOLDBERG J.M., LEVY D.D. & SMITH Q.R. (1978) Raman spectroscopic evidence of porphyrinphenyl resonance interactions in tetraphenylporphin, tetraphenylporphindication, and copper (II) tetraphenylporphin. Bioinorganic Chem. 9, 461-467.

SMITH Q.R. & JOHANSON C.E. (1980) Effect of ouabain and potassium on ion concentrations in the choroidal epithelium. Am. J. Physiol. 238, F399-F406.

SMITH Q.R. & JOHANSON C.E. (1980) Effect of carbonic anhydrase inhibitors and acidosis on choroid plexus epithelial cell sodium and potassium. J. Pharmacol. Exp. Ther. (in press).

Abstracts

SMITH Q.R. & JOHANSON C.E. (1977) Ouabain and acetazolamide-induced changes in choroid plexus electrolyte concentrations. The Pharmacologist 19, 449.

JOHANSON C.E. & SMITH Q.R. (1977) Phenytoin-induced stimulation of the Na-K pump in the choroid plexus-cerebrospinal fluid system. Soc. Neuroscience Abstracts 3, 1012.

SMITH Q.R. & JOHANSON C.E. (1978) Stimulation of the choroid plexus Na-K pump after acetazolamide treatment. Fed. Proc. 37, 1585.

SMITH Q.R. & JOHANSON C.E. (1978) Distribution of Na and K in the submaxillary salivary gland subsequent to carbonic anhydrase inhibition. The Pharmacologist 20, 261.

SMITH Q.R. & JOHANSON C.E. (1978) Localization of rat blood-CSF barrier Na-K ATPase. Soc. Neuroscience Abstracts 4, 779.

SMITH Q.R., JOHANSON C.E. & WOODBURY D.M. (1979) Uptake of chloride-36 by the in vivo rat choroid plexus. Fed. Proc. 38, 2483.

SMITH Q.R., JOHANSON C.E. & WOODBURY D.M. (1979) Kinetics of ^{22}Na and ^{36}Cl distribution in the postnatal rat choroid plexus. Soc. Neuroscience Abstracts 5, 592.

SMITH Q.R., JOHANSON C.E. & WOODBURY D.M. (1980) Regulation of in vitro choroid plexus cell electrolytes. Fed. Proc. 39, 2475.

SMITH Q.R., JOHANSON C.E. & WOODBURY D.M. (1980) Relative permeability of the blood-brain and blood-CSF barriers to ^{22}Na and ^{36}Cl. Soc. Neuroscience Abstracts (in press).